



SAPIENZA
UNIVERSITÀ DI ROMA

PhD Course in Molecular design and characterization for the promotion of health and well-being: from drug to food

XXXVII Cycle

Synthesis and Application of Symmetric Organocatalysts, Stability Studies of Atropisomeric Hydrazides by Dynamic-HPLC and Off-Column HPLC experiments

PhD dissertation by

Shilashi Badasa Oljira

Advisor

Professor Alessia Ciogli

Dept. of Chemistry and Drug Technologies at the University of Roma "Sapienza"
P.le A. Moro 5, 00185 Roma, Italy

Academic year 2023/2024

General Introduction

This Ph.D. research program in Molecular Design and Characterization for the Promotion of Health and Well-being: From Drug to Food (XXXVII Cycle) at the Department of Chemistry and Drug Technologies at the University of Roma "Sapienza", under the supervision of Prof. Alessia Ciogli, aimed different topics whose the common unit is chirality. We studied the preparation of Symmetric Chiral Organocatalysts and their applications in the synthesis of enantioriched molecules together with the investigation of the Stereochemical Stability of Atropisomeric Hydrazides by dynamic-HPLC and Off-Column HPLC experiments. The Ph.D. research and obtained results were collected in three distinct chapters.

Part-A has been focused on the asymmetric synthesis of warfarin and analogues catalyzed by C_2 -symmetric amido and C_3 -symmetric amino-organocatalysts. The use of small chiral organic molecules as catalysts for stereoselective reactions has captured great attention and shown impressive advancement for the past two decades to attain enantiopure molecules mainly intermediates of pharmaceutical products with green chemistry principles and without purification. Today, organocatalysts are established as the third fundamental pillar in asymmetric catalysis, next to enzymes and metal-based catalysts. As concern the topic of my thesis, despite the advances of organocatalysts, applications in the synthesis of enantioenriched warfarin and its analogues still a significant synthetic challenge remained. We developed, in high yield, C_2 -symmetric amido and C_3 -symmetric amino-organocatalysts with easy synthetic procedures. The asymmetric Michael addition of 4-hydroxycoumarin to α , β -unsaturated ketones promoted by C_2 -symmetric amido-organocatalysts have shown good performance in yield and enantioselectivity than C_3 -symmetric amide prepared by installation of 1,3,5-benzenetricarbonyl trichloride onto a (2-Amino-1,2-diphenyl-ethyl)-carbamic acid tert-butyl ester.

For C_3 -symmetric amino-organocatalysts, we have evaluated the chiral 1,2-diphenylethylenediamine (DPEDA) as scaffold where the core was the 1,3,5-benzoltricarboxyltrichloride. A small library of 4-hydroxycoumarin and 4-hydroxyquinoline derivatives was provided through a Michael addition. In addition, this novel C_3 -symmetric amino catalyst was used in gram-scale synthesis and transformation of product was well deserved.

The second chapter (Part B) shows the results concerning the stereo stability studies of the atropisomeric hydrazides by dynamic HPLC and off-column-HPLC experiments. The synthesis and analysis of the energy barrier needed for the racemization process of the studied molecules using a computational approach were done by collaborating with Prof. Giorgio Bencivenni at the University of Bologna. In this section, our aim focuses on the experimental determination of energy barriers through chromatographic approaches. Compounds that can exhibit optical properties due to the presence of axial chirality are widely studied and well-developed, while hydrazides represent a new class of atropisomers to be investigated. The knowledge of the rotational stability of such molecules is crucial for designing and developing newly important pharmaceutical drugs as well as gives the highest contribution in the separation of desired active enantiomer. Mainly, we focused on dynamic-HPLC and off-column HPLC experimental studies of these chiral molecules capable of interconverting their enantiomers upon rotation of the σ bonds. Experimental data were then used to extract the kinetic parameters and the free energy barrier of hindered rotation. Specifically for the dynamic-HPLC experiments, kinetic data were obtained by using the simulation software, Auto-D-HPLC-Y2K.

The study of the symmetric amido-thiourea organocatalysts for the synthesis of α -aminonitriles (Part-C) was carried out at the Institute of Organic Chemistry in the research group of Prof. Olga Garcia, University of Munster (Germany). In this part, our goal is to develop C_2 -symmetric thiourea-organocatalysts using a spacer containing pyridine structure where hydrogen-bonding catalysis, anion-binding and Lewis-base have become the prime focus. The performance of the prepared catalysts was evaluated in the enantioselective Strecker reaction. Unfortunately, despite the very high product yields, the catalysts are not able of inducing stereoselection. To understand this trend, the analysis of anion binding abilities of dual hydrogen bond donor symmetric amido-thiourea (for the selected Cat-2) has been performed by titration experiments.

Finally, these 3-years gave me a well-rounded view of different working environment and groups that prepare me for the next endeavors.

Table of contents

Part A	5
1.1 Introduction	6
1.1.1 Overview of Organocatalysis.....	6
1.1.2 Asymmetric Organocatalysis-----	6
1.1.3 Amine Catalysis (via enamine/iminium catalysis)-----	8
1.1.4 Symmetric Organocatalysts in Asymmetric Synthesis-----	12
1.1.5 Asymmetric Michael reactions for synthesis of Warfarin and its analogues-----	15
1.2 Results and discussion -----	20
1.2.1 Synthesis of C ₂ -symmetric amide Organocatalysts-----	20
1.2.2 Synthesis of C ₃ -Symmetric Organocatalysts-----	23
1.2.3 Synthesis of Warfarin-----	25
1.2.4 Scope of the reactions-----	28
1.2.5 Scale-up of synthesis of the active compound-----	31
1.2.6 ESI-MS offline reaction monitoring: identification of active intermediates-----	32
1.3 Conclusion Remarks	35
1.4 Experimental Section	35
References	52
Part B	59
2.1 Introduction	60
2.1.1 Overview of Chirality.....	60
2.1.2 Classification of chiral molecules.....	61
2.1.3 Classification of atropisomers stereochemical stabilities.....	63
2.1.4 Atropisomerism in drug discovery.....	64
2.1.5 N–N atropisomers and Atropisomeric Hydrazides.....	66
2.1.6 Dynamic and kinetic studies for Stereochemistry analysis.....	68
2.1.6.1 Off-column HPLC approach.....	68
2.1.6.2 Dynamic-HPLC: On-column Enantiomerization.....	69

2.2	Aim of the work and research strategies.....	71
2.3	Synthesis of the investigated hydrazides.....	72
2.4	Results and Discussion.....	73
2.4.1	Energy barrier values at different temperatures.....	77
2.4.2	Energy barrier values versus temperatures: Eyring Plots.....	81
2.4.3	Comparison: experimental and computational data.....	84
2.5	Conclusion.....	85
2.6	Experimental Section.....	86
	References.....	89
Part C	93
3.1	Aim of the Research Work.....	94
3.2	Introduction.....	96
3.2.1	H-bond donor catalysis: Focus of thiourea Organocatalysts.....	96
3.2.2	Hydrogen bond catalyzed synthesis of α -aminonitriles	98
3.3	Results and discussion.....	104
3.3.1	Synthesis of symmetric amido-thiourea (Cat-1 to Cat-5)	104
3.3.2	Enantioselective Strecker reaction.....	108
3.3.3	Anion-binding studies of the catalyst Cat-2.....	112
3.4	Conclusion.....	116
3.5	Experimental Section.....	117
	References.....	128
	List of Publications.....	132

Part-A

Asymmetric Synthesis of Warfarin and Analogues Catalyzed by C₂ and C₃-symmetric Amino-Organocatalysts

1.1 Introduction

1.1.1 Overview of Organocatalysis

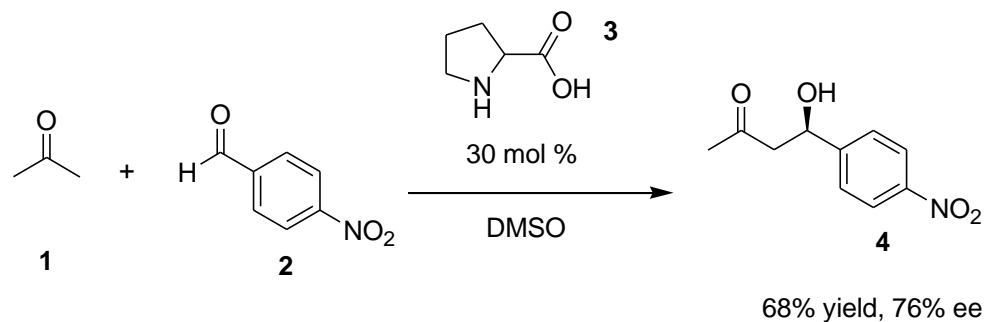
Racemic resolution, chiral synthesis based on substrate induction, and chiral catalytic synthesis are three common methods to obtain enantioenriched molecules. In modern organic synthesis, the most interesting area is to design and prepare chiral molecules with structural diversity using effective reaction approaches. Sustainable chiral catalysts in organic reactions are used to boost the yield, enantioselectivity, purity of the product, and safety of the environment. The use of organic molecules as catalysts to facilitate the reaction has become the most advanced in the enantioselective synthesis of the desired enantiomer. The discovery of proline as a catalyst in the year 2000 was taken as an impressive season that resulted in the development of multiple organocatalysts for different asymmetric reactions.¹ Over decades, the state-of-the-art in asymmetric synthesis largely relies on organo-catalysts due to the inherent nonmetal feature, broad functional group tolerance, and mild reaction conditions. Today, organocatalysis is a fast-growing research field in synthetic chemistry, which has been shown as a powerful catalysis approach in the construction of enantiopure molecules. To date, a large number of organo-catalysts was synthesized and applied successfully in a great number of asymmetric reactions which results in the construction of various enantiopure molecules with structural diversity.

1.1.2 Asymmetric Organocatalysis

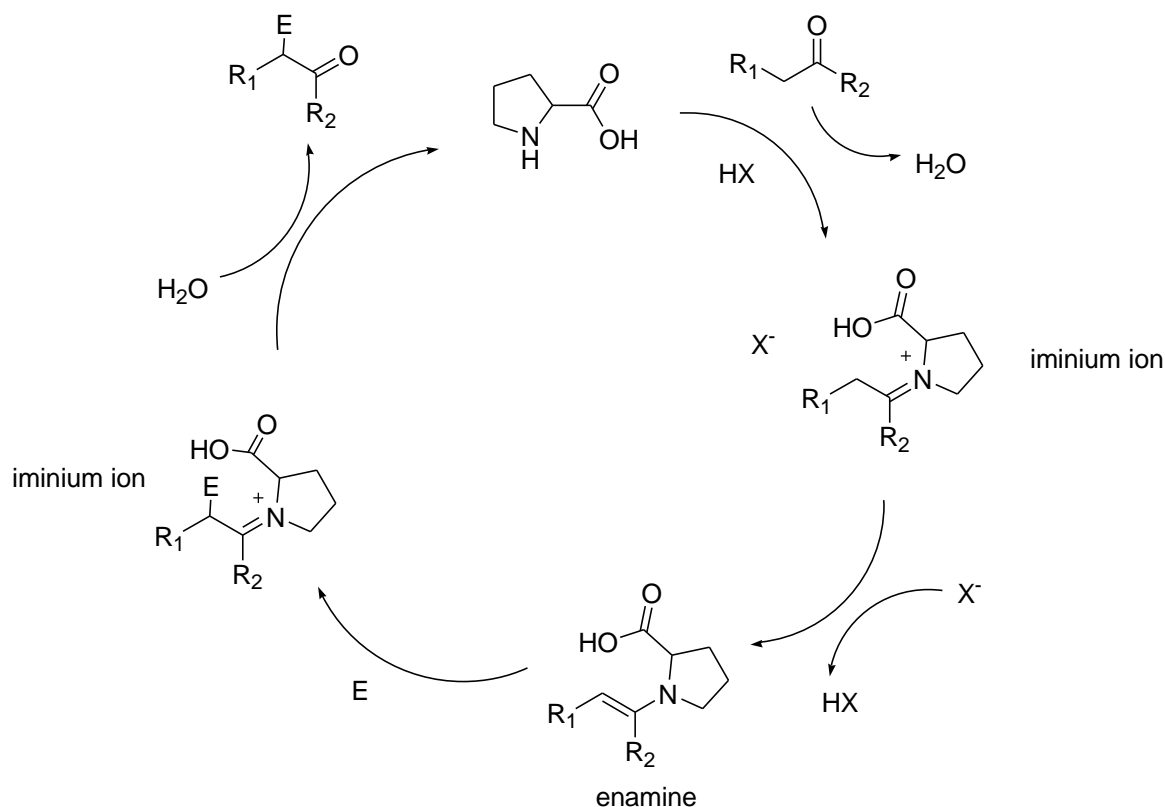
Investigation of efficient strategies for the construction of enantiopure molecules that active pharmaceutical ingredients are a continuing challenge in synthetic chemistry. Depending on the general point of view of organic synthesis, there are different criteria for one method to be efficient during the synthesis of enantioenriched molecules. In a synthesis of desired enantiopure compounds in high yield and environmentally friendly, the use of sustainable catalysts in reaction

protocol is recognized as superior quality. To encounter these problems, researchers in the area of organic synthesis have been officially struggling for a long period. It is known that the design of an efficient reaction strategy that provides pure enantiomer needs the assistance of safe catalysis with a well-matched activation mode.

Over the years, the field of asymmetric synthesis has been dominated by transition metal catalyst¹. The activation of organic reactions by this catalysis approach still constitutes as one of the useful tools in organic synthesis, however, the continued use of metal catalysis has not matched with the main object of sustainable catalysis. To encounter this problem, organic chemists have working continuously for a long time. The use of organic molecules instead of metal catalysts in asymmetric synthesis has been around for more than half a century. The application of organocatalytic in Hajos–Parrish–Eder–Sauer–Wiechert reaction was reported in the early 1970s^{2,3}, however, the use of this catalysis approach remained unexplored for several decades. The year 2000 became a sensational period for the official start of the organocatalysis concept. In this season, proline was recognized as a very simple enzyme-like catalyst for asymmetric aldol reactions by List, Lerner, and Barbas.⁴ Following this remarkable example of simple amine-mimicking enzyme, several organocatalysts for various enantioselective catalytic transformations have been developed.



Scheme 1.1 Proline Catalyzed Asymmetric Aldol Reaction of Acetone with 4-Nitrobenzaldehyde.



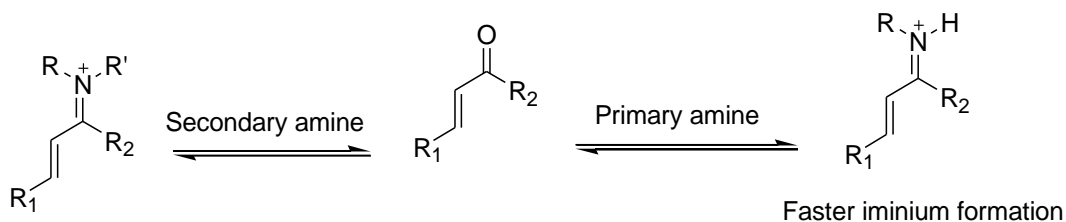
Scheme 1.2. The general mechanism for acid-promoted condensation of the carbonyl with the amine.

To date, organocatalysis has become a major catalytic approach along metal^{5,6,7} and enzymatic reportcatalysis^{8,9,10}, have attracted extensive attention because it provides multiple advantages like the low cost, tolerant of water and air, robustness, environmental friendly, easy structural modification of their scaffolds and their nontoxic nature.¹¹

1.1.3 Amine Catalysis (via enamine/iminium catalysis)

The development of novel and efficient catalysis has allowed for the discovery of novel transformations of asymmetric reaction and improvement of the stereocontrol, minimizing waste, minimizing contamination, and increase efficiency of the product. Use of amino-organocatalysts in asymmetric synthesis of chiral molecule is among these novel and efficient catalysis for

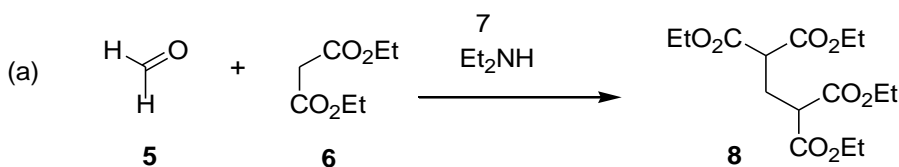
different reaction approach in which primary or secondary of these molecules are able to activate carbonyl carbon/ α,β -unsaturated carbonyl compound¹² like Michael reactions. Mainly, the concept of enamine/iminium catalysis has already demonstrated its invaluable importance and will continue to be widely applied in the enantioselective construction of bioactive molecule and active pharmaceutically ingredient. Due to steric and electronic similarity of the two carbonyl groups in iminium ion activation of unsaturated ketones (Michael addition reaction), asymmetric catalysis with metal is challenging task.^{13,14} This is one reason for the rise of concept about iminium ion activation approach.

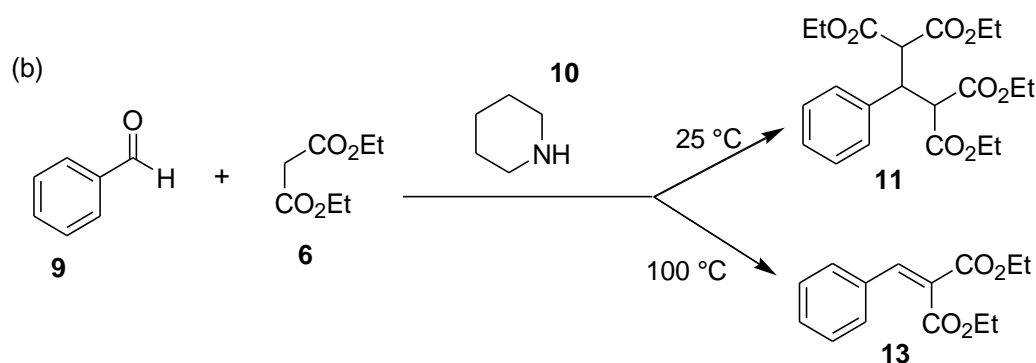


Overcrowded iminium adduct

Scheme1. 3: Steric effect in iminium ion activation approach.

E. Knoevenagel, reported the first amine-promoted (primary) reaction in which condensation was facilitated by the formation of the iminium intermediate between the amine catalyst and the carbonyl substrate.¹⁵ Almost, all the Knoevenagel work was carried out with tertiary amines, secondary amines, primary amines, and ammonium salts known as nitrogen-based catalysts. This research approach opened new research opportunities for organic synthesis communities and offer concept using e-factor in quantitative analysis in of green chemistry.¹⁶



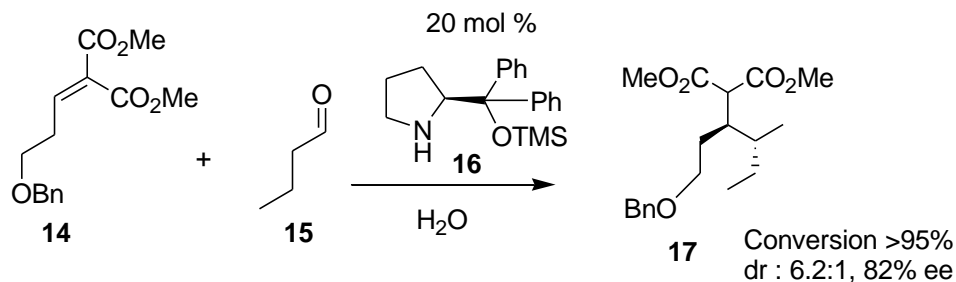


Scheme 1.4 Knoevenagel condensation reaction: **a)** formaldehyde and diethyl malonate under alkaline conditions yielding the bis adduct, **b)** benzaldehyde with diethyl malonate producing the bis adduct at 298 K, and the unsaturated compound at 373 K.

In 1950, Stork and co-workers' introduction of stoichiometric enamine became a milestone in the field of amino catalysis, and the general utility of enamines as nucleophiles was amply demonstrated in their elegant studies.^{17,18} The Hajos–Parrish–Eder–Sauer–Wiechert reactions were reported in the 1970s, in which proline-catalyzed intramolecular aldol reactions via the enamine intermediates accounted for the observed high enantioselectivity.^{19,20}

Takemoto and Rawal developed various Lewis or Brønsted base- or acid-bifunctional tertiary amine-based organocatalysts that attract considerable attention due to their versatility and high level of stereocontrol^{21,22,23,24}. These catalysts activate carbonyl-free reagents and properly locate them in a transition state via stereoselective formation of hydrogen bonds rather than covalent enamine or iminium intermediates. The mechanism of enamine and iminium catalysis has been established by Barbas, Lerner, List, and MacMillan in the years 2000.^{25,26,27} In this trend, the first highly enantioselective reaction promoted by a chiral iminium intermediate was reported by MacMillan and co-workers.²⁸ Chiral secondary and primary amines have been used to catalyze several important enantioselective such Michael reaction^{28,29}, aldol reaction^{28,29,30}, Mannich reaction,^{29,30} α -aminations^{29,30} and α -aminoxylation reactions. Domino reactions and one-pot operations have been easily catalyzed by amino-organocatalytic because it is tolerant of several subsequent reactions.^{32,33,34,35}. It is an excellent approach to the synthesis of bioactive natural

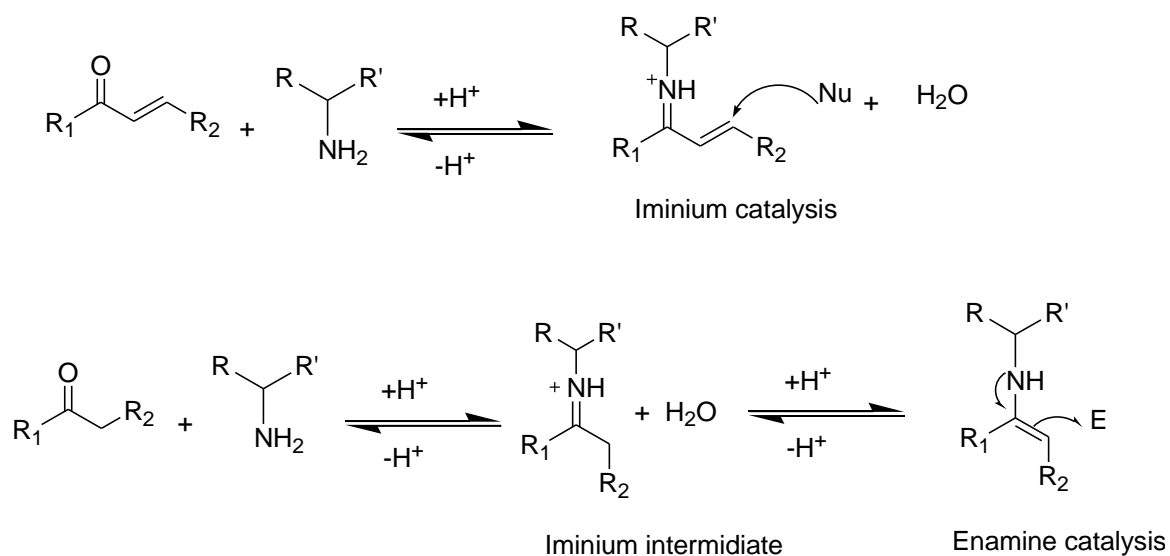
products at both laboratory and industrial scale. At this time, the use of chiral amines especially primary amine in iminium ion activation of α,β -unsaturated ketones become well-known.



Scheme 1.5 Proline derivatives catalyzed Michael addition of a functionalized malonate and *n*-butanal³³.

The mechanistic study during enamine and iminium catalysis is used to understand the change in energy of nucleophiles and electrophiles which implies types of activation modes.

The first work on iminium catalysis was applied on cycloadditions,³⁶ and Michael additions³⁷ respectively. Currently, it is accepted as a general approach for the asymmetric conjugate addition of nucleophiles to α,β -unsaturated carbonyl molecules. According to this, the transformation of a carbonyl group into an enamine intermediate increases the HOMO of the nucleophile which is used to facilitate its reaction with an electrophile while the iminium activation lowers the LUMO of the electrophile, increasing its susceptibility towards nucleophilic attack. Examples of iminium and enamine activations are shown in Scheme 1.6



Scheme 1.6 Primary amines in iminium and enamine catalysis.

Imine activation describes the reactions promoted by an in situ-generated imine intermediate while enamine activation describes the reactions promoted by an in situ generated enamine, which is a nucleophilic enolate equivalent (Figure 1.6)^{36,37}. These intermediates resulted from the reaction between a carbonyl compound and an amine, which activates an α,β -unsaturated carbonyl compound towards a nucleophilic attack. In enamine activation, cleavage of an α -proton converts an iminium into an enamine, which enhances the nucleophilicity of the original carbonyl compound. Despite the advanced progress witnessed over the past two decades, activation of carbonyl carbon in an excellent enantioselective manner remains a challenging issue.

1.1.4 C₂- and C₃-symmetric Organocatalysts for Asymmetric Synthesis

The C₂- and C₃-symmetric catalysts have become the center of interest in different research due to their importance in asymmetric synthesis. This type of catalyst has the advantage of reducing the number of possible interaction pathways compared to catalysts lacking rotational symmetry.³⁶ In addition, symmetry used to facilitate structure elucidations, mechanistic interpretations, and for studies of dynamic molecular processes.³⁵ Molecules with rotational symmetry have been used as

ligands, catalysts, molecular receptors, gelators, and metal-organic materials.^{39,40,41,42,43,44} In asymmetric synthesis, chiral organocatalysts with the 2-fold or 3-fold symmetry axis usually afford considerable advantages over its nonsymmetric counterpart because the presence of rotational symmetry enhances the chances for activation of the substrate which enhances the reaction rates and improve the selectivities.^{44,45} The performance of these organocatalysts has been evaluated in different types of organic reactions like asymmetric Michael addition reactions⁴⁷; asymmetric aldol reactions,⁴⁶ asymmetric Mannich reactions, and others.

C_2 -symmetry molecules have been widely used in catalysis⁴⁸, and many of the so-called privileged ligands have two-fold symmetry.⁴⁹ The chance to activate substrate with this class of catalyst becomes greater, which results in increasing reaction rates and improving selectivity.⁴⁶ This condition might be particularly appropriate in amino-organocatalyzed reactions due to the long reaction times. There were different new classes of chiral C_2 -symmetric amine/amide developed that performed better in most common organic reactions like Michael addition reactions⁴⁵; asymmetric aldol reactions,⁴⁴ and asymmetric Mannich reactions.

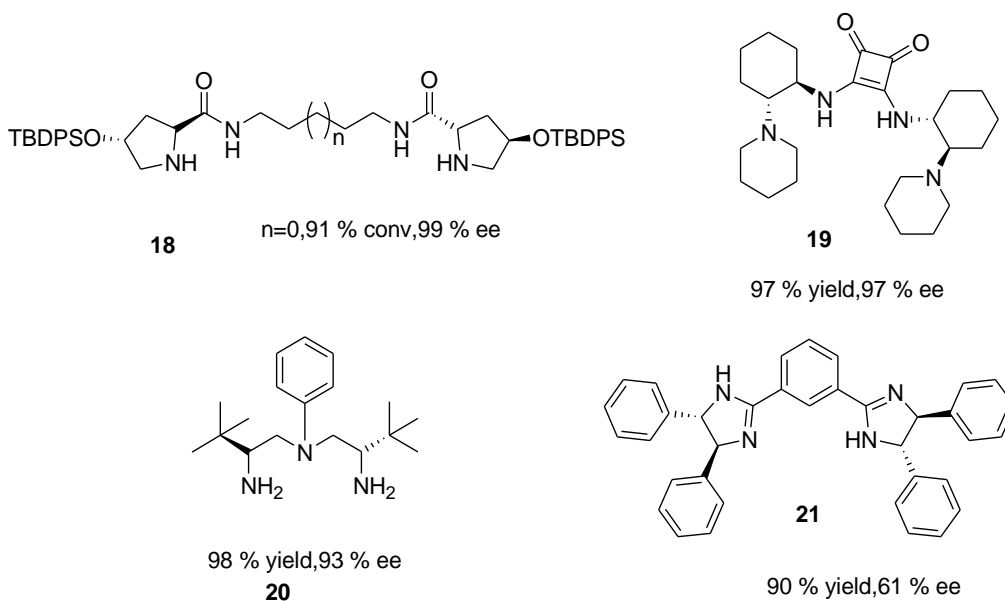


Figure 1.1 Sample of C_2 -Symmetric amine/amide-organocatalysts in asymmetric catalysis

For instance, in 2012, C₂-symmetric organocatalysts composed of two diprolineamide units joined by a symmetric alkyl bridging group provide the best reaction outcomes in asymmetric aldol reaction at low catalyst loading (1 mol%) in terms of conversion (up to >99%) and enantiomeric excess (up to 97% ee).⁵⁰ C₂-symmetric bifunctional tertiary amine-squaramide has been tested for asymmetric Michael reactions and it proved the product with enantioselectivity up to 99% ee in the presence of 1 mol % .⁵¹ Newly designed C₂-symmetric chiral bifunctional triamines has been studied in the aldol reaction of cyclic ketones with isatin, provides enantioenriched compounds up to 98% yield with 93 %ee.⁴⁶

Organocatalysts containing three equal catalytic units might have shown good to excellent performance on enantioselectivity for more powerful reaction approaches in organic synthesis like asymmetric Michael addition ^{49,52} and Friedel–Crafts Reactions.⁵³ For instance, the use of C₃-symmetric chiral tris-imidazoline for enantioselective control in the conjugate addition of α -substituted β -ketoesters to nitroolefins was achieved in 2010 by Hiromichi Fujioka and coworkers⁵⁴ This work briefly shown advantage of using of C₃-symmetric chiral tris-imidazoline when compared with C₂-symmetric chiral bis-imidazoline. These results indicated that at least two imidazolines on the benzene ring were essential for this reaction and the structure of tris-imidazoline **22** was much more effective than that of bis-imidazoline. This study revealed that C₃-symmetric chiral tris-imidazoline organocatalysts had better enantioselectivity (up 89% ee) than bis-imidazoline where a moderate selectivity was obtained (61% ee).

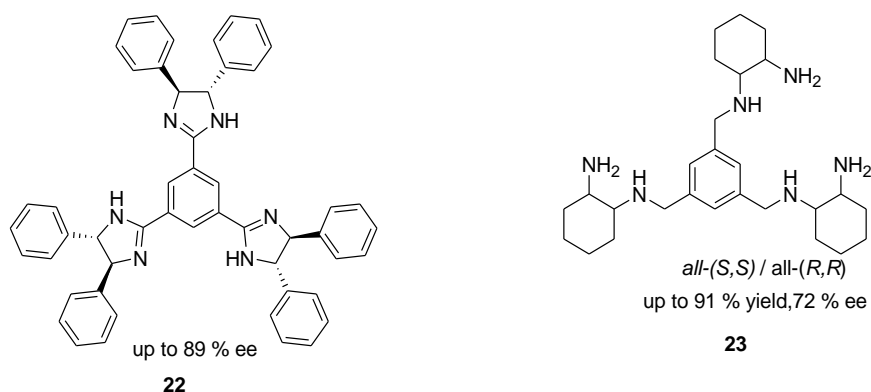


Figure 1.2 Sample of C₃-symmetric amino catalyst for enantioselective reactions.

Four structurally different C₃-symmetric cinchona organocatalysts were prepared, in which the catalytic units are covalently anchored to a trifunctional central core. These catalysts were compared with the parent hydroquinone and results were promising.⁵³ Very recently, in 2024, attractive work on a novel C₃-symmetric multi-amino catalyst that has shown great performance in the synthesis of warfarin and analogues has been reported from Alessia Ciogli's group (**23** in Figure 1.2).⁴⁷

1.1.5 Asymmetric Michael Reactions for the synthesis of warfarin and its analogues.

As mentioned previously, asymmetric organocatalytics have captured great attention and shown dramatic advancement for the past two decades to attain chiral molecules and essential intermediates of pharmaceutical products with green chemistry principles and without purification of the intermediates.⁵⁵⁻⁶⁰ In asymmetric synthesis, we have to develop an appropriate catalytic activation mode to get a valid and effective platform for designing new enantioselective reactions which help us to synthesize enantioenriched molecule.⁶¹ A valid solution for the synthesis of the enantiopure compounds, mainly biologically active, is represented by the use of asymmetric Michael reactions catalyzed by chiral aminocatalyst.^{62,63,64} In this contest, my PhD project aimed the synthesis of symmetric chiral organocatalyst to apply in the production of warfarin and analogues.

Warfarin^{65,66}, chemically known as 4-hydroxy-3-(3-oxo-1-phenyl butyl)-2H-chromen-2-one is an efficient chiral anticoagulant drug for preventing thrombosis and embolism^{69,70}; prescribed as a racemate but the (R)-enantiomer and (S)-enantiomer demonstrated different activity and metabolism.⁷¹ Warfarin is known for its excellent potency and good pharmacokinetic profile. According to the report released by the Royal Flying Doctoral Service from State of Queensland health sector in 2024, warfarin remains the treatment of choice for more health problems like kidney impairment, heart valve replacements, left ventricular thrombus, or antiphospholipid syndrome, valvular atrial fibrillation and a high risk of stroke or systemic embolism.⁷²

Isolation or synthesis of optically pure R or S enantiomer of warfarin would be of great importance because (S)-warfarin had higher anticoagulant activity than the R enantiomer.^{73,74} Michael addition

of 4-hydroxycoumarin with benzal acetone in presence of catalysts is a well-known reaction approach to synthesis this clinically active molecule.⁷⁵ The applicability of chiral amine catalysts for asymmetric synthesis of warfarin with higher activation ability and excellent levels of efficiency have been demonstrated by many researchers (Figure 1.3).^{46,75,76} For the first time, organocatalytic asymmetric Michael addition was used in warfarin synthesis in the presence of chiral imidazolidine catalysts.⁷⁶ In this work, Jørgensen and coworkers obtained enantioenriched warfarin by a single recrystallization. Next, a proline-based chiral amide catalyst was used by Feng and coworkers.⁷⁵ In Michael additions of coumarins to benzalacetone, primary amine-organocatalysts were recognized well.^{78,79} In 2018, Mlynarski and Zlotin showed the synthesis of warfarin in water using (*S,S*)-diphenyl ethylenediamine.^{80,82} In 2018, Sergei G. Zlotin and coworkers showed the performance of C₂-symmetric trans-1,2-diamines **12**, which provides the desired warfarin with good enantioselectivity (90 % ee).⁸²

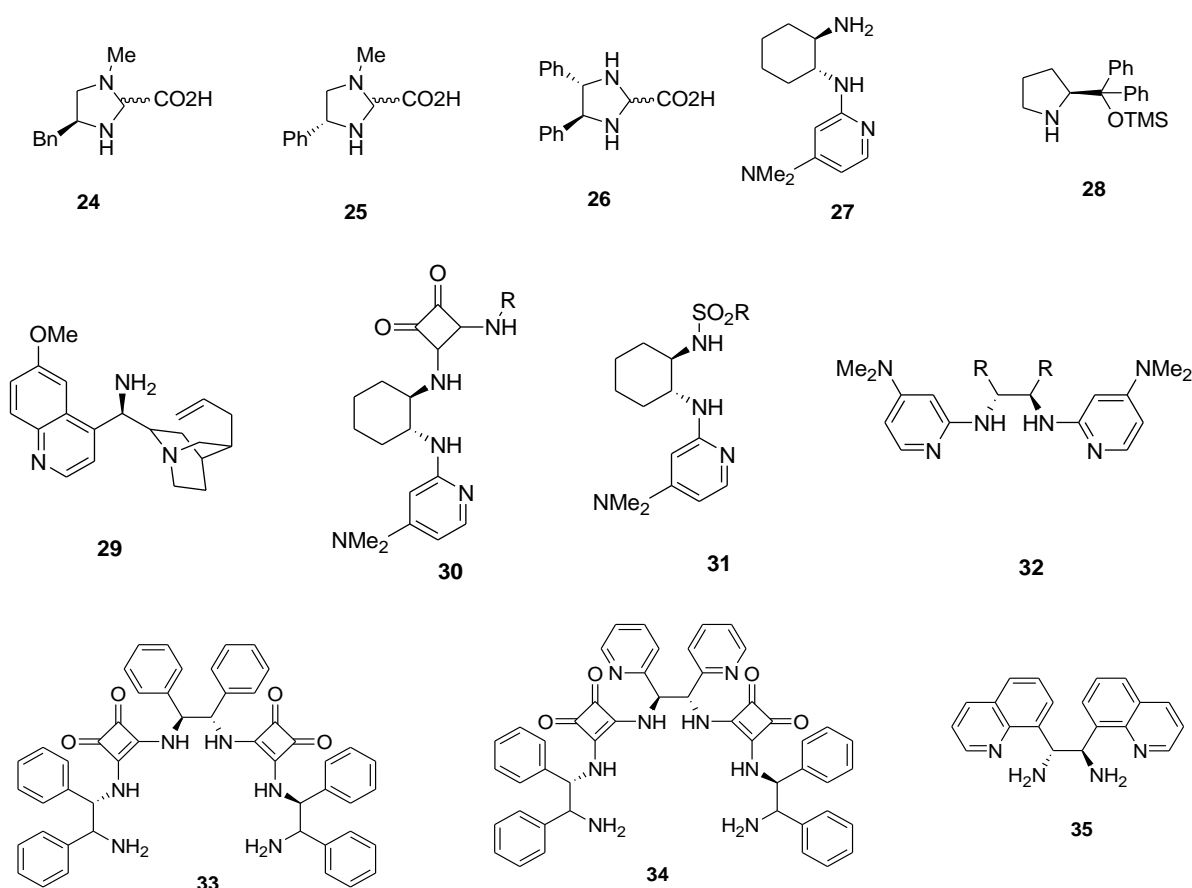
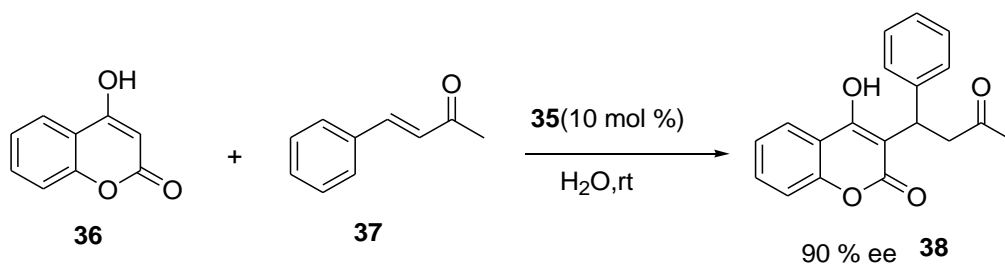


Figure 1.3: Example of amino-organocatalysts used in asymmetric warfarin synthesis.

In our group, Michael reaction between 4-hydroxycoumarin with benzylideneacetone catalyzed by 1,2-trans-diamino cyclohexane (DACH) based C₃-symmetric primary amine was chosen to be model reactions for warfarin synthesis in THF, and this C₃-symmetric catalyst furnished good results. For the same model reactions, Sergei G. Zlotin and coworkers found that 10 mol% of C₂-Symmetric-1,2-diamines **12** was the most useful catalyst.⁸²



Scheme 1.7 Warfarin synthesis with C₂-symmetric-1,2-diamines **35**.

The C₃-symmetric primary amine-mediated imine mechanism was illustrated by our group in a previously reported paper by ESI-MS offline experiment and DFT calculation.⁴⁷ The benzylideneacetone reacts with the C₃-symmetric amine, affording an imine, which consequently adds to the 4-hydroxycoumarin to obtain the enantiomerically enriched product. The ESI-MS investigation demonstrated that two aminic sites of catalyst work separately and a bis-imine intermediate was generated. In addition, the computational outcomes confirmed that the primary amine function of the catalyst can express a much more effective nucleophilic attack to the carbonyl of the benzylideneacetone compared to the secondary amine moiety. Calculations also suggested that once the carbinolamine is synthesized (generated as an intermediate species before it evolved into the expected imine structure), it can be easily involved (with a very low activation barrier, estimated to be about 12 kcal) in the formation of the C-C bond with coumarin, in concerted way with the breaking of the carbinolamine N-C bond, so resulting in the release of a warfarin tautomer and the regeneration of catalyst.

Despite the advances of organocatalysts, application in synthesis of enantioenriched warfarin and its analogues still a significant synthetic challenge remained. We know that the synthesis of new and efficient catalysts needs more time which consumed during applying trial-and-error protocols. Therefore, it is still necessary to develop environmentally and economically advantageous organocatalysts to synthesize this anticoagulant in high yield and enantiopure. In this PhD project, we developed symmetric amido (C-1, C-2, C-3, C-4) and C₃-symmetric amino-organocatalysts (C-

5) (figure 1.4) to synthesize warfarin and its analogues. To the best of our knowledge, the application of C_3 -symmetric amino-organocatalysts in the asymmetric synthesis of warfarin and its analogues has been studied less than the use of C_2 -symmetric catalysts. In this project, we have evaluated the 1,2-diphenyl ethylenediamine (DPEDA) as a scaffold for the novel C_3 -symmetric catalyst, where the core was the 1,3,5-benzenetricarbonyl trichloride. The resulting structures have a combination of i) primary and secondary amines or ii) primary amine and amide. In addition, we synthesized three different C_2 -symmetric organocatalysts introducing the pyridine-2,6-dicarbonyl dichloride as the connector of DPEDA or 1,2-diamino cyclohexane and amino phenyl diethylamine. All C_2 -symmetric structures possess amine and amide moieties. Once prepared, the five organocatalysts were tested in the formation of warfarin and in a small library of analogues using 4-hydroxycoumarin and 4-hydroxyquinoline. The following sections show the obtained results and conclusions; at the end, the reader can find all experimental details and data.

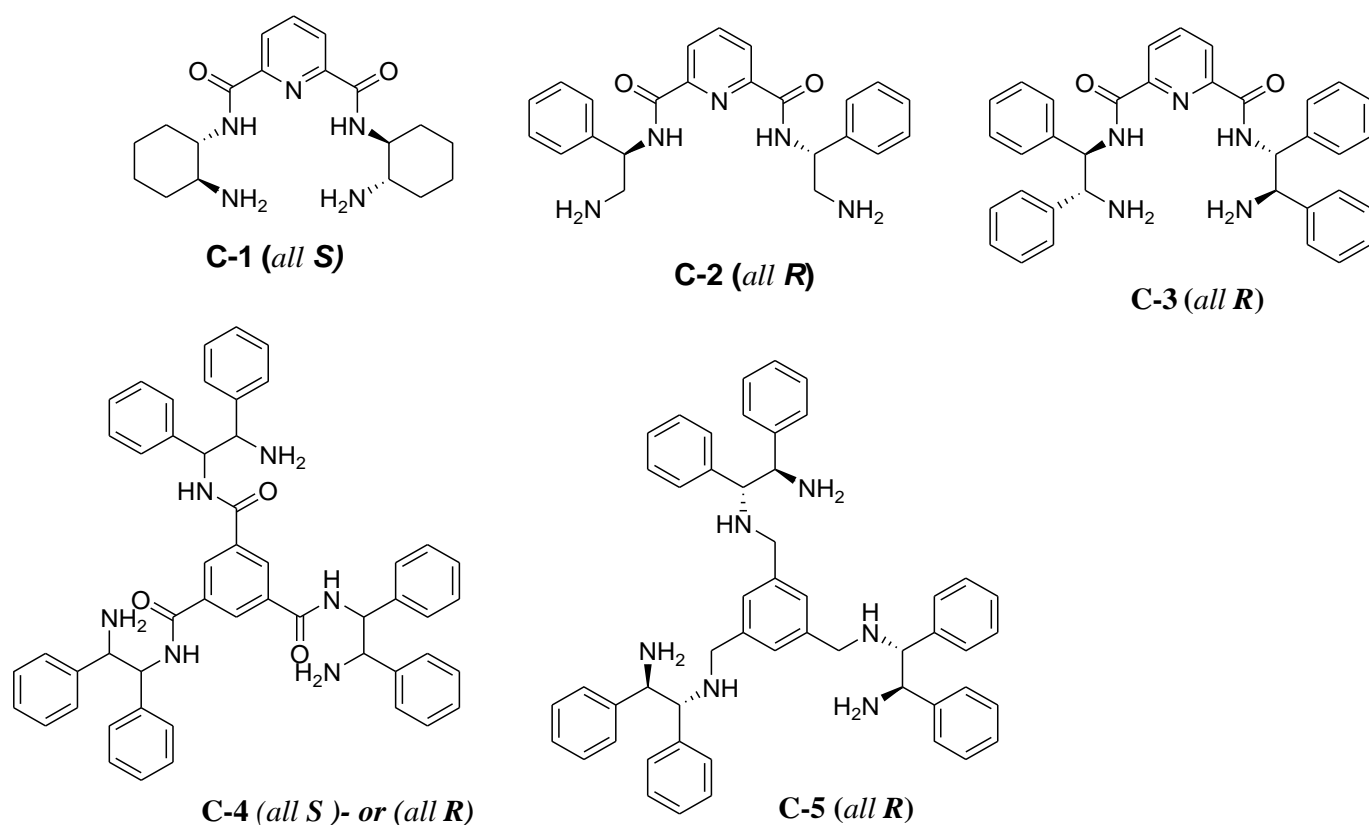


Figure-1.4 Developed Chiral symmetric organocatalysts for synthesis of enantioenriched warfarin and its analogues

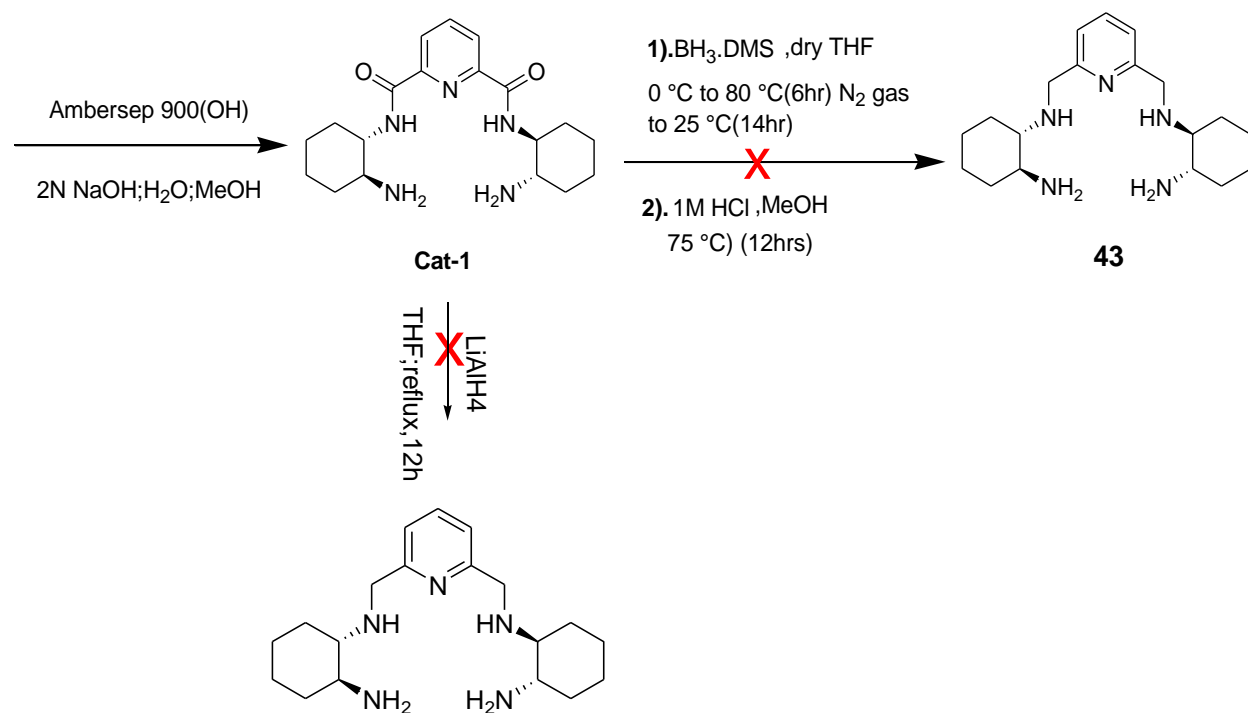
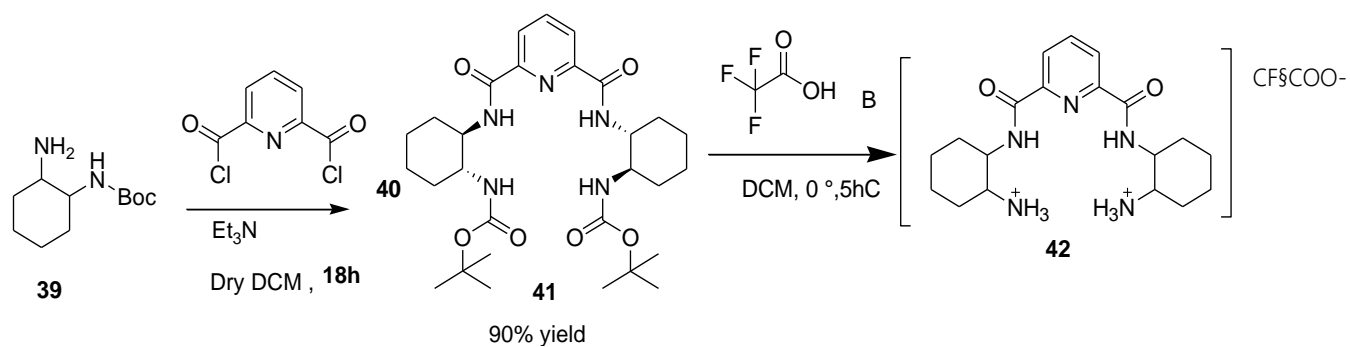
C₂-symmetric amide-catalyzed Michael addition reaction of α,β -unsaturated ketone with 4-hydroxycoumarin at room temperature using only 5 mol % and 10 mol %, resulting in the formation of warfarin in moderate to good yields with moderate enantioselectivity (table 2). While the C₃-symmetric amide formed by installation of 1,3,5-benzenetricarbonyl trichloride onto a (2-Amino-1,2-diphenyl-ethyl)-carbamic acid tert-butyl ester performed less both by yield and enantioselectivity than the pyridine based C₂-symmetric amide (table 3). Installation of a spacer contain a more basic nature in C₂-symmetric amido-organocatalysis was employed as a new valuable player to this imine catalysis. Our next hypothesis was that the reduction of pyridine-based C₂-symmetric amide to amine increased its catalytic performance to the same this type of reaction, however, with this concept, we didn't succeed due to the unfit reduction protocol with this pyridine-based C₂-Symetric amide.

As we have observed in our previous work, C₃-symmetric amide showed low performance in enantioselectivity than C₃-symmetric amine. One possible reason may be the weak basicity nature of the amides when we compare with amine. We hypothesized that by introducing spacer containing hetero atom like nitrogen may increase the catalyzing performance of amide by increasing the basicity nature of the catalysts. we expected that increasing the basicity nature of our catalyst to positively influence the yield and enantioselectivity of warfarin and warfarin analogues.

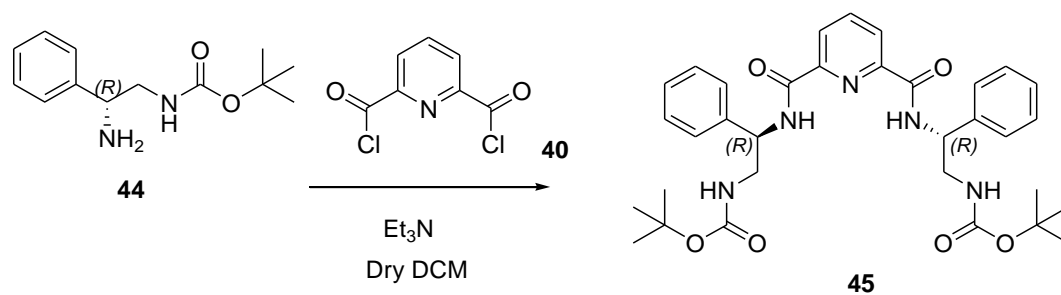
1.2. Results and discussion

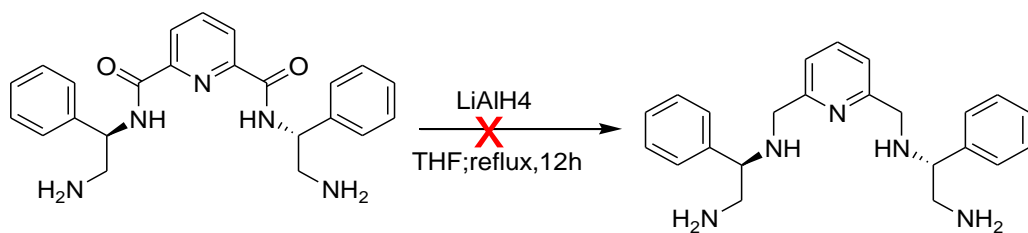
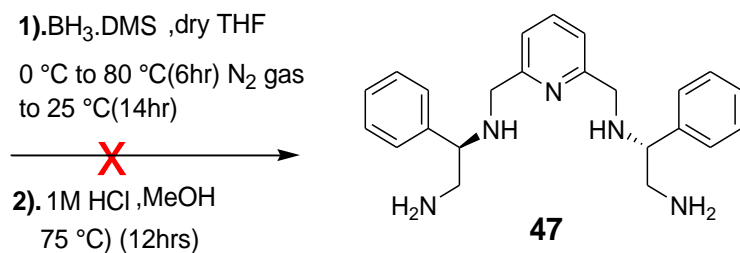
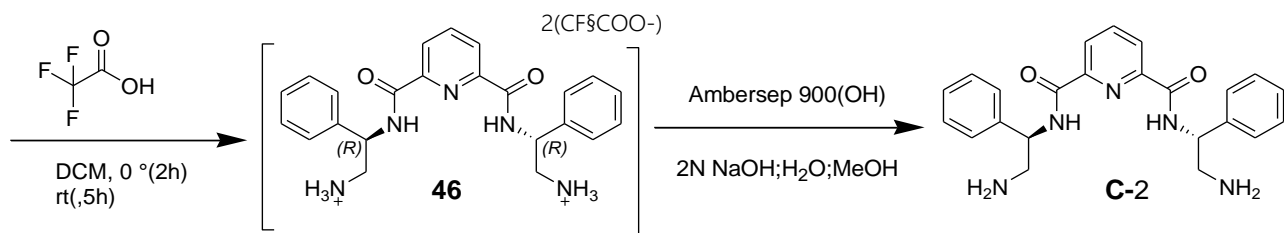
1.2.1. Synthesis of C₂-Symmetric amide Organocatalysts *Pyridine-2,6-dicarboxylic acid bis-[(2-amino-cyclohexyl)-amide] C-1(all S)*, *Pyridine-2,6-dicarboxylic acid bis-[(2-amino-1-phenyl-ethyl)-amide]C-2(all R)* and *Pyridine-2,6-dicarboxylic acid bis-[(2-amino-1,2-diphenyl-ethyl)-amide] C-3 (all R)*

C₂-symmetric chiral amido-catalysts C-1, C-2, and C-3 were synthesized in quantitative yield by reaction of commercially available chiral diamine **39,44,48** with spacer **40** respectively. During the preparation of C₂-symmetric chiral amido-catalysts, reactions were carried out in dry dichloromethane in the presence of Et₃N and completed after 18 hours by stirring at room temperature (**Scheme 1.8,1.9,1.10**). In well-dried flask equipped with a stir bar, compound (1S,2S)-N-Boc-1,2-cyclohexanediamine (**39**) was stirred with one equivalence of spacer pyridine-2,6-dicarbonyl dichloride (**40**) in presence of triethyl amine in dry DCM provided 90% yield; followed by its deprotection by TFA in DCM afford 99% yield. Deprotection of compound **41** was carried out by stirring it at 0 °C for 5 hours with TFA in DCM to get non-neutral compound (**42**). The solution of **42** in methanol was passed through activated ambersep 900-OH that provided catalysts C-1. After evaporating on the vacuum and dried well on high vacuum, 99% of the product was recovered. C₂-symmetric chiral amido-catalysts (C-2 and C-3) were prepared following the same procedures of C-1 provide 98% and 96% yield respectively. The reduction of these chiral amido-catalysts (C-1, C-2, and C-2) with BH₃·SMe₂ in dry THF failed to give the corresponding amine (43,47 and 51). Fortunately, this reduction couldn't be carried out with the use of Lithium aluminum hydride in dry THF followed with the addition of an NaOH solution. This was surprising, given that C₃-symmetric amido-organocatalytic was reduced to a corresponding amine with BH₃·SMe₂ in dry THF under similar reaction conditions.

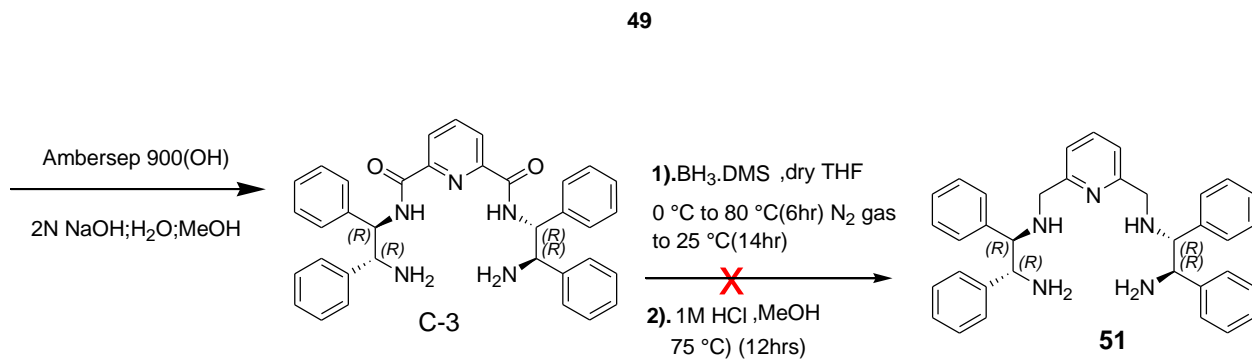
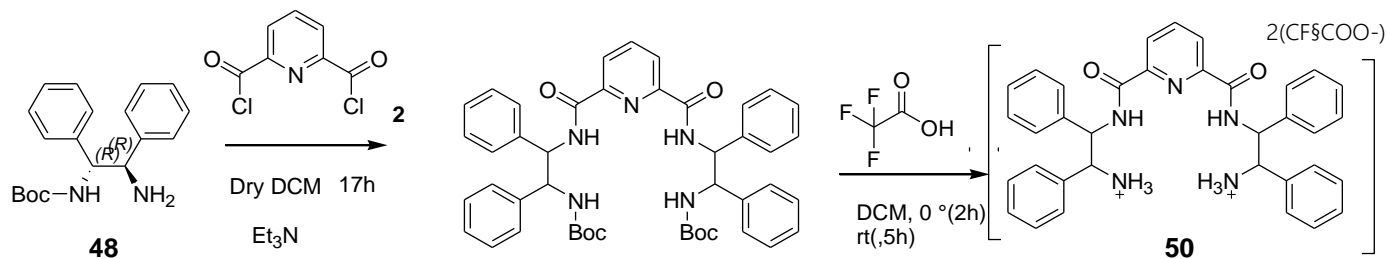


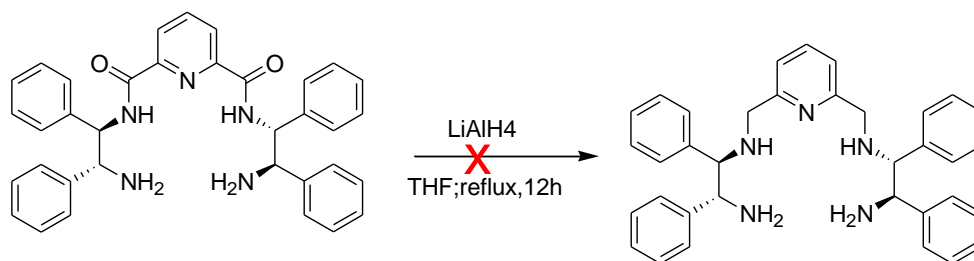
Scheme-1.8 Synthesis of **C-1** catalyst.





Scheme-1.9 Synthesis of **C-2** catalyst.

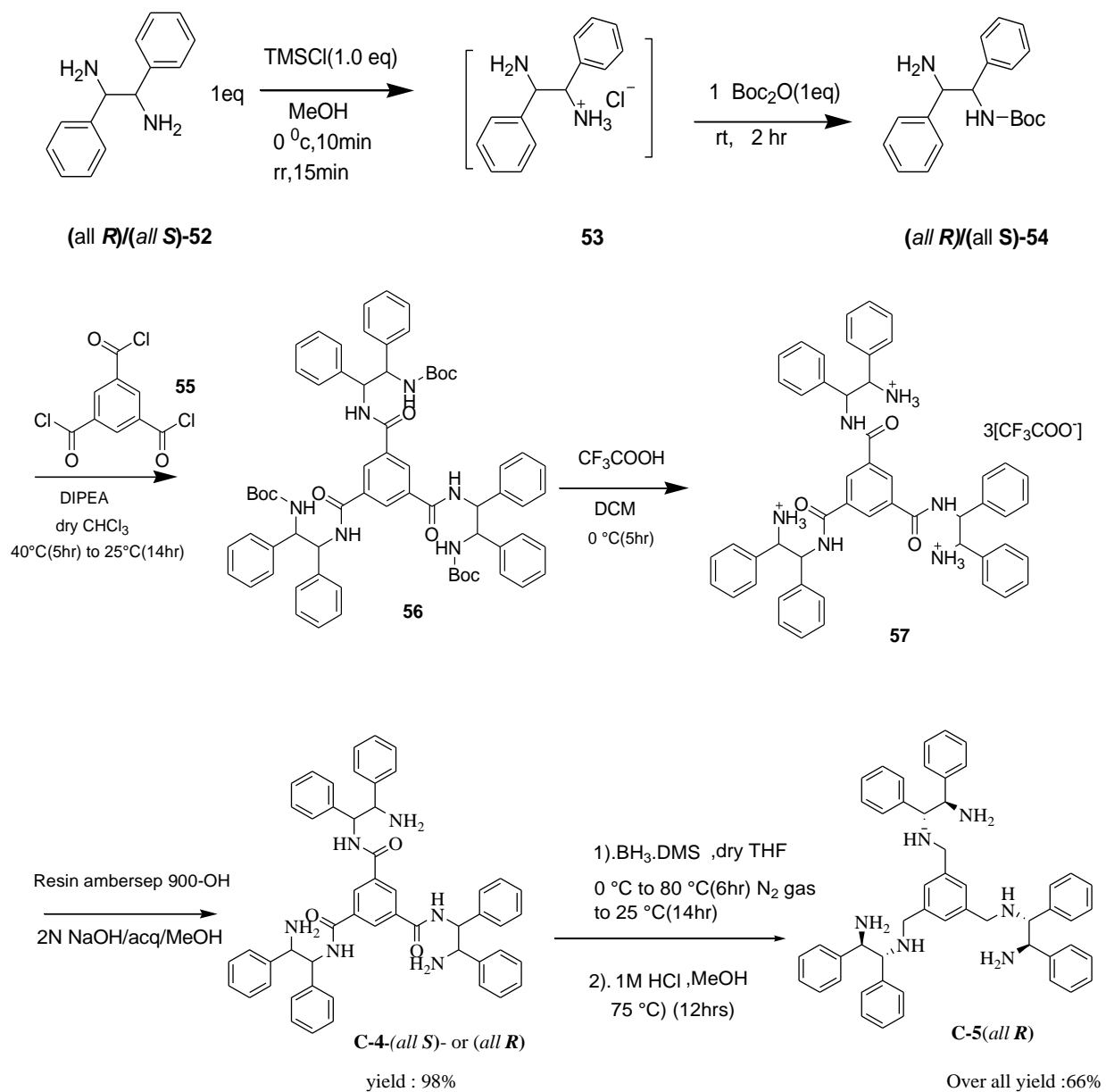




Scheme-1.10 Synthesis of C-3 catalyst.

1.2.2. Synthesis of C₃-Symmetric Organocatalysts *benzene-1,3,5-tricarboxylic acid tris-[(2-amino-1,2-diphenyl-ethyl)-amide] C-4 (all R)/(all S) and N-{3,5-bis-[(2-amino-1,2-diphenyl-ethylamino)-methyl]-benzyl}-1,2-diphenyl-ethane-1,2-diamine C-5 (all R)*

To synthesize C₃-symmetric organocatalysts (C-4 and C-5), we used di-*tert*-butyl dicarbonate as protecting group⁶⁴. In 2012, Alexander S. Kucherenko and his coworkers used benzyl chloroformate as Cbz-C-1 to protect the amine functional group of this diamine, however, the corresponding product (**54**) obtained in moderate yield (61%); but in 2018, when, Sergei G. Zlotin and co-workers used N-Boc, the yield was dramatically increased to 86%⁶⁸. By following the second protocol, anhydrous solutions of hydrochloric acid were formed in alcohol with trimethylsilyl chloride resulted in mild synthesis of protected compound⁶⁸. The construction proceeded with the formation of a minor side product known as (2-*tert*-Butoxycarbonylamino-1,2-diphenyl-ethyl)-carbamic acid *tert*-butyl ester. Intending to improve the yield, we decided to extend the time for dropwise Boc₂O solution at constant concentration (see table-1.1). The mono-protected diamine **54** could be obtained in excellent yield when the time of drop of Boc₂O solution was performed at prolonged minutes. As the time of the dropwise of Boc₂O solution increased, the yield of this competent product (side product) was decreased, in an opposite way, the yield of product **54** was increased from **65%** (10min) to **87%** (30min). The pale-yellow mono-protected diamine **54** was successfully separated from the untargeted product by column chromatography on silica gel and afforded a reasonable yield (**87%**) (see supportive material). The structure of the product **54** and the undesired product were characterized by both NMR and mass spectra. The optical rotation was recorded for product **54** in chloroform at wavelength 589 nm and reported as: $[\alpha]_D^{27.90} = +29.15$ (c=0.5, CHCl₃) where temperature = 27.90 °C.



Scheme-1.11 Synthesis of **C-4** (*all R*)/(*all S*) and **C-5** (*all R*) catalysts.

Table:1.1 Optimization of the time for addition of Boc₂O solution

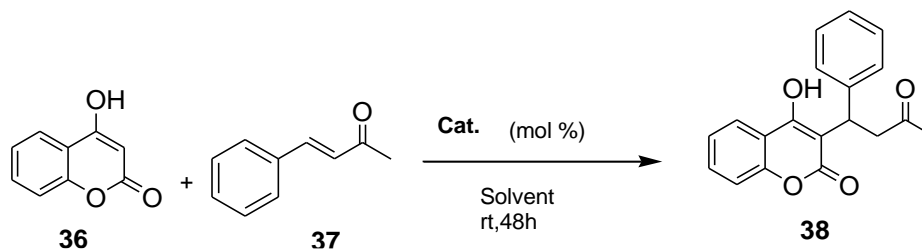
Entry ^[a]	Time (Min) ^[b]	Yield (%) ^[c]
1	10	65
2	15	77
3	30	87

^[a] the reactions were performed with TMSCl (1 equivalent), **52**-diamine (1 equivalent) and Boc₂O (1 equivalent), MeOH, rt ^[b] time needed for the dropwise of Boc₂O solution. ^[c] Yield of the mono-protected chiral 1,2-diamines **54** isolated after silica gel column chromatography.

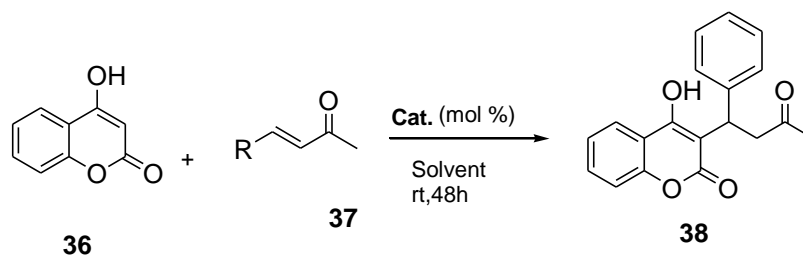
With a protocol for addition reaction in our hand from our previous reported work ^[27], we proceeded addition of (2-amino-1,2-diphenyl-ethyl)-carbamic acid tert-butyl ester **3** with 1,3,5-benzenetricarbonyl trichloride in presence of N-ethyl-diisopropylamine afforded 82 % of product **56**. The installation of compound **54** with the spacer **55** was accomplished in smooth way without any side product. The deprotection reaction using TFA in DCM resulted in the preparation of C3-symmetric C4-(*all S*) in excellent yield (98%) after passing through basic resin (Ambersep 900-OH) (see experimental section). The C-4 (*all S*) or (*all R*) was reduced with BH₃·SMe₂ in dry THF, and then in methanol in the presence of 1M HCl. To get amino-catalyst C-5 (*all R*), the concentrated crude was passed through resin (ambersep900-OH) and dried for 20h at 80 °C that afforded overall yield of 67%.

1.2.3 Synthesis of warfarin

In the preliminary evaluation of efficacy of catalysts, we checked all catalysts in the synthesis of warfarin with standard conditions of **36** (0.2mmol), **37**(0.24mmol), catalysts (mol %), THF (2mL) for 48hrs at room temperature.

Table 1.2 Optimization of solvent and C₂-symmetric catalysts loading

Entry	Solvent	Catalyst	Mol%	Yield (%)	e.r (%)
1	THF	C-1	5	61	31/69
2	THF	C-2	5	58	64/36
3	THF	C-3	5	65	70/30
4	THF	C-1	10	68	31/69
5	THF	C-2	10	62	69/31
6	THF	C-3	10	74	47/53
7	Toluene	C-1	5	58	44/56
8	Toluene	C-2	5	52	63/37
9	Toluene	C-3	5	49	74/26

Table 1.3 Optimization of C₃-symmetric catalysts loading

Entry ^[a]	R	Solvent	Cat.	(Mol %)	Yield (%) ^[b]	e.r(%) ^[c]
1	C ₆ H ₅ -	THF	C-5(<i>all R</i>)	2	62	74/26
2	4-ClC ₆ H ₄ -	THF	C-5(<i>all R</i>)	2	70	70/30
3	C ₆ H ₅ -	THF	C-4(<i>all R</i>)	2	30	61/39
4	C ₆ H ₅ -	THF	C-4(<i>all S</i>)	2	33	40/60
5	4-ClC ₆ H ₄ -	THF	C-4(<i>all R</i>)	2	43	64/36
6	4-ClC ₆ H ₄ -	THF	C-4(<i>all S</i>)	2	40	37/63
7	C ₆ H ₅ -	THF	C-5(<i>all R</i>)	5	87	78/22
8	C ₆ H ₅ -	THF	C-5(<i>all R</i>)	5	95	76/24

^[a]The reactions were performed with **36** (0.2mmol), **37**(0.24mmol), catalysts (2 mol %), THF (2mL) at room temperature, time (48hrs) ^[b] Yield of the isolated product after silica gel column chromatography ^[c] Determined by chiral HPLC analysis.

Initially, we have started to investigate catalyst activity with 2 mol % of catalyst. For this purpose, we examined the reaction between 4-hydroxy-chromen-2-one **36** with Michael acceptors **37**. This preliminary examination was carried out in THF at room temperature in the presence of 1 equiv of Michael acceptors **37** (Table 1.3). With this loading, amino-organocatalyst C-5(*all R*) could catalyze the reaction that afforded the desired product **38** (table 1.3, entry1) with a moderate yield 62% and good enantiomeric ratio (74/26), The activity of catalyst C-5 (*all R*) was further investigated at the same loading for the synthesis of warfarin analog **38** (table 1.3, entry 2) provided 70% yield with 70/30 enantiomeric ratio. In our attempt with the same substrate, catalysts C-4(*all S*) provided the product **38** in 40% yield with the moderate enantiomeric ratio of 37/63 (table 3, entry 6). This result may indicate the leading role of C-4(*all R*)/(*all S*) in both yield and stereocontrol would be a structural factor. In chiral C3-symmetric amide, -N-H---O bonds formation may determine the partial deactivation of the catalyst (figure 1.5). This initial

investigation revealed that amino catalyst **C-5** showed good performance that furnished product **38** within 48h reaction time. To decide the loading for the scope of the reaction, we increased catalysts **C-5**(*all R*) from 2 mol % to 5 mol %. With these reaction conditions, the desired Michael product **38** was increased to 87 % yield with 78/22 e.r (table 1.3, entry 7). The last attempt for this round was performed between 4-hydroxy-chromen-2-one **36** and 4-(4-chloro-phenyl)-but-3-en-2-one **37c** with 5mol % of **C-5** (*all R*) that provided 95 % of yield with good enantiomeric ratio (76/24). By keeping the reaction time and temperature constant, an increase of catalyst loading from 2 mol % to 5 mol % resulted in an enhanced yield and superior enantiomeric ratio. We found that high yield and good enantioselectivity could be achieved by **C-5**(*all-R*) (5%) for the synthesis of warfarin analogs.

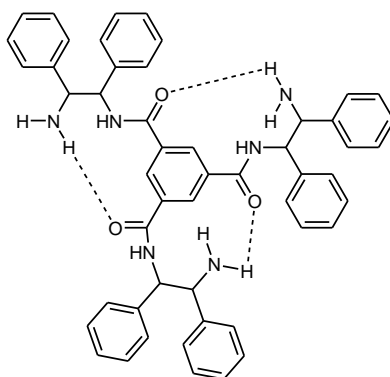


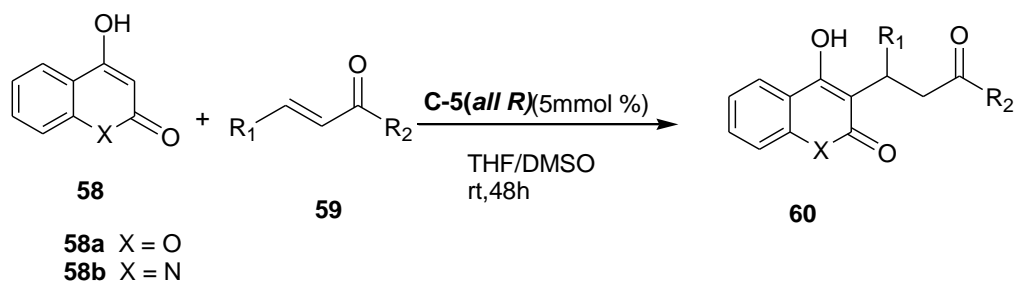
Figure 1.5. Plausible N-H-O bonds formation which determine the partial deactivation of catalyst **C-4**

1.2.4 Scope of the reactions

The scope of the warfarin analogs synthesis was investigated by **C-5**(*all R*)(5% mol) in THF or DMSO at room temperature. Different α,β -unsaturated ketones **59** were employed with two different cyclic Michael donors (nucleophiles) **58** to synthesis the expected Michael products **60**. Based on our previously reported work⁴⁵, DMSO was used as a solvent for the reactions performed with 4-hydroxy-1H-quinolin-2-one. Confirmed that the reaction of nucleophile **58** with electrophile **59** does proceed well in the presence of **C-5**(*all R*)(5% mol). The corresponding products **60a-i** were obtained from low to excellent yields with good enantioselectivities.

Consistently high yield and good enantioselectivity were achieved with 4-hydroxy-chromen-2-one **58a** (table 1.4) except for product **60i**. When using 4-hydroxy-1H-quinolin-2-one **8b** instead of 4-hydroxy-chromen-2-one **58a**, the reaction also worked to give the product from good to low yields. This revealed that the type of heteroatom (oxygen/ nitrogen) in the Michael donors **58** has influenced the yield of each warfarin analogues. The C₃-symmetric amino-catalyst **C-5**(*all R*) performed well for most of the tested substrates, however, the reaction between **58b** and **59i** did not afford the product. The reason for the lack of performance of catalysis for this reaction (**58b** with **59i**) is under investigation. The R₁ and R₂ phenyl substituted Michael acceptor **59** provided the lowest yield and enantioselectivity when reacting with Michael donor **58b**, compared to the reaction with **58a** (table 1.4, entries 7-8). This compound has been synthesized and enantiomerically separated by this work for the first time. In addition, the newly synthesized **25i** having cyanide substituent was the second lowest yield, however, the HPLC conditions are not optimized for enantiomeric separation. In this scope of reactions, the highest yield (95%) (table 1.3, entry 3) and best enantiomeric ratio (80/20) (table 1.3, entry 5) was attained in THF in the presence of 5mol % of the multifunctional **C-5**(*all R*).

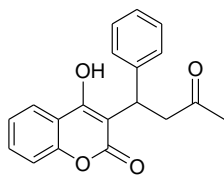
Table 1.4 **C-5**(*all R*) Catalyzed reactions between 4-hydroxycoumarin/4-hydroxy-1H-quinolin-2-one and α , β -unsaturated ketone



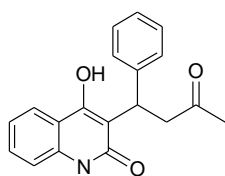
^[a]The reactions were performed with **58**(0.2mmol), **59** (0.24mmol), catalysts (5 mol %), and

Ent ^[a]	R1	R2	X	Solvent	Yield (%) ^[b]	e.r.(%) ^[c]
1	C ₆ H ₅ -	CH ₃	O	THF	87	78/22
2	C ₆ H ₅ -	-CH ₃	N	DMSO	52	77/23
3	4-ClC ₆ H ₄	CH ₃	O	THF	95	78/22
4	4-ClC ₆ H ₄	-CH ₃	N	DMSO	56	76/24
5	-CH ₃	CH ₃	O	THF	54	80/20
6	-CH ₃	CH ₃	N	DMSO	25	68/32
7	C ₆ H ₅ -	C ₆ H ₅ -	O	THF	19	75/25
8	C ₆ H ₅ -	C ₆ H ₅ -	N	DMSO	8	55/45
9	CNC ₆ H ₄ -	C ₄ H ₉	O	THF	21	----

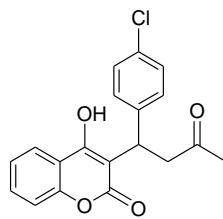
solvent (2mL), at room temperature, time(48hrs) ^[b] Yield of the isolated product after silica gel column Chromatography ^[c] Determined by HPLC



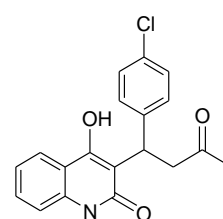
60a
Yield 87 %
e.r : 77/23



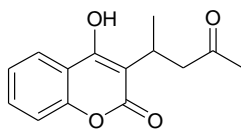
60b
Yield 52%
e.r.78/22



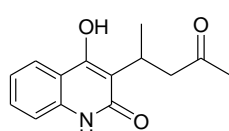
60c
Yield 95%
e.r.78/22



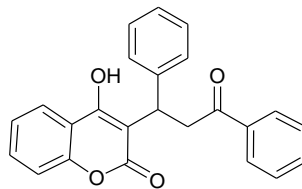
60d
Yield 56 %
e.r. 76/24



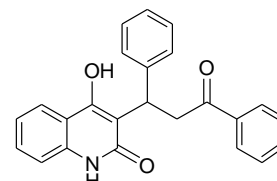
60e
Yield 53 %
e.r. 80/20



60f
Yield 25%
e.r. : 68/32



60g
Yield 6%
e.r. . 73/27



60h
Yield :8 %
e.r. : 55/45

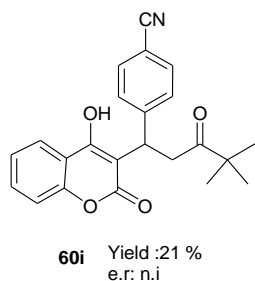
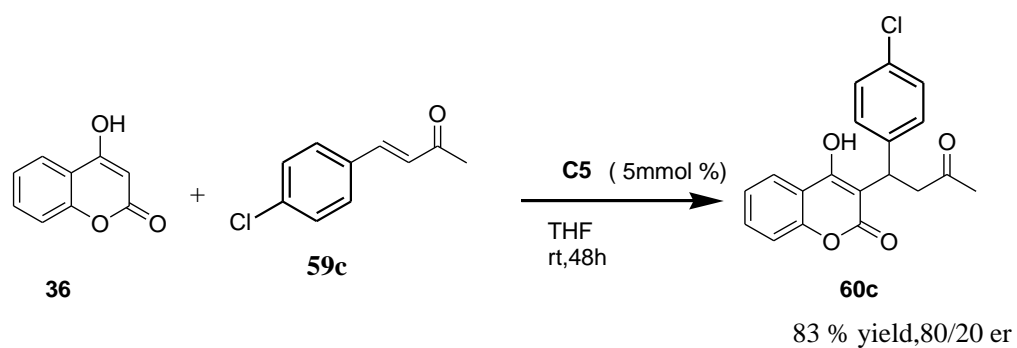


Figure 1.6- Structures of obtained compounds from scope of reactions

In summary, this work revealed that the yield has been influenced by the type of heteroatoms (oxygen and nitrogen) of Michael donors **58**, the structure of Michael acceptors **59**, and catalyst loading.

1.2.5 Scale-up of synthesis of the active compound **60c**

To verify our procedure, we performed scale-up synthesis using 4-hydroxy-chromen-2-one **58a** (1g, 6.20mmol) and 4-(4-Chloro-phenyl)-but-3-en-2-one **59c** (1.34g, 7.44 mmol) under the same standard reaction conditions. To our delight, product **60c**, a rodenticide, was generated in high yield with a good enantiomeric ratio (80/20) (Scheme 1.12).



Scheme 1.12 Scale-up synthesis of product **60c**

1.2.5 ESI-MS offline reaction monitoring: identification of active intermediates

Finally, to confirm the catalytic activity of multiple amine units for **C-5**(*all R*), we performed off-column ESI-MS studies. By flow-injection of the reaction mixture, we identify the more relevant intermediates. The reaction consists formation of a covalent bond between Michael acceptor and multifunctional aminocatalyst **C-5**(*all R*), followed by nucleophile addition of **58** via imine activation. As we observed, the three expected imine intermediates of the catalytic cycle are observed in reasonable abundance (Figure 1.7).

Here the high-resolution ESI-MS spectra acquired between the catalyst and ketone (Figure 1.7). m/z 913.4737 for $C_{61}H_{62}Cl_1N_6$, m/z 1075.4979 for $C_{71}H_{69}Cl_2N_5$ and m/z 1237.5222 for $C_{81}H_{76}Cl_3N_6$ are the mono- bis- and tris-imine intermediates respectively. As indicated from the mass spectrum of the reaction mixture after 22h (figure 1.8), the signal corresponding to the mono-imine species was observable and exhibited the highest intensity while the signal corresponding to the tris-imine species exhibited the lowest intensity. The high-resolution mass spectra attest to the agreement with the proposed reaction mechanism.

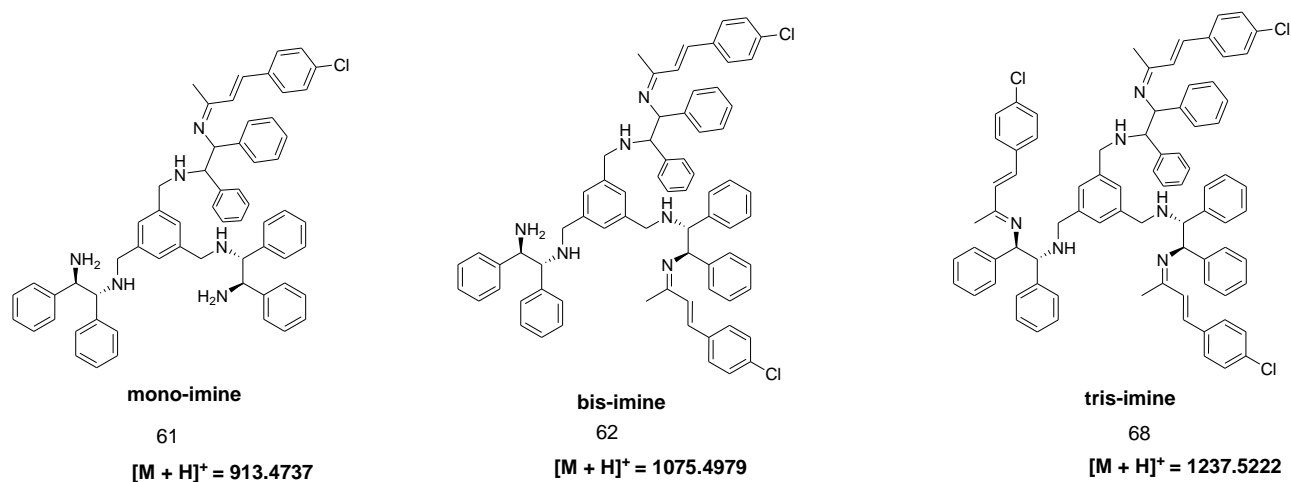


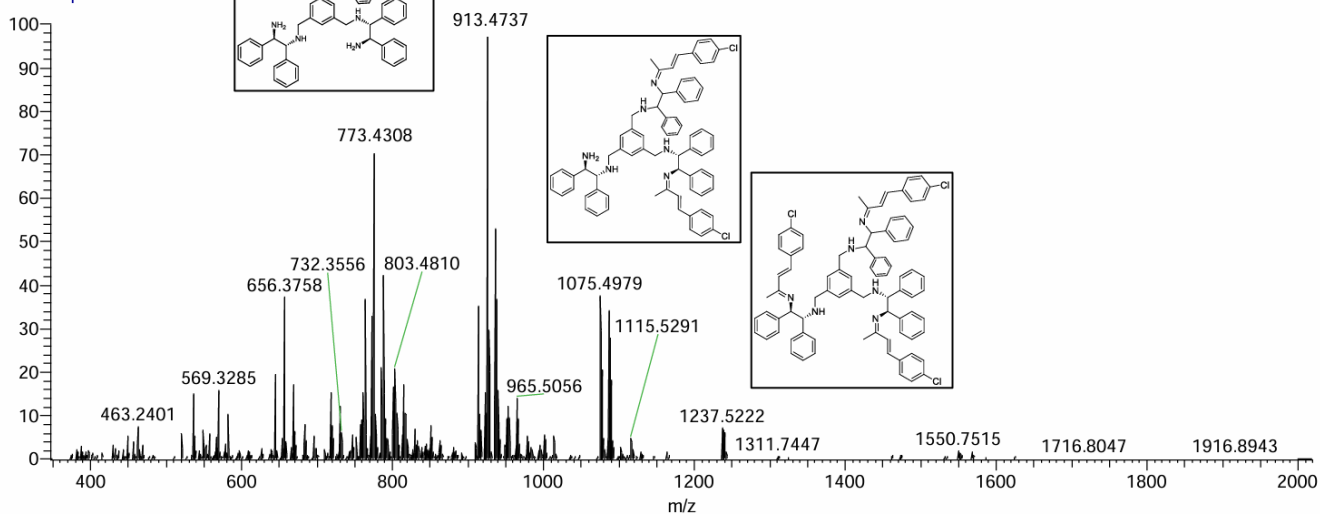
Figure: 1.7 Mono- bis- and tris-imine intermediate

REACTION2_ 2h_Alessia_1604

05/17/24 09:09:25

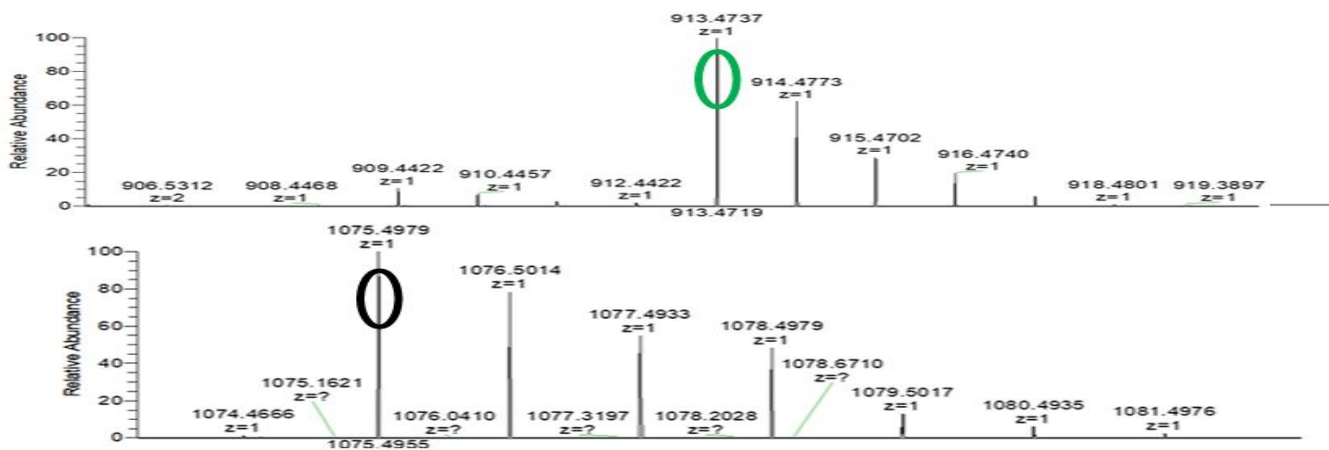
REACTION2_ 2h_Alessia_160
T: FTMS + p NSI Full ms2 1000.

1 NL: 3.74E4



REACTION2_22h_Alessia_16042024_hcd150-2

05/17/24 09:09:25



REACTION2_22h_Alessia_16042024_hcd150-2

05/17/24 09:09:25

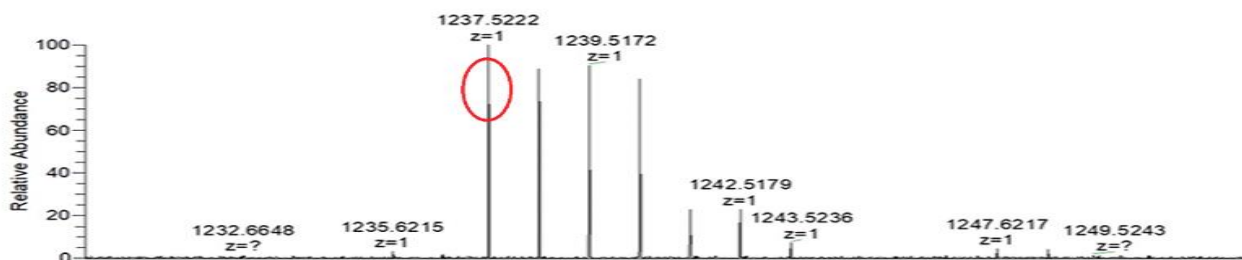


Figure 1.8 HR-MS spectrum of reaction mixture after 22h using catalyst C-5 (*all-R*): zooms in the region of active species. (see experimental section for additional information)

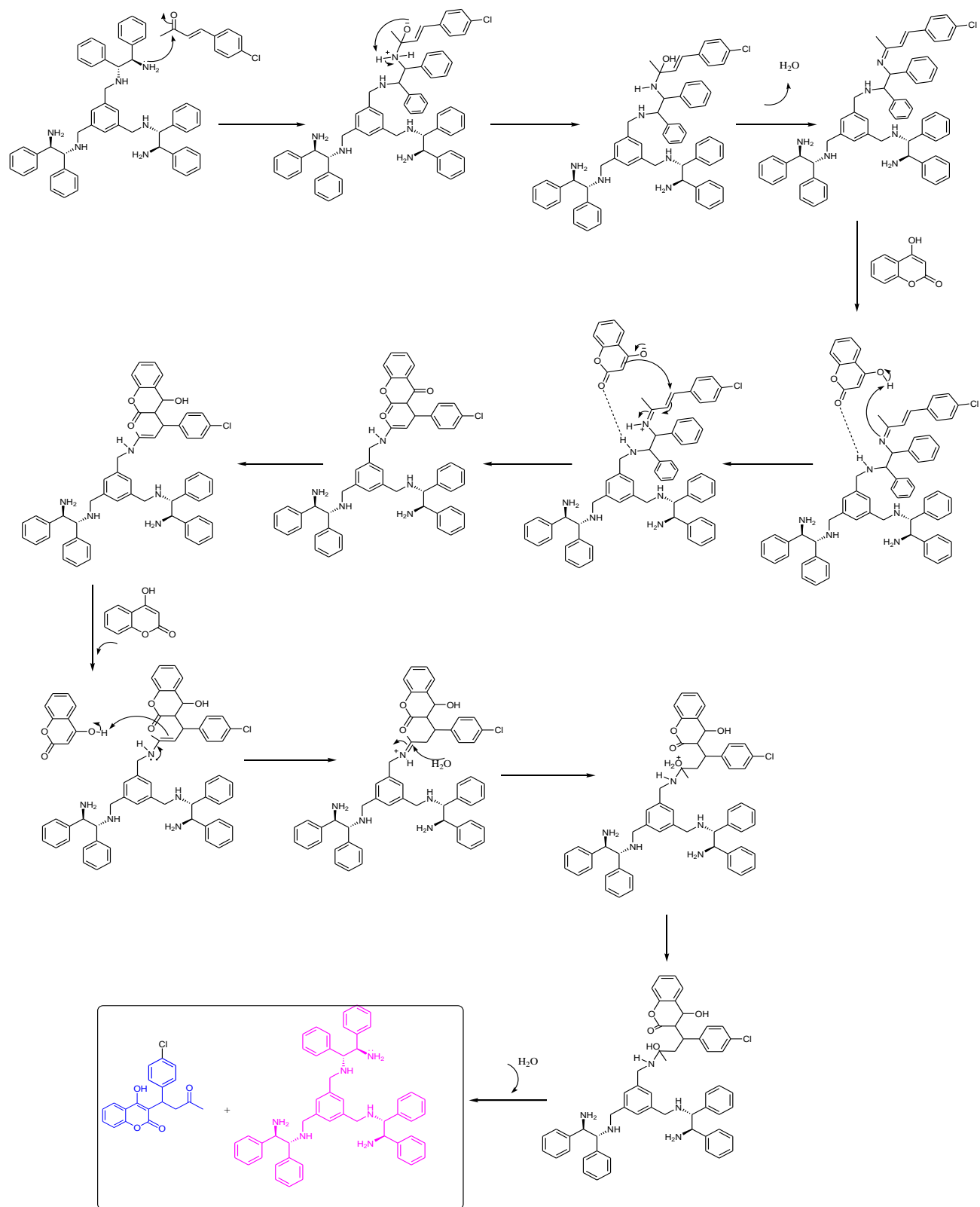


Figure 1.9. Proposed reaction mechanism

1.3 Conclusion Remarks

Novel chiral C₃-symmetric N-{3,5-bis-[(2-amino-1,2-diphenyl-ethylamino)-methyl]-benzyl}-1,2-diphenyl-ethane-1,2-diamine (**C-5**) with 1,3,5-benzotricarbonyltrichlorid spacer group has been synthesized from readily available chiral 1,2diamines. This amino catalyst has been applied in the asymmetric synthesis of warfarin and analogues under room temperature and metal-free conditions, shown superior performance which provided the corresponding warfarin and analogues products in high yield (up to 95%) and enantioselectivities up to 80:20 e. r.

The mechanism of **C-5**(*all-R*)-catalyzed reaction between α - β -unsaturated ketones and coumarin were studied using ESI-MS and it was demonstrated as an effective technique for the off-line analysis of reaction intermediates.

1.4 Experimental section

1.4.1 General experimental conditions

All reactions were conducted under the atmosphere unless otherwise noted. All commercial reagents, solvents used for analysis, and HPLC solvent were purchased from Sigma Aldrich or Fluorochem. Column chromatography used 60 Å (230-400 mesh) silica gel purchased from Sigma Aldrich. All reactions were monitored by thin layer chromatography using Merck TLC Silica gel 60 F254 aluminum sheets(20X20cm), and then UV light (254 nm) was used for visualization. NMR spectra were recorded at 298 K by Bruker AM 400 in CDCl₃, MeOD and DMSO-d₆ except spectra of one sample were recorded by Bruker AM 300. Coupling constants were reported in Hz. For multiplicity (s (singlet), m (multiplet), d (doublet), t (triplet), q (quatriplet), dd (doublet of doublets), ddd (double doublet of doublets), dt (doublet of triplets), ddt (double doublet of triplets), dq (doublet of quatriplets). The exact mass of catalysts was obtained on ESI-MS. Optical rotation [α] was measured at a specific temperature. Isolation of enantiomers was performed by HPLC equipped with UV detection at 254nm or 280nm with ChiralPak columns. All the reported product yields were calculated based on pure material isolated after column purification. The analysis of the catalytic cycle was performed by ESI-MS.

1.4.2 Synthesis of C₂-symmetric organocatalysts

Synthesis of molecule 41

In well dried flask equipped with a stir bar, commercially available chiral amine-**39** (500 mg, 2.334 mmol) was dissolved in dry CH₂Cl₂ (6 mL) under argon gas. Triethylamine Et₃N (325.34 μL, 0.9333 mmol) was added to the solution at 0 °C. Then, the solution of 2,6-pyridinedicarbonyl dichloride-**40** (238.10g, 1.167 mmol) in dry CH₂Cl₂ (4 mL) was added dropwise. The mixture was stirred overnight at room temperature. The progress of the reaction was monitored via TLC. After completion, the crude product was concentrated and purified by column chromatography on silica gel (Hex/EA)50/50). 90% of the white product was recovered. The obtained product was characterized by NMR and mass spectroscopy. 90% of the white product.

¹H NMR (400 MHz, CDCl₃) δ 8.01 (d, *J* = 8.5 Hz, 2H), 7.54 (d, *J* = 7.7 Hz, 2H), 7.26 (t, *J* = 7.7 Hz, 1H), 3.90 (d, *J* = 9.0 Hz, 2H), 3.19 – 2.91 (m, 4H), 1.39 (dd, *J* = 28.4, 12.6 Hz, 4H), 1.09 (s, 4H), 0.99 – 0.85 (m, 2H), 0.79 – 0.54 (m, 7H), 0.45 (s, 18H). 560.3445 m/z calculated for C₂₉H₄₆N₅O₆ [M+H]⁺ found: 560.34, [M +Na]⁺ 582.32615 m/z, C₂₉H₄₅N₅O₆Na₁ [M +Na]⁺ 582.3261 m/z.

Synthesis of Catalyst-1(C-1)

Compound **41** (196g;0.3680mmol) was dissolved in DCM (10ml) and kept at 0°C. TFA (170.10μL,2.21mmol) was added to the solution. Then reaction was stirred at 0°C for 2hrs and temperature of the reaction was increased to room temperature for another 5h. The progress of reaction was controlled by TLC (Pentane/EOAc:50/50). After completion of reaction, solvent was removed in rotavapor. Catalyst-1(C-1) was obtained after passing through Ambersep 900-OH. To obtain neutral compound(C-1) from **42**, Ambersep 900-OH resin was activated with 2N NaOH. Then, water and MeOH were passed consecutively. At the end, compound-**42** was dissolved in methanol and loaded to column. The solution was collected and evaporated. Finally,99% of desired product-**C-1** was obtained.

^1H NMR (400 MHz, CDCl_3) δ 7.92 (d, $J = 7.8$ Hz, 2H), 7.58 (dd, $J = 18.1, 10.2$ Hz, 1H), 7.49 (d, $J = 8.3$ Hz, 2H), 3.26 (qd, $J = 11.1, 3.7$ Hz, 2H), 2.19 (td, $J = 10.3, 3.8$ Hz, 2H), 1.74 (dd, $J = 7.2, 4.2$ Hz, 2H), 1.66 – 1.54 (m, 2H), 1.37 (dd, $J = 23.0, 20.2$ Hz, 4H), 0.92 (tt, $J = 22.0, 11.2$ Hz, 10H). 360.23928 m/z calculated for $\text{C}_{19}\text{H}_{29}\text{N}_5\text{O}_2$ found: 360.24 $[\text{M} + \text{H}]^+$, $\text{C}_{19}\text{H}_{29}\text{N}_5\text{O}_2\text{Na}$ $[\text{M} + \text{Na}]^+$ 382.22116, $[\text{2M} + \text{H}]^+$ 719.47191.

Synthesis of molecule-45

To the solution of **44** (400mg, 1.70mmol) in dry CH_2Cl_2 (7mL), triethylamine Et_3N (237mL, 1.70mmol) was added under argon gas. Then, the solution of 2,6-pyridinedicarbonyl dichloride (173.41mg, 1.70mmol) in CH_2Cl_2 (4mL) was added dropwise. The mixture was stirred in room temperature overnight. The crude product was concentrated and purified by column chromatography on silica gel (Hex/EA)50/50). 93% yield

^1H NMR (400 MHz, CDCl_3) δ 9.00 (d, $J = 4.5$ Hz, 2H), 8.20 (d, $J = 7.7$ Hz, 2H), 7.91 (t, $J = 7.8$ Hz, 1H), 7.27 (ddd, $J = 29.9, 24.4, 7.0$ Hz, 10H), 5.27 (d, $J = 91.5$ Hz, 4H), 3.84 – 3.32 (m, 4H), 2.04 (d, $J = 49.6$ Hz, 2H), 1.21 (s, $J = 21.2, 13.9$ Hz, 18H). 626.29486 m/z calculated for $\text{C}_{33}\text{H}_{41}\text{N}_5\text{O}_6\text{Na}$ $[\text{M} + \text{Na}]^+$ found: 625.30, $[\text{2M} + \text{Na}]^+$ 1229.60120.

Synthesis of Catalysts-2(C-2)

Compound **45**(306mg;0.51mmol) was dissolved in DCM (14ml) and kept in ice(0°C). TFA (391 μL ,5.10mmol) was added to the reaction solution at 0°C and stirred at rt for 5h. Reaction was stopped and solvent was removed in rotavapor. The ambersep 900-OH resin was run with 2N NaOH, followed by water, then MeOH. Sample was dissolved in methanol and loaded to the column by pipette. The solution was collected, evaporated, weighted, characterized by NMR and ESI-MS. 98% yield. ^1H NMR (400 MHz, MeOD) δ 8.21 – 8.13 (m, 2H), 8.08 – 7.97 (m, 1H), 7.39 – 7.16 (m, 12H), 5.13 (dd, $J = 7.9, 5.7$ Hz, 2H), 3.15 – 2.98 (m, 4H), 1.80 (s, 4H). 426.19010 m/z calculated for $\text{C}_{23}\text{H}_{25}\text{N}_5\text{O}_2\text{Na}$ $[\text{M} + \text{Na}]^+$ found: 426.19, $[\text{2M} + \text{Na}]^+$ 829.3909

Synthesis of molecule 49

To the solution of **48** (400mg, 1.280 mmol) in dry CH_2Cl_2 (7 mL), triethylamine Et_3N (237mL, 1.70 mmol) was added. The solution of 2,6-pyridinedicarbonyl dichloride (173.41mg, 1.70 mmol) in CH_2Cl_2 (4 mL) was added dropwise. The mixture was stirred at room temperature overnight. The crude product was concentrated and purified by column chromatography on silica gel (Hex/EA)50/50). 94% yield. ^1H NMR (400 MHz, CDCl_3) δ 9.21 (s, $J = 8.4$ Hz, 2H), 8.24 (d, $J = 7.8$ Hz, 2H), 7.93 (t, $J = 7.8$ Hz, 1H), 7.40 – 7.08 (m, 21H), 5.79 (d, $J = 8.9$ Hz, 2H), 5.35 (t, $J = 8.9$ Hz, 4H), 1.02 (s, 18H). 754.3603 m/z calculated for $\text{C}_{45}\text{H}_{48}\text{N}_5\text{O}_6[\text{M} + \text{H}]^+$ found: 754.36 m/z for ${}_{45}\text{H}_{48}\text{N}_5\text{O}_6\text{Na}[\text{M} + \text{Na}]^+$ 778.3566, $[2\text{M} + \text{Na}]^+$ 1534.7272

Synthesis of catalyst-3(C-3)

Compound **49**(950 gm;2.19 mmol) was dissolved in DCM (7 mL) and kept in ice(0°C). TFA (169 μL ,2.19mmol) was added to the reaction solution at 0°C and stirred at rt for 5 h. Reaction was stopped and the solvent was removed in rotavapor. Ambersep 900-OH in the column was activated with 2N NaOH, followed by water, then MeOH. The sample was dissolved in methanol and transferred to the column by pipette. The solution was collected, evaporated, weighted, characterized by NMR and ESI-MS. 96% yield. ^1H NMR (400 MHz, MeOD) δ 8.22 (d, $J = 7.7$ Hz, 2H), 8.08 (dd, $J = 8.3, 7.2$ Hz, 1H), 7.60 – 7.02 (m, 22H), 5.41 (d, $J = 6.6$ Hz, 2H), 4.61 (d, $J = 6.6$ Hz, 2H), 3.32 (m, $J = 1.6$ Hz, 2H). 554.2556 m/z calculated for $\text{C}_{35}\text{H}_{32}\text{N}_5\text{O}_2$ found, $[\text{M} + \text{H}]^+$ found 554.66, 578.25147, $[2\text{M} + \text{Na}]^+$ 1133.5143

Synthesis of (2-Amino-1,2-diphenyl-ethyl)-carbamic acid tert-butyl ester-54

Round bottom flask containing methanol(3ml) was charged with TMSCl (1.415 mmol,178.50 μ L) at 0 °C. After 10min stirring, 1,2-diphenyl ethylenediamine (DPEDA) (1.415 mmol, 300 mg) was added. The solution was continued to be stirred at room temperature for 15 min. The solution of di-tert-butyl dicarbonate (Boc)₂O (1.41 mol, 308.47mg) in MeOH (2 mL) was added dropwise for 30 min. The resulting solution was stirred for 2h at room temperature. The mixture was concentrated in a vacuo. The residue was washed with diethyl ether (3 \times 4mL) and the pale-yellow solid was treated with the 3N NaOH solution (1.2mL) and water (3 \times 1.5mL). The product was dried in a vacuo at low pressure. 87% of white product **54** was isolated by column chromatography with Hex/EA (50/50) +1%TEA and characterized by ¹H-NMR,¹³C NMR, and ESI spectra. Confirmation was done by comparing its ¹H-NMR spectrum with previously reported literature. ¹H NMR (400 MHz, CDCl₃) δ 7.47 – 7.24 (m, 10H), 5.88 (1, *J* = 8.1 Hz, 1H), 4.89 (s, 1H), 4.37 (s, 1H), 1.44 (s, *J* = 27.6 Hz, 2H), 1.36 (s, 9H). 313.17 m/z calculated for C₁₉H₂₄N₂O₂ found: 313.18 and [M +Na]⁺:335.17

Synthesis of Molecule-56

Compound-**54**(380 mg, 1.22 mmol) was dissolved in 8 mL of dry CHCl₃. Then, 167.7 μ Lof DIPEA was added to the reaction mixture. Then, the solution of 1,3,5-benzenetricarbonyl trichloride **17**(107.80 mg,0.41mmol) in 4 mL of dry CHCl₃ was added to the reaction mixture dropwise. The solution was stirred under nitrogen atmosphere at 40 °C. After 5hours stirring, the temperature of the reaction was decreased to 25°C for 14hr. The reaction progress was controlled with TLC (Hex/EA)50/50) +1%MeOH, Rfspot1 =0.037, Rfspot2 =0.278, Rfspot3 =0.667). Then, 2ml of MeOH was added slowly. The crude of reaction was concentrated in vacuo. The residue was purified by column chromatography on silica gel with Hex/EA)50/50) +1%MeOH. Based on the third spot,85% yield was obtained. The structure was confirmed by both NMR and mass spectroscopy,¹H NMR (400 MHz, DMSO) δ 9.02 (d, *J* = 9.1 Hz, 3H), 8.23 (s, 3H), 7.69 (d, *J* = 9.7 Hz, 3H), 7.35 (m, *J* = 13.2, 7.5 Hz, 11H), 7.28–7.11 (m, 10H), 5.52 (dd, *J* = 8.9, 6.4 Hz, 3H),

5.13 (dd, $J = 9.4, 6.3$ Hz, 3H), 1.23 (d, $J = 9.9$ Hz, 27H). 569.33 m/z found for $C_{66}H_{72}N_6O_9$ $[M + H]^{2+}$ found and 1115.58 m/z $[M + Na]^+$

Synthesis of Catalyst-4(C4-(*R, R*) and C4(*S, S*))

Compound-**56** (233mg, 0.2134 mmol) was dissolved in DCM(7ml) and kept in ice(0°C). Next, TFA (165 μ l) was added and reaction was stirred at room temperature for 5hrs. After the progress of reaction was controlled by TLC (hex/EA (50/50) +1% methanol), the crude of reaction was concentrated in vacuo. Then the concentrated crude product was dissolved in methanol and passed through Ambersep 900 OH. Before load the sample, the resin was activated with 2N water and methanol consecutively. Finally, the dissolved crude product was loaded. After collection, the solvent was evaporated in vacuo and 98% of product was recovered. Finally, the product was characterized by ¹H NMR and mass spectroscopy (ESI). ¹H NMR (400 MHz, MeOD) δ 8.41 (s, 1H), 7.29 – 7.15 (m, 12H), 7.12 (t, $J = 6.7$ Hz, 1H), 5.30 (dd, $J = 20.6, 6.1$ Hz, 1H), 4.34 (d, $J = 8.2$ Hz, 1H). 815.3800 m/z found for $C_{51}H_{48}N_6O_3Na[M + Na]^+$

Synthesis of N-{3,5-Bis-[(2-amino-1,2-diphenyl-ethylamino)-methyl]-benzyl}-1,2-diphenyl-ethane-1,2-diamine (C5)

In well dried round bottom flask, (185mg; 0.233mmol) of catalysts **C-4** was dissolved in 10ml of anhydrous THF. Next, (296 μ L; 3.12mmol) of B (Borane dimethyl sulfide) was added at 0 °C. The solution was heated to reflux under N₂ atmosphere for 6h. The temperature was dropped to 25°C for another 14hours. Then reaction was quenched by adding 4mL of MeOH at 0°C and then, the crude of the reaction was dried in vacuo. Then, 250mg of concentrated material was dissolved in 10mL of MeOH. Followed by 1M HCl (10mL) was added to the solution and continued to reflux for 8hr. washed with MeOH. Then the concentrated material was passed through resin Ambers per 900. The product was dried in rotavapor and lead to vacuum pump at 80°C for 24hr. Yield :95% with overall yield 67%. ¹H NMR (400 MHz, MeOD) δ 7.12 (d, 30H), 6.97 (s, 3H), 3.94 (d,

$J = 9.0$ Hz, 3H), 3.74 (s, 3H), 3.57 (dd, $J = 12.0, 5.3$ Hz, 3H), 3.49 – 3.38 (m, 3H). 773.44 m/z found for $C_{51}H_{54}N_6 [M + Na]^+$

General procedure for the synthesis of Michael Reactions

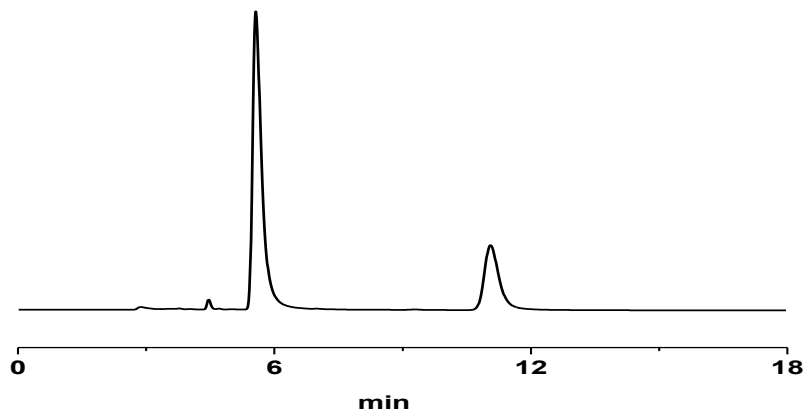
Compounds (**60a-60j**) were synthesized by mixing 4-hydroxy-2H-chromen-2-one(**58a**) (0.2mmol) or Hydroxy-1H-quinolin-2-one(**58b**) (0.2mmol), α, β -unsaturated ketone (**59**) (0.24mmol) and catalyst(5% mol) in THF(BHT)(2ml) or DMSO(2ml). The solution was stirred at room temperature for 48hours. The reactions were controlled by TLC. After 48h, the solution was concentrated in vacuo. Crude residue was purified via column chromatography on silica. The eluent conditions were Hex/EA (70/30) for coumarin based reaction or Hex/EA(60/40) for Hydroxy-1H-quinolin-2-one based reaction. The purified compounds were stored at 5°C until analyzed. Separation of enantiomers were performed using chiral HPLC (Daicel Chiralpak IA or IB).

In these asymmetric Michael addition reactions, warfarin and warfarin analogs(**60a-60i**) were synthesized by mixing 4-hydroxy-2H-chromen-2-one(**58a**) (0.2mmol) or Hydroxy-1H-quinolin-2-one(**58b**) (0.2mmol), α, β -unsaturated ketone (**59**) (0.24mmol) and catalyst(5mol%) in THF(2ml)(X=O) or DMSO(2ml)(X=N) respectively. The solution was stirred at room temperature for 48hours. The progress of the reaction was controlled by TLC analysis. After completion of time, the solution concentrated in vacuo and the crude residue was purified via column chromatography on silica with Hex/EA (70/30) for coumarin based substrates and Hex/EA(60/40) for Hydroxy-1H-quinolin-2-one based michael product. The purified compounds were stored at 5°C until analyzed. Separation of enantiomers were performed using chiral HPLC (Daicel Chiralpak IA and IB (0.46 cm x 250cm).

Synthesis of 4-Hydroxy-3-(3-oxo-1-phenylbutyl) coumarin(**60a**)

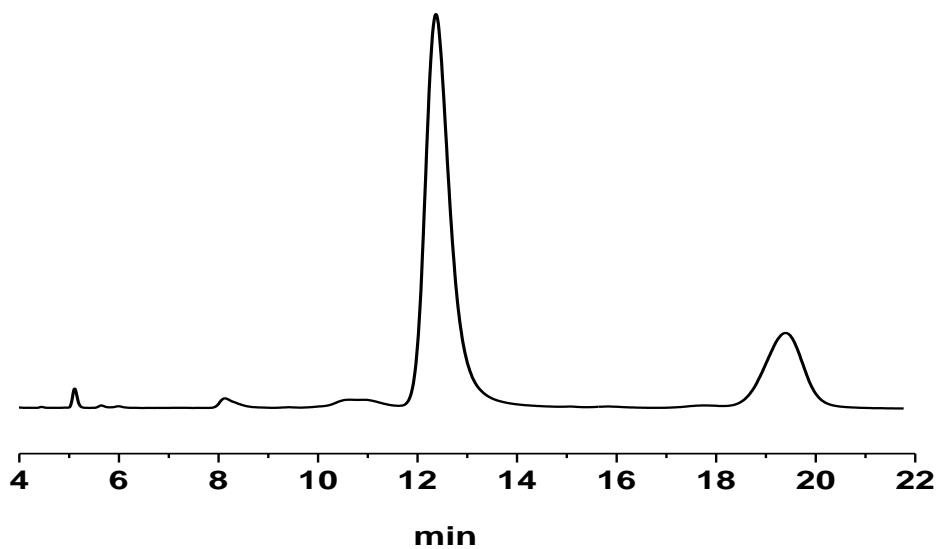
White solid, yield (87%), 1H NMR (400 MHz, DMSO) δ 7.84 (d, $J = 7.6$ Hz, 1H), 7.63 (t, 1H), 7.38 (d, $J = 8.4$ Hz, 3H), 7.28 – 7.13 (m, 5H), 4.01 (dt, $J = 13.2, 6.9$ Hz, 1H), 2.40 – 2.26 (m, 1H),

1.90 (t, $J = 12.4$ Hz, 1H), 1.61 (d, $J = 25.9$ Hz, 3H). Enantiomeric ratio :77/23 where major peak at $t_r = 5.57$ and minor peak is at $t_r = 11.11$.



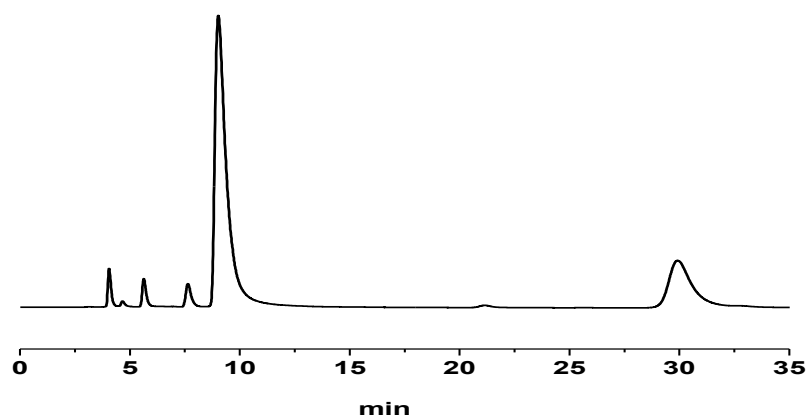
Synthesis of 4-Hydroxy-3-(3-oxo-1-phenyl-butyl)-1H-quinolin-2-one(60b)

^1H NMR (400 MHz, DMSO) δ 11.28 (d, $J = 42.9$ Hz, 1H), 7.81 (s, 1H), 7.54 – 7.44 (m, 1H), 7.36 – 7.08 (m, 8H), 4.02 (d, $J = 5.9$ Hz, 1H), 2.36 – 2.28 (m, 1H), 2.21 – 2.06 (m, 1H), 1.89 – 1.71 (m, 1H), 1.56 (d, $J = 15.1$ Hz, 3H). Enantiomeric ratio :78/22 where major peak at $R_t = 12.37$ and minor peak is at $R_t = 19.39$.



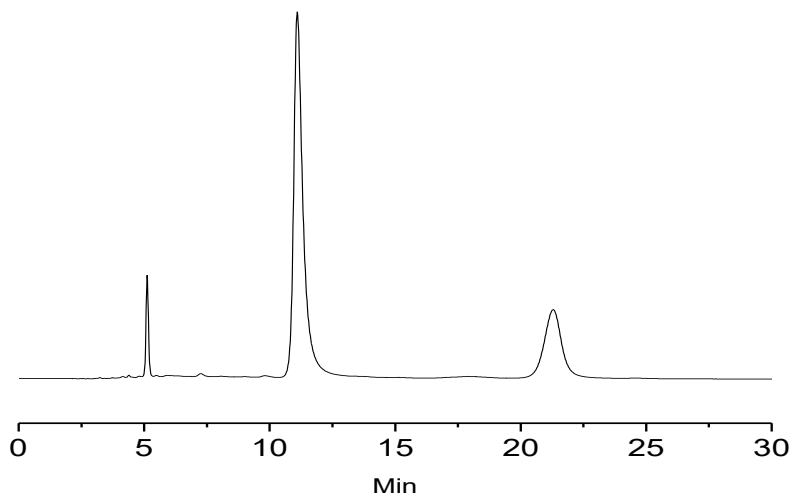
Synthesis of 3-[1-(4-Chloro-phenyl)-3-oxo-butyl]-4-hydroxy-chromen-2-one(60c)

^1H NMR (400 MHz, MeOD) δ 7.92 (d, $J = 6.3$ Hz, 1H), 7.59 (t, $J = 16.8, 9.8$ Hz, 1H), 7.40 – 7.11 (m, 6H), 4.09 (t, $J = 17.4, 6.5$ Hz, 1H), 2.38 (m, $J = 13.4, 6.6$ Hz, 1H), 2.06 – 1.88 (m, 1H), 1.69 (d, $J = 29.3$ Hz, 3H). Enantiomeric ratio :81/19 where major peak at $t_r = 11.60$ and minor peak is at $t_r = 35.87$.



Synthesis of 3-[1-(4-Chloro-phenyl)-3-oxo-butyl]-4-hydroxy-1H-quinolin-2-one(60d)

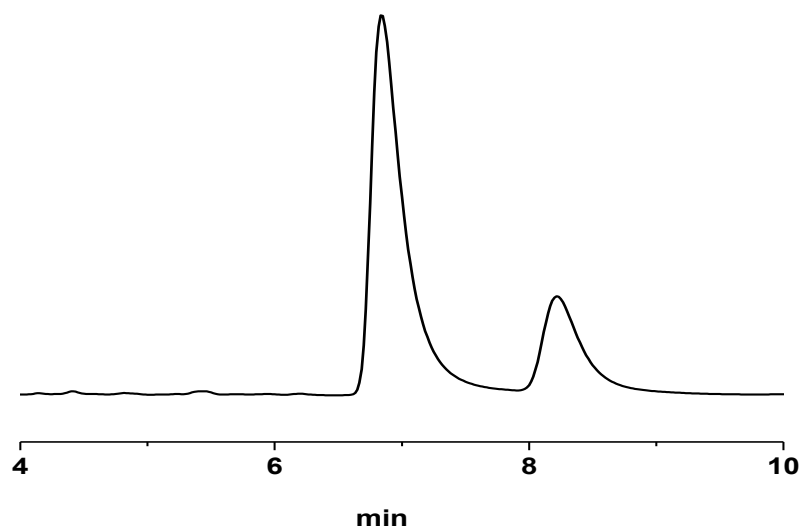
^1H NMR (400 MHz, DMSO) δ 11.24 (d, $J = 32.4$ Hz, 1H), 7.81 (d, $J = 7.5$ Hz, 1H), 7.47 (s, 1H), 7.29 – 7.08 (m, 8H), 4.01 (s, 1H), 2.37 – 2.20 (m, 1H), 1.83 (s, 1H), 1.54 (d, $J = 11.6$ Hz, 3H).
Enantiomeric ratio :76/24 where major peak at $R_t = 11.11$ and minor peak is at $R_t = 21.39$.



Synthesis of 4-Hydroxy-3-(1-methyl-3-oxo-butyl)-chromen-2-one(60e)

^1H NMR (400 MHz, MeOD) δ 7.86 – 7.79 (m, 1H), 7.58 – 7.51 (m, 1H), 7.33 – 7.26 (m, 2H), 2.99 – 2.83 (m, 1H), 2.31 – 2.19 (m, 1H), 2.10 – 1.98 (m, 1H), 1.69 (d, 4H), 1.41 (dd, 3H).

Enantiomeric ratio :80/20 where major peak at $R_t = 6.85$ and minor peak is at $R_t = 8.24$.

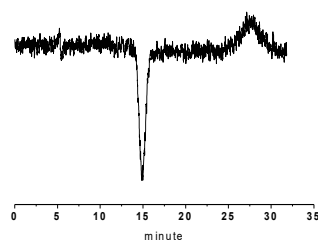
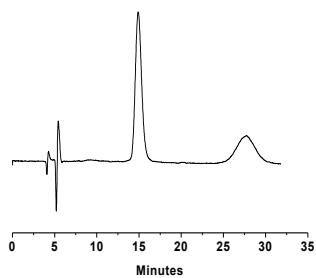


Synthesis of 4-Hydroxy-3-(1-methyl-3-oxo-butyl)-1H-quinolin-2-one(60f)

^1H NMR (400 MHz, DMSO) δ 11.26 (d, $J = 19.2$ Hz, 1H), 7.73 (t, $J = 8.8$ Hz, 1H), 7.47 – 7.36 (m, 1H), 7.29 – 7.21 (m, 1H), 7.13 (dd, $J = 14.3, 7.1$ Hz, 1H), 2.83 (m, $J = 20.2, 10.3, 6.8$ Hz, 1H), 1.96 – 1.87 (m, 1H), 1.79 (d, $J = 7.3$ Hz, 1H), 1.59 (d, $J = 17.0$ Hz, 3H), 1.41 – 1.28 (m, 3H).

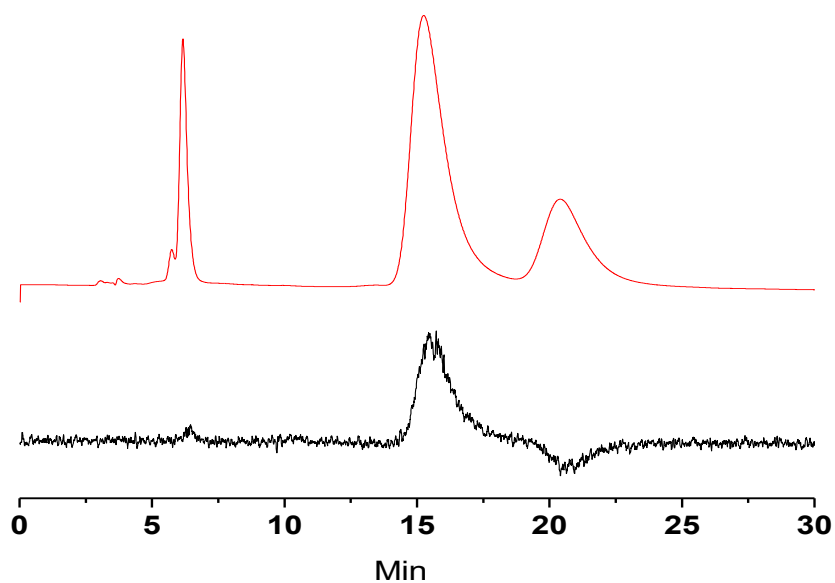
Enantiomeric ratio :68/32 where major peak at $R_t = 14.80$ min and minor peak is at $R_t = 27.70$ min

HRMS (ESI): m/z calculated for $\text{C}_{14}\text{H}_{15}\text{NO}_3$ $[\text{M} + \text{Na}]^+$, found:



4-Hydroxy-3-(3-oxo-1,3-diphenyl-propyl)-chromen-2-one(60g)

^1H NMR (400 MHz, DMSO) δ 8.08 – 7.86 (m, 3H), 7.72 – 7.11 (m, 12H), 5.21 (d, J = 87.4 Hz, 1H), 3.98 (tdd, J = 14.7, 11.9, 7.2 Hz, 2H).

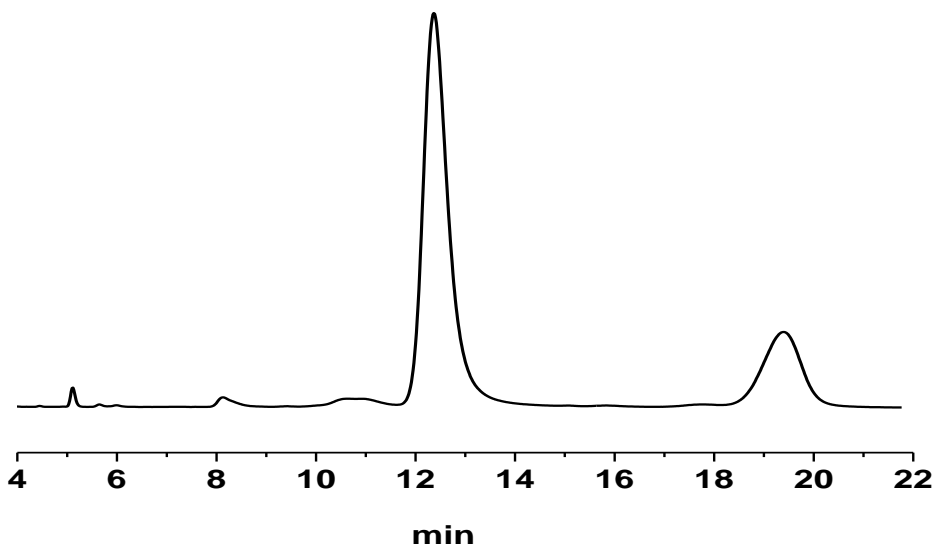


Enantiomeric ratio :75/25 where major peak at $R_t = 15.27$ and minor peak is at $R_t = 20.39$.

HRMS (ESI): m/z calculated for $C_{24}H_{18}O_4[M + Na]^+$ 370.12 , found: 393.1103

4-Hydroxy-3-(3-oxo-1,3-diphenyl-propyl)-1H-quinolin-2-one (60h)

1H NMR (400 MHz, $CDCl_3$) δ 9.72 (s, 1H), 8.15 – 7.95 (m, 3H), 7.84 (d, $J = 15.7$ Hz, 1H), 7.54 (dddd, $J = 37.3, 29.8, 9.3, 7.0$ Hz, 8H), 7.23 (d, $J = 7.3$ Hz, 2H), 5.09 (d, $J = 8.6$ Hz, 1H), 4.59 (dd, $J = 18.7, 10.1$ Hz, 1H), 3.86 (d, $J = 18.3$ Hz, 1H). Enantiomeric ratio: 55/45 where major peak at $R_t = 11.68$ min and minor peak is at $R_t = 28.99$ min HRMS (ESI): m/z calculated for $C_{14}H_{15}NO_3 [M + Na]^+$, found:

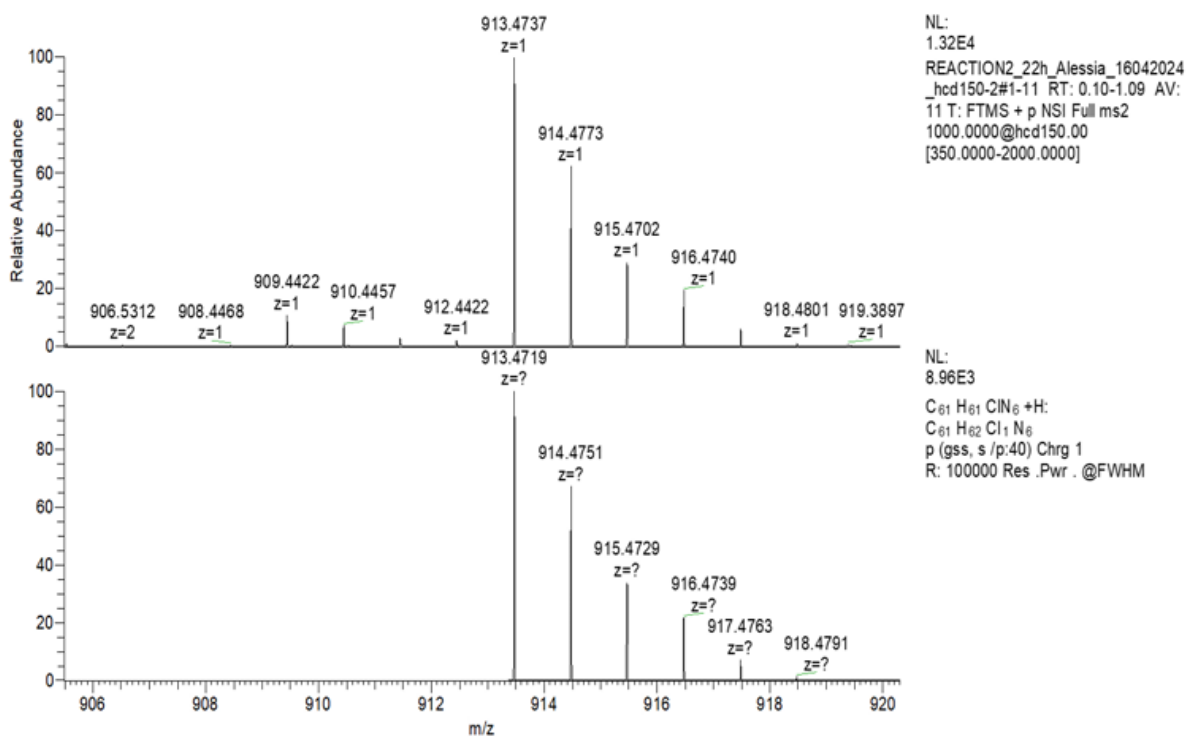


4-[1-(4-Hydroxy-2-oxo-2H-chromen-3-yl)-4,4-dimethyl-3-oxo-pentyl]-benzointrile (60i)

$^1\text{H NMR}$ (400 MHz, CDCl_3) δ 7.81 (d, $J = 7.5$ Hz, 1H), 7.61 – 7.47 (m, 3H), 7.43 – 7.21 (m, 5H), 4.36 – 4.04 (m, 1H), 2.43 (dd, $J = 20.5, 12.5$ Hz, 1H), 2.15 – 1.69 (m, 1H), 1.33 – 1.05 (m, 13H).
376.1543 m/z calculated for $\text{C}_{23}\text{H}_{22}\text{N}_1\text{O}_4[\text{M} + \text{H}]^+$ found to be 375.15 m/z, 773.2839 m/z for $\text{C}_{23}\text{H}_{22}\text{N}_1\text{O}_4\text{Na} [2\text{M} + \text{Na}]^+$

REACTION2_22h_Alessia_16042024_hcd150-2

05/17/24 09:09:25



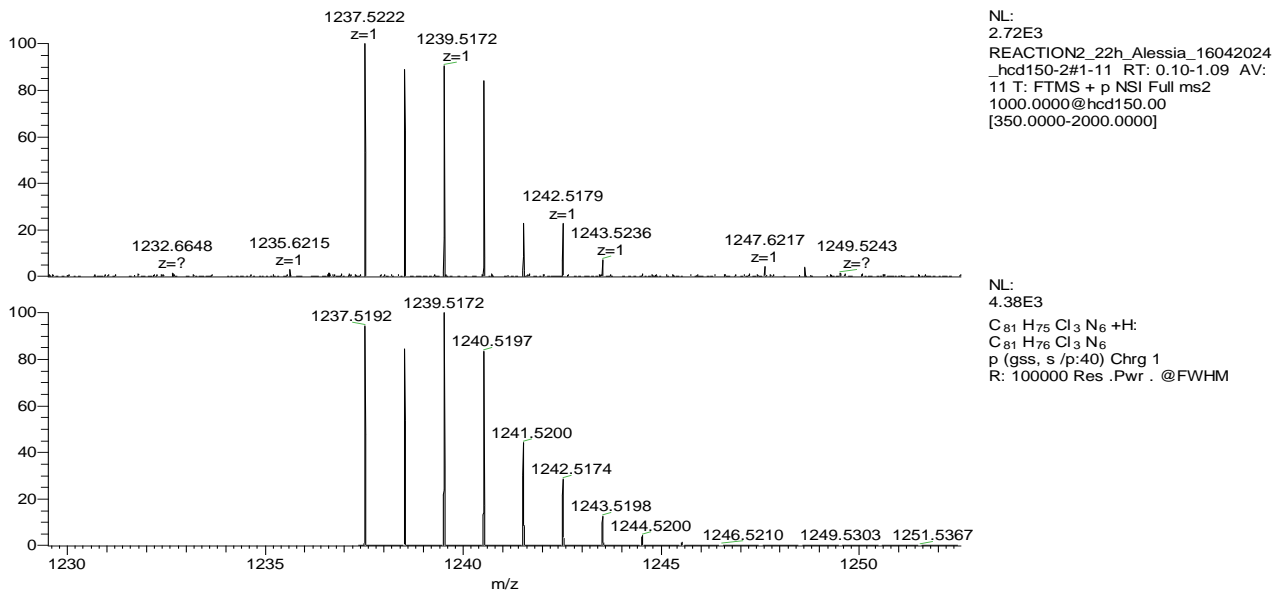
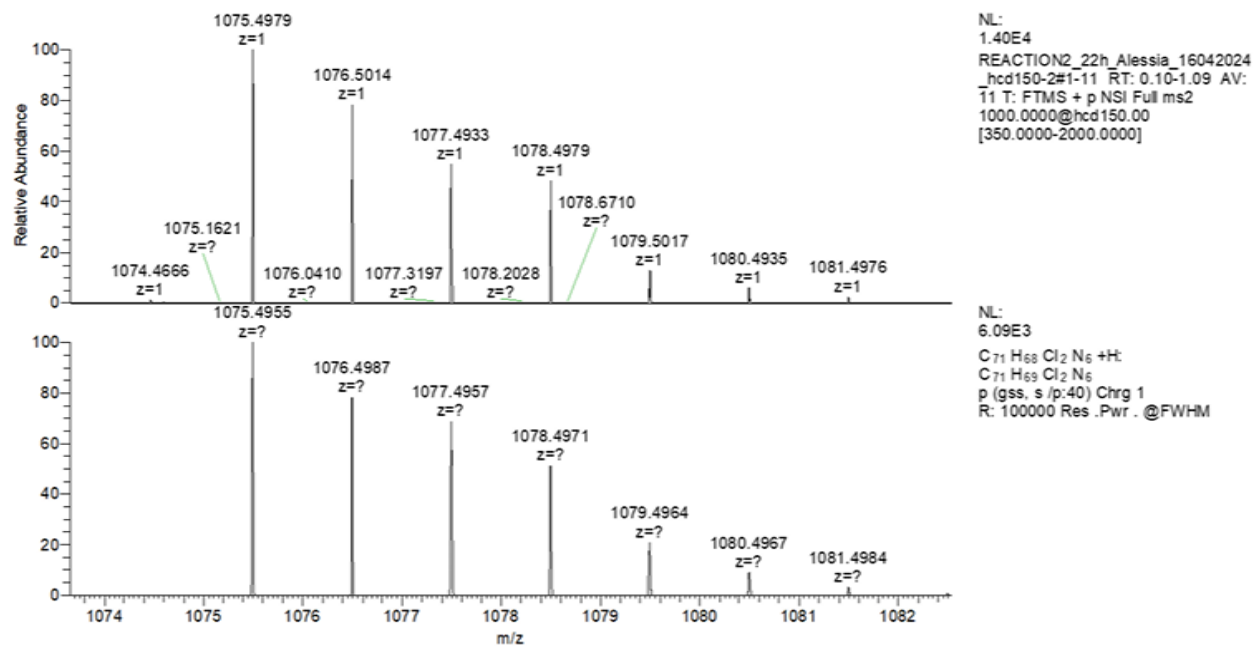


Figure 1.9 Zooms in the region of active species from HR-MS spectrum of reaction mixture after 22h with catalyst C-5 (*all-R*)

Reference

1. Anebousely, K.; Ramachary, D.; Kumar, I. *Dienamine Catalysis for Organic Synthesis*. The Royal Society of Chemistry. 2018.
2. Eder, U.; Sauer, G.; Wiechert, R. New Type of Asymmetric Cyclization to Optically Active Steroid CD Partial Structures. *Angew. Chem. Int. Ed. Engl.* 1971, 10, 496
3. Hajos, Z.; Parrish, R. Asymmetric Synthesis of Bicyclic Intermediates of Natural Product Chemistry. *J. Org. Chem.* 1974, 39, 1615.
4. List, B.; Lerner, R.; Barbas, C. F. Proline-Catalyzed Direct Asymmetric Aldol Reactions. *J. Am. Chem. Soc.* 2000, 122, 2395–2396.
5. Liu, C.; Yuan, J.; Gao, M.; Tang, S.; Li, W.; Shi, R.; Lei, A. Oxidative Coupling between Two Hydrocarbons: An Update of Recent C–H Functionalizations. *Chem. Rev.* 2015, 115, 12138–12204.
6. Wencel-Delord, J.; Glorius, F. C–H bond activation enables the rapid construction and late-stage diversification of functional molecules. *Nat. Chem.* 2013, 5, 369–375.
7. Díaz-Requejo, M.; Pérez, P.; Coinage, J. Metal Catalyzed C–H Bond Functionalization of Hydrocarbons. *Chem. Rev.* 2008, 108, 3379–3394.
8. Lewis, J.; Coelho, P.; Arnold, F. Enzymatic Functionalization of Carbon-Hydrogen Bonds. *Chem. Soc. Rev.* 2011, 40, 2003–2021.
9. Schramm, V. Introduction: Principles of Enzymatic Catalysis. *Chem. Rev.* 2006, 106, 3029–3030.
10. Ramos, M.; Fernandes, P. Computational Enzymatic Catalysis. *Acc. Chem. Res.* 2008, 41, 689–698.
11. MacMillan, D. The advent and development of organocatalysis. *Nature.* 2008, 455, 304–308
12. Santiago, C.; Pedro, A.; Miquel, A. Development of C₂-Symmetric Chiral Bifunctional Triamines: Synthesis and Application in Asymmetric Organocatalysis. *Org. Lett.* 2018, 20, 4806–4810
13. Suman K.; Anupriya, B.; Soniya, S.; Nirmal, K. Asymmetric Catalytic Approaches Employing α,β Unsaturated Imines. *Eur. J. Org. Chem.* 2023, 26, e202201470

14. Tapaswini D.; Seetaram.M.; Nilima.P; Sabita.N., Bishnu.I. Recent Advances in Organocatalytic Asymmetric Michael Addition Reactions to α,β -Unsaturated Nitroolefins. *ChemistrySelect* 2021, 6, 3745–3781E.
15. Niklas.F.; Jan.N.; Dieter.K.; René.W. Intramolecular Phosphine-Promoted Knoevenagel Based Redox-Reaction. *Molecules*. 2022, 27, 4875
16. Koen.B.; Steffijn.K.; Dennis.M.; ack.S. The Knoevenagel reaction: a review of the unfinished treasure map to forming carbon–carbon bonds. *Green Chemistry letters and Reviews*. 2020, 13, 4, 349–364
17. Stork, R.; Szmuszkovicz, I. New Type of Asymmetric Cyclization to Optically Active Steroid CD Partial Structures. *J. Am. Chem. Soc.*, 1954, 76, 2029
18. Stork.G.; Landesman, H. Codeinone Dimethyl Ketal and its Conversion to Thebaine. *J. Am. Chem. Soc.* 1956, 78, 5128
19. Ulrich, E.; Gerhard, S.; Priv, D.; Rudolf, W. New Type of Asymmetric Cyclization to Optically Active Steroid CD Partial Structures†. *Angew. Chem., Int. Ed. Engl.*, 1971, 10, 496
20. Hajos.Z.; Parrish, R. The Hajos–Parrish–Eder–Sauer–Wiechert Reaction. *J. Org. Chem.*, 1974, 39, 16
21. Okino, T.; Hoashi, Y.; Takemoto, Y. Enantioselective Michael Reaction of Malonates to Nitroolefins Catalyzed by Bifunctional Organocatalysts. *J. Am. Chem. Soc.* 2003, 125, 12672–12673.
22. Okino, T.; Hoashi, Y.; Takemoto, Y. Thiourea-catalyzed nucleophilic addition of TMS-CN and ketene silyl acetals to nitrones and aldehydes. *Tetrahedron Lett.* 2003, 44, 2817–2821
23. Malerich, J.; Hagihara, K.; Rawal, V. Chiral Squaramide Derivatives are Excellent Hydrogen Bond Donor Catalysts. *J. Am. Chem. Soc.* 2008, 130, 14416–14417.
24. Zhu, Y.; Malerich, J.; Rawal, V. Squaramide-catalyzed enantioselective Michael addition of diphenyl phosphite to nitroalkenes. *Angew. Chem., Int. Ed.* 2010, 49, 153–156.
25. List, B.; Lerner, R.; Barbas, C. Proline-Catalyzed Direct Asymmetric Aldol Reactions. *J. Am. Chem. Soc.* 2000, 122, 2395–2396.
26. Ahrendt, K.; Borths, C.; MacMillan, D. New Strategies for Organic Catalysis: The First Highly Enantioselective Organocatalytic Diels–Alder Reaction. *J. Am. Chem. Soc.* 2000, 122, 4243–4244.
27. Erkkila, A.; Majander, I.; Pihko, P. Iminium Catalysis. *Chem. Rev.* 2007, 107, 5416–5470

- K. A. Ahrendt, C. J. Borths and D. W. C. MacMillan, New Strategies for Organic Catalysis: The First Highly Enantioselective Organocatalytic Diels-Alder Reaction. *J. Am. Chem. Soc.*, 2000, 122, 4243.
28. Choon-Hong, T.; Benjamin, L. Cluster Preface: Asymmetric Brønsted Base Catalysis. *Synlett* 2017, 28, 1270–1271
29. Benjamin, L. *Comprehensive Enantioselective Organocatalysis: Catalysts, Reactions, and Applications*, ed. P. I. Dalko, Wiley-VCH, Weinheim, 2013.
30. Mase, N.; Hayashi, Y. *Comprehensive Organic Synthesis*, Elsevier, Amsterdam, 2nd edn, 2014, 2, 273–339.
31. Enders, D.; Matthias, H.; Hüttl, R.; Grondal, C.; Raabe, G. Control of four stereocentres in a triple cascade organocatalytic reaction. *Nature*, 2006, 441, 861–863
32. Dieter, E.; Christoph, G.; Matthias, R. Asymmetric Organocatalytic Domino Reactions. *Angew. Chem., Int. Ed.*, 2007, 46, 1570–1581.
33. Ishikawa, H.; Honma, M.; Hayashi, Y. One-Pot High-Yielding Synthesis of the DPP4-Selective Inhibitor ABT-341 by a Four-Component Coupling Mediated by a Diphenylprolinol Silyl Ether. *Angew. Chem., Int. Ed.*, 2011, 50, 2824–2827.
34. Hayato, I.; Shinya, S. Alkaloid synthesis using chiral secondary amine organocatalysts. *Org. Biomol. Chem.*, 2016, 14, 409–424
35. Xin-Qi, Z.; Qian, W.; Jieping, Z. Organocatalytic Enantioselective Diels–Alder Reaction of 2-Trifluoroacetamido-1,3-dienes with α,β -Unsaturated Ketones. Organocatalytic Enantioselective Diels–Alder Reaction of 2-Trifluoroacetamido-1,3-dienes with α,β -Unsaturated Ketones. *Angew. Chem.* 2023, 135, e202214925
36. Brandau, S.; Landa, A.; Franzén, J.; Marigo, M.; Jørgensen, K. Organocatalytic Conjugate Addition of Malonates to α,β -Unsaturated Aldehydes: Asymmetric Formal Synthesis of (-)-Paroxetine, Chiral Lactams, and Lactones. *Angew. Chem. Int. Ed.* 2006, 45, 4305–4309
37. Christina, M. Symmetry as a Tool for Solving Chemical Problems *Bull. Chem. Soc. Jpn.* 2021, 94, 558–564
38. Gibson, S.; Castaldi, M. Applications of chiral C₃-symmetric molecules. *Chem. Commun.* 2006, 37, 3045–3062.

39. Rodríguez, L.; Roth, T.; Fillol, J.; Wadepohl, H.; Gade, L. The More Gold-The More Enantioselective: Cyclohydroaminations of γ -Allenyl Sulfonamides with Mono-, Bis-, and Trisphospholane Gold(I) Catalysts. *Chem. A Eur. J.* 2012, 18, 3721–3728.
40. Yamanaka, M.; Nakagawa, T.; Aoyama, R.; Nakamura, T. Synthesis and estimation of gelation ability of C3-symmetry tris-urea compounds. *Tetrahedron.* 2008, 64, 11558–11567.
41. Cri, san, C.; Soran, A.; Bende, A.; Hadade, N.D.; Terec, A.; Grosu, I. Synthesis, Structure and Supramolecular Properties of a Novel C3 Cryptand with Pyridine Units in the Bridges. *Molecules* 2020, 25, 3789.
42. Yu, M.; Liu, X.; Space, B.; Chang, Z.; Bu, X..Metal-organic materials with triazine-based ligands: From structures to properties and applications. *Co-ord. Chem. Rev.* 2021, 427, 213518.
43. García, A.; Insuasty, B.; Herranz, M.; Martínez-Álvarez, R.; Martín, N. New Building Block for C3-Symmetry Molecules: Synthesis of s-Triazine-Based Redox Active Chromophores. *Org. Lett.* 2009, 11, 5398–5401
44. Péter, K.; Zsuzsanna, F.; Sándor, N.; Péter, B.; Petra, K.; Zsófia, G.; Miklós, D.; Péter, H.; Béla, M.; József, K. Synthesis of C3-Symmetric Cinchona-Based Organocatalysts and Their Applications in Asymmetric Michael and Friedel–Crafts Reactions. *Symmetry* 2021, 13, 521.
45. Santiago, C.; Pedro, A.; Miquel, À..Development of C2-Symmetric Chiral Bifunctional Triamines: Synthesis and Application in Asymmetric Organocatalysis. *Org. Lett.* 2018, 20, 4806–4810
46. Andrea Sorato; Martina DeAngelis; Shilashi Badasa Oljira; Marco Pierini; Giulia Mazzocanti; Maria Pia Donzello; Alessia Ciogli. A C3-Symmetric Amino Organocatalyst for Asymmetric Synthesis of Warfarin and Analogues: Mechanistic Insight From ESI-MS Spectrometry and Computational Calculations. *ChemCatChem*, 2024, e202400031
47. Uraguchi, D.; Ohmatsu, T.; Dalko, P. *Comprehensive Enantioselective Organocatalysis: Catalysts, Reactions, and Applications*, 1st Ed., 2013, 161.
48. Yoon, T.; Jacobsen, E. Privileged Chiral Catalysts. *Science* 2003, 299, 1691
49. Joshua P; Hannah L; Luke C. Henderson. Synergistic effects within a C2-symmetric organocatalyst: the potential formation of a chiral catalytic pocket. *Org. Biomol. Chem.*, 2013, 11, 2951–2960

50. Alexander,S.; Alexey A.; Andrey N.;Boris V.;Michael ,Y; Sergei,G.C₂-Symmetric Chiral Squaramide, Recyclable Organocatalyst for Asymmetric Michael Reactions. *J. Org. Chem.* 2019, 84, 4304–4311
51. Shinobu,T.;Makoto,S.;Mohamed,A.;Kenta,K.;Wathsala,P.;,Shuichi,H.; Kenichi,M.;, Hiromichi,F.;,Hiroaki,S. Enantio-and Diastereoselective Betti/aza-Michael Sequence: Single Operated Preparation of Chiral 1,3-Disubstituted Isoindolines. *Org. Lett.* 2017, 19, 5426–5429
52. Péter,K.;Zsuzsanna,F.;Miklós,D.;Péter,H.;Sándor,N.;,Péter,B.;Petra,K.;Zsófia,G.;Béla,M. ; József,KSynthesis of C₃-Symmetric Cinchona-Based Organocatalysts,their applications in Asymmetric Michael and Friedel–Crafts Reactions. *Symmetry* 2021, 13, 521.
53. Kenichi,M; Shunsuke,F; Shoko,H;Yusuke,T; Hiromichi,F. C₃-Symmetric Chiral Trisimidazoline: Design and Application to Organocatalyst. *Org.Lett* 2010.12,964-966.
54. List,B.; Lerner,R.;Barbas,C., Proline-Catalyzed Direct Asymmetric AldolReactions.*J. Am. Chem. Soc.* 2000, 122, 2395–2396.
55. Jie.G.;John,G.Organocatalyzed asymmetric Michael reaction of β -aryl- α -ketophosphonates and nitroalkenes*Tet. Lett.* 2013, 54, 5703–5706.
56. Liu.;Y. Wang, G.;Song.H; Zhou.Z;Tang.Organocatalyzed Enantioselective Michael Addition of 2-Hydroxy-1,4-naphthoquinone to β,γ -Unsaturated r-Ketophosphonates*J. Org. Chem.* 2011,76, 4119–4124.
57. Husmann,R.;Jçrres,M;Raabe,G.;Bolm,C.Silylated Pyrrolidines as Catalysts for Asymmetric Michael Additionsof Aldehydes to Nitroolefins.*Chem. Eur..* 2010, 16,12549–12552.
58. Wang, Y; Du,M.Recent advances in organocatalytic asymmetric oxa-Michael addition triggered cascade reactions *Org. Chem. Front.* 2020, 7, 3266–3283.
59. Wang,W .; Wang, X.; Kodama, K.;Hirose,T.; Zhang,G. Novel chiral ammonium ionic liquids as efficient organocatalysts for asymmetric Michael addition of aldehydes to nitroolefins.*Tetrahedron.*2010, 66, 4970–4976.
60. Kelleher,F.;Kelly,S., Watts,J.;McKee,V.Structure–reactivity relationships of L-proline derived spirolactams and α -methyl prolinamide organocatalysts in the asymmetric Michael addition reaction of aldehydes to nitroolefins.*Tetrahedron.* 2010, 66, 3525–3536.

61. Wei,W;Qi,X.Chiral Aldehyde Catalysis Enabled Asymmetric α -Functionalization of Activated Primary Amines. *Acc. Chem. Res.* 2024,57,776–794
62. Tapaswini,D.; Seetaram,M.; Mishra,P.; Nayak,S.;Raiguru,P.Recent Advances in Organocatalytic Asymmetric MichaelAddition Reactions to α , β -Unsaturated Nitroolefins. *Chemistry Select* 2021, 6, 3745 – 3781.
63. Ishii, T.; Fujioka, S.; Sekiguchi, Y.; Kotsuki, H. New Class of Chiral Pyrrolidine-Pyridine Conjugate Base Catalysts for Usein Asymmetric Michael Addition Reactions*J. Am. Chem. Soc.* 2004, 126, 9558-9559
64. Zhenhua,D;Lijia W;Xiaohong,C;Xiaohua,L; Lili,L;Xiaoming.F.Organocatalytic Enantioselective Michael Addition of 4-Hydroxycoumarin to α , β -Unsaturated Ketones: A Simple Synthesis of Warfarin.*Eur. J. Org. Chem.* 2009, 5192–5197
65. Mattia, R.; Belen, P; Miriam, D.;Markus,L;Richard,G; Benjamin,L.Activation of Carboxylic Acids in Asymmetric Organocatalysis.*Angew.Chem. Int. Ed.*2014,53,7063 – 7067
66. Diana, V.; Stephanie, K.; Jorge.D;Cornelis,V; Torsten,S; Jean-Christophe,M.Continuous Flow Intensification for the Synthesis of High-Purity Warfarin. *Org. Process Res. Dev.* 2024, 28, 1704–1712
67. Kochetkov, S; Kucherenko, A.; Sergei G..Asymmetric synthesis of warfarin and its analogs catalyzed by C2 symmetric squaramidebased primary diamines. *Org. Biomol. Chem.*, 2018.
68. Malde, Alpeshkumar, Stroet, Martin, Caron, Bertrand, Visscher, Koen, Mark, Alan Predicting the Prevalence of Alternative Warfarin Tautomers in Solution.*J.Chem.Theory Comput.* 2018, 14, 4405–4415
69. Ilya D.;Ruslan,A.;Alexander,S.;Olga Y. ;Sergei G.Chiral Bis(8-Quinolyl)Ethane-Derived Diimine: Structure Elucidation and Catalytic Performance in Asymmetric Synthesis of (S)-Warfarin.*Catalysts* 2023,13, 136
70. Jee,S.; Nour,B.;Sepideh,S.;Wenyao.P.;Debasis.M.,Michael.G.The Synthesis of Warfarin Using a Reconfigurable-Reactor PlatformIntegrated to a Multiple-Variable Optimization tool.*Chem.Eur.J.*2020,26,15505–15508
71. Queensland Health.State of Queensland.Guideline for Warfarin Management in the Community February 2024

72. Tao.S; Zhiwei.G.; Huixian, Y.; Jianwu.X; Yijun.Z.; Weidong.Z. Atom-Economic Synthesis of Optically Active Warfarin Anticoagulant over a Chiral MOF Organocatalyst. *Adv. Synth.Catal.* 2013, 355, 2538–2543
73. Arulcova,A; Prokopova,L; Kra.u.;Bitman,M.;Vrzal,R.; Dvorak,Z.; BLAHOS.J.; P a v e k .P.Stereoselective interactions of warfarin enantiomers with the pregnane X nuclear receptor in gene regulation of major drug-metabolizing cytochrome P450 enzymes. *Journal of Thrombosis and Haemostasis*, 2010,8,2708–2717
74. Steven, L; Sameh.A.; Ellen.H.; Ivan.M; Andrea.L.; Jorgensen;Panos D.;Ann K.;Kevin B Kayode O., Farhad.K; Dyfrig.H;Munir.P. The population pharmacokinetics of R- and S-warfarin: effect of genetic and clinical factors. *Br J Clin Pharmacol* ,2011,73(1),66–76
75. Halland, N.; Hansen, T.; Jørgensen, K. A. Organocatalytic Asymmetric Michael Reaction of Cyclic 1,3-Dicarbonyl Compounds and α , β -Unsaturated Ketones A Highly Atom-Economic Catalytic One-Step Formation of Optically Active Warfarin Anticoagulant. *Angew. Chem., Int. Ed.* 2003, 42, 4955–4957.
76. Dong, Z.; Wang, L.; Chen, X.; Liu, X.; Lin, L.; Feng, X. Organocatalytic Enantioselective Michael Addition of 4-Hydroxycoumarin to α , β -Unsaturated Ketones: A Simple Synthesis of Warfarin. *Eur. J. Org. Chem.* 2009, 2009, 5192–5197.
77. Zhu, X; Lin,A; Shi;Y;Guo, J; Zhu;C. Cheng, Y. Enantioselective Synthesis of Polycyclic Coumarin Derivatives Catalyzed by an in Situ Formed Primary Amine-Imine Catalyst. *Org. Lett.* 2011, 13, 4382–4385.
78. Zhu, L.; Zhang, L.; Luo, S. Catalytic Asymmetric β -C–H Functionalizations of Ketones via Enamine Oxidation. *Org. Lett.* 2018, 20, 1672–1675
79. Kucherenko, A.; Kostenko, A.;Zhthankina,G.; Kuznetsova, O.;Zlotin,S. Green asymmetric synthesis of Warfarin and Coumachlor in pure water catalyzed by quinoline derived 1,2-diamines. *Green Chem.* 2018, 20, 754–759.
80. Rogozinska-Szymczak, M.;Mlynarski, J.;Asymmetric synthesis of warfarin and its analogues on water. *Tetrahedron: Asymmetry* 2014, 25, 813–820.
81. Rogozinska, M.; Adamkiewicz, A.; Mlynarski, J. Efficient “on water” organocatalytic protocol for the synthesis of optically pure warfarin anticoagulant. *Green Chem.* 2011, 13, 1155–1157.

- 82.** Alexander S.;Alexey A.;Galina M.;Olga.Y;Sergei-G.Green asymmetric synthesis of Warfarin and Coumachlor in pure water catalyzed by quinoline-derived 1,2-diamines. *Green Chem.*,2018,20,754–759

Part-B

Stability Studies of Atropisomeric Hydrazides by Dynamic-HPLC and Off-Column HPLC experiments.

2.1 Introduction

2.1.1 Overview of Chirality

Chirality is the geometric property of an object that cannot superimpose with its mirror image¹. This historic concept returned back to 19th century, in particular, unconventional work by Louis Pasteur on the omnipresence and significance of chirality in 1848¹ and he recognized the existence of chiral object as pair of enantiomorphous mirror images. He became the father of molecular chirality because of his exceptionally famous discovery of the resolution of tartrates.²

According to the IUPAC, ‘‘The geometric property of a rigid object (or spatial arrangement of points or atoms) of being non-superposable on its mirror image; such an object has no symmetry elements of the second kind (a mirror plane, σ = S1, a center of inversion, i = S2, a rotation-reflection axis, S2).’’ This work opened the door for chemists to generate rules and theories to describe chiral compound and their properties.

Studies on chirality have been one of the most essential research areas in pharmaceutical science because it is a basic step in the investigation of biologically chiral active molecules.^{3,4} Chiral molecules have stereogenic carbon, which is ubiquitous, their enantiomers are not mutually convertible without bond dissociation and recombination⁵. The other class of chiral molecules are capable of interconverting their enantiomers upon rotation of the σ bonds without bond dissociation and recombination. Different types of configurations of atoms in molecules cause the chirality is classified as the chiral center, chiral plane, chiral axis, and helical chirality.^{5,6,7,8} The existence of one of these types of configurations in a molecule makes it non-superimposable with its mirror image. Plane of chirality is a property of chiral systems in which a planar unit is connected to an adjacent part of the structure by a bond which results in restricted torsion so that the plane cannot lie in a symmetry plane.⁷ Helical chirality rises when the molecule has a helical structure. Helicity is a structural property that can be described by a curve in three-dimensional space which can be defined as an entity with an axis yet not superimposable on its mirror image. Here are some representatives of molecules contain a chiral center, chiral plane, chiral axis, and helical chirality are indicated below (Figure 2.1).

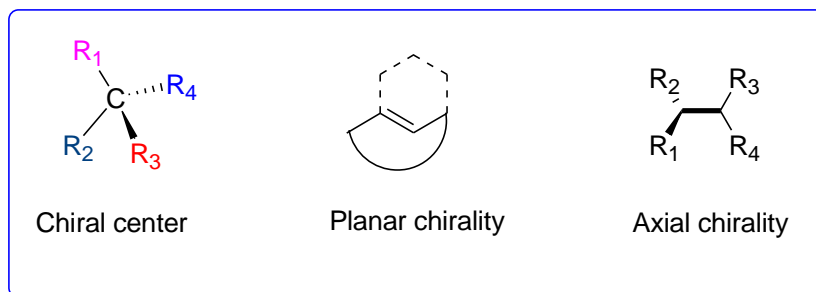


Figure 2.1 Types of Chirality based on configurations of atoms

2.1.2 Classification of chiral molecules

Chirality has a central role in drug design and development which commands a great deal of importance in modern organic chemistry because most of the interested pharmaceutical molecules are chiral. The existence of this property is directly connected with the biological activity of molecules. As we tried to indicate in the overview part, chirality can be classified as the chiral center, chiral plane, chiral axis, and helical chirality.⁵ Here, we have introduced the description of this chirality for bioactive molecules using the concept of stereoisomerism with selected examples. The majority of molecules in the organic world show this type of isomerism. These two enantiomers interact differently with another chiral organic compound. This is noticeable in interactions between drugs and the human body since all receptors are chiral.

The absolute configuration of organic molecules indicates the spatial arrangement of the atoms with stereochemical descriptors that command properties and functions of a chiral molecule. Mefloquine, as an example, is one of the pharmaceutical molecules used to prevent and treat malaria that contains two chiral centers.^{9,10} This molecule was discovered in the 1970s during malaria research being done by the U.S. military in response to high cases of malaria in American soldiers during the Vietnam War.¹⁰ This molecule is the biologically active compound that becomes pharmaceutically important because of the presence of stereogenic carbons.

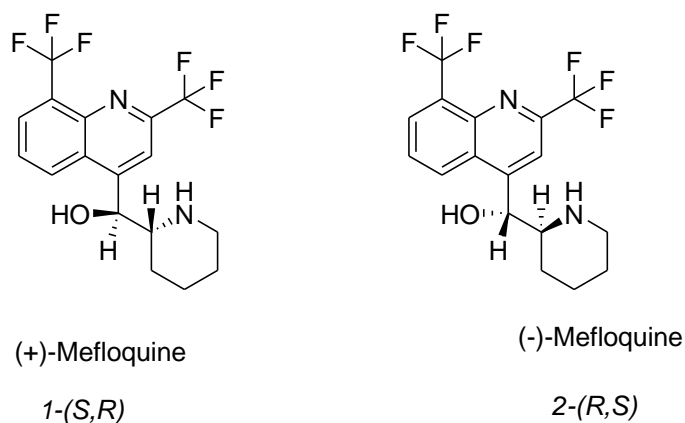


Figure 2.2: Example of molecule contains chiral center

Axially chirality is a well-known structural character of several organic compounds that lack asymmetric centers where some of them are widely studied and well-developed, while others may get very limited consideration. Most important molecules are classified as stereoisomers that can be interconverted by rotation about single bonds with a high enough rotational barrier to avoid interconversion at room temperature.¹¹ These molecules can exhibit optical properties due to the presence of axial chirality, as well as their enantiomers, can exhibit different chemical and physical properties. The finding of axial chirality has led chemists to design new atropisomeric molecule used as pharmaceutical drugs. During drug development from axially chiral molecules, understanding the rotational stability of the axis is a crucial precondition. This type of stereoisomer differs from other chirality in that racemization can occur spontaneously via bond rotation, rather than the process of bond breaking and bond making.¹ Here are representatives of atropisomerism that is likely present in many common scaffolds in drug design and development (Figure 3).^{12,13} For instance, due to their relevant biological properties, chiral ligands, and catalysts, BINOL biaryl scaffolds have attracted the interest of the scientific community (Figure 2.3A). There are also more scaffolds used in the synthesis of important axially chiral molecules. (Figure 2.3C). In general, this type of molecule can exist as either stable isolable enantiomers or rapidly interconverting racemizing mixtures.

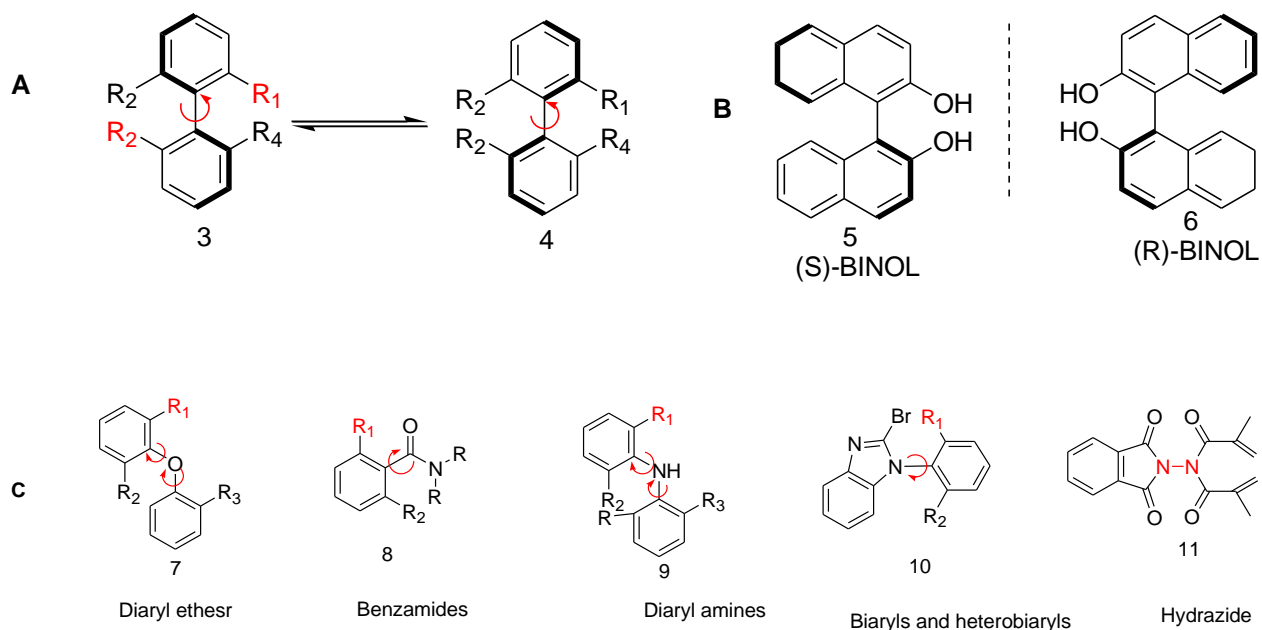


Figure 2. 3 Atropisomerism present in common scaffolds in drug development

2.1.3 Classification of atropisomers stereochemical stabilities

Energy barriers and rotation rates are the two main features that researcher rely on for the classification of atropisomer into groups. Steric hindrance and stereoelectronic effects are the two common electronic effect that control the rate of interconversion of enantiomers

In 1983, Oki has proposed a border rule between atropisomers and conformers defined that atropisomers are conformers which interconvert with a minimum threshold of a 1000 second half-life at +25 °C, correlate with a racemization barrier of 21.8 kcal/mol.¹⁴

Furthermore, atropisomers were classified by LaPlante et al. into three groups based upon tendency to interconvert as evaluated by their barrier to rotation and half-life.^{15,16} This classification was supported by computational approach based on the amount of energy needed for the chiral axis to racemize via rotation. For this purpose, he has collected several industrial screening decks for potentially atropisomeric compounds.

Class 1 Compound possess fast axial rotation rates which rapidly convert on the order of seconds and the energy barriers involved are generally lower than 19 kcal/mol. Molecules in this group

display no axial chirality and are developed as single molecule. This class of atropisomers comprise all scaffolds wherein the isomers cannot be isolated due to their fast interconversion properties, and cannot display atropisomeric character and thus should be developed as single compounds.

Class 2 These compounds have intermediate stability in which the rotational barriers are between 20 kcal/mol and 30 kcal/mol and the half-life time ($t_{1/2}$) spans from few minutes to years. Within this class of compounds, challenges may arise from moderate interconversion rates. There may high probability to form racemization during biological analysis, analytical characterization and through shelf-life storage leading to challenges during drug design and development. It is possible to get a more appropriate analogue by modifying the structure for designing of related compounds that have slower or faster axial rotation rates. This class further grouped into two subclasses were rotational energy barrier ranged within $20 \text{ kcal/mol} \leq \Delta E_{\text{rot}} \leq 23 \text{ kcal/mol}$ or $23 \text{ kcal/mol} < \Delta E_{\text{rot}} < 30 \text{ kcal/mol}$.

Class 3 Atropisomers are stable, $t_{1/2}$ on the order of years. These are chiral stable compounds with a $\Delta E_{\text{rot}} \geq 30 \text{ kcal/mol}$ and the single enantiomers can be considered kinetically stable. Therefore, little to no axial rotation is expected to occur at +25 °C.

2.1.4 Atropisomerism in drug discovery

Chirality plays crucial role in modern pharmaceutical industry where the studies of atropisomerism have received considerable attention following the increased its prevalence in modern drug discovery.¹⁷ The discovery of new atropisomeric compounds has used to guide us to develop new pharmaceutical drugs which have differ biological activity towards to target and pharmacokinetic properties like others chiral-centered stereoisomers.¹⁸ These molecules can exist as either stable isolable enantiomers or rapidly interconverting racemizing form. As we have seen at classification of atropisomers at stereochemical stabilities section, drug discovery and development processes become more complex for atropisomerism than chiral-centered molecules because the interconversion take place via bond rotation which subject to time and temperature-dependent.¹⁹

Each possible atropisomeric conformation of a molecule can possess different drug properties and target profiles.

A significant role for atropisomers in drug discovery and development has been established via substantial studies on the characteristics of molecules exhibiting this form of chirality. Atropisomerism plays a significant role in altering pharmacodynamic and pharmacokinetic properties and thereby the success of any proposed drug candidate. It is advised that all vital pharmacological attributes related to the safety and efficacy of both the isomers are studied and evaluated. The activity toward the choice target of stable atropisomers (class 3) take the majority in drug discovery while others provide minor contributions. Here are examples of significant small molecule atropisomeric FDA-approved drugs: telenzepine (12), colchicine (13), and lesinurad (14) (Figure 2.4). The antimuscarinic telenzepine is an atropisomeric FDA-approved drug that discussed many times in the literature possesses a $t_{(1/2)}$ to racemization at 20 °C of approximately 1000 years, and a 500-fold difference in potency between atropisomers^{20,21} (R_a,7S)-colchicine is another FDA-approved atropisomeric natural product which inhibits microtubule polymerization is (~40-fold) less cytotoxic.^{22,23} Lesinurad is an oral selective inhibitor of the URAT1 and OAT4 uric acid (UA) transporters of the kidney, exist as a mixture of stable atropisomers after initially approved for the treatment of gout, with the (S_a)-atropisomer proving to be a three times more potent hURAT1 inhibitor²⁴.

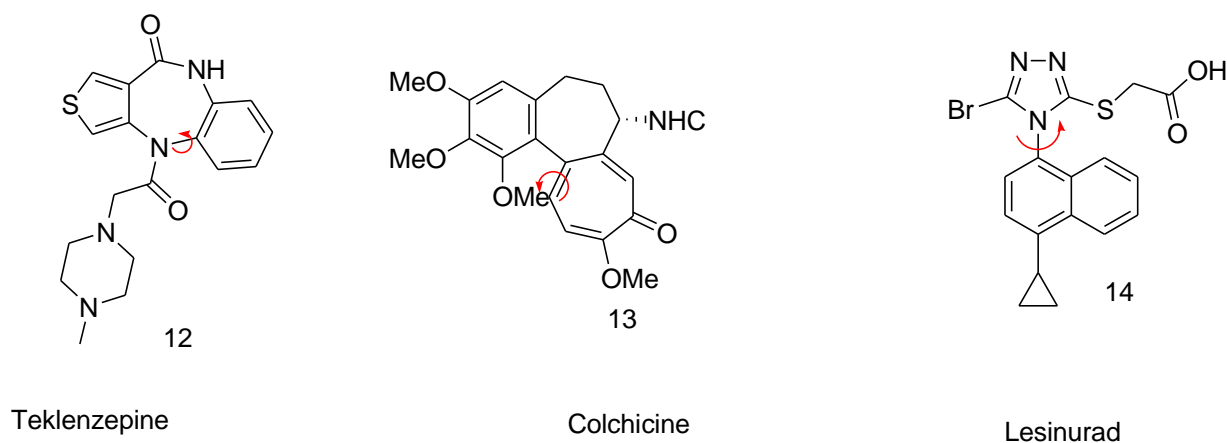


Figure 2.4 US FDA-approved small-molecule drugs that are atropisomerically stable.

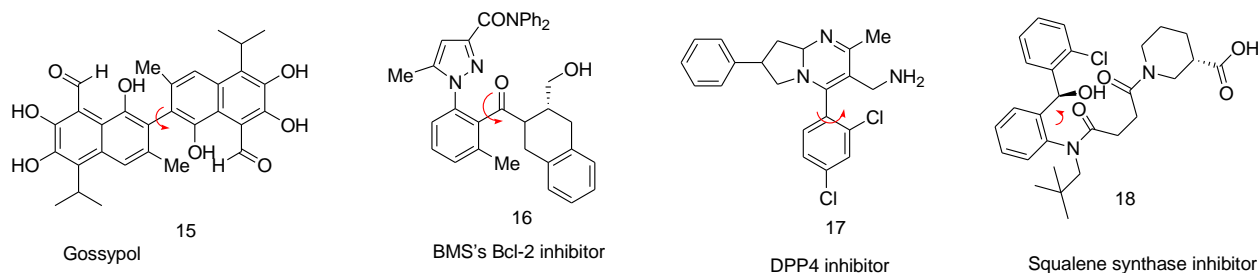


Figure:2.5 Representative of atropisomeric stable compounds from the medicinal chemical literature.

As briefly described in the literature, class 1 atropisomers have become frequently used in drug discovery. About 30 % of FDA-approved small molecule drugs since 2011 possess at least one interconverting axis of chirality.^{25,26} Generally, atropisomer scaffolds that are prevalent throughout drug discovery are biaryls, heterobiaryls, and diaryl amines.

2.1.5 N–N atropisomers and Atropisomeric Hydrazides

Axially chiral compounds that possess N–N axes are widespread in natural products, bioactive compounds, and ligands, and their study holds promise for discoveries of important molecules, especially in pharmaceutical drug design and development. For example, in atropisomers featuring an aza axis that contains restricted rotations in N–N single bonds was shown by Adamas and Chang in 1931.²⁷ N–N biaryl atropisomers have drawn increasing interest due to their unique structure and relatively stable axes. The successful separation of N–N biaryl atropisomers via the resolution of 2,2',5,5'-tetramethyl-1,1'-bipyrrole-3,3'-dicarboxylic acid with brucine was one of interesting work that push this research area one step forward.²⁷ In 2014, Pierini and coworkers obtained the N–N biaryl atropisomers that made a feature of N–N bibenzimidazoles scaffold by means of chiral high-performance liquid chromatography (HPLC).²⁸ Seven year later, Higashibayashi and coworkers characterized the racemization of the obtained N–N bicarbazole atropisomer using HPLC, that revealed a stable chiral axis that could withstand higher temperatures than its decomposition temperature.²⁹ When racemic tetra-orthoportograph-substituted substrates were utilized, a typical kinetic resolution procedure was conducted to provide the N–N atropisomers with excellent enantioselectivity and up to 173 selectivity factors.³⁰

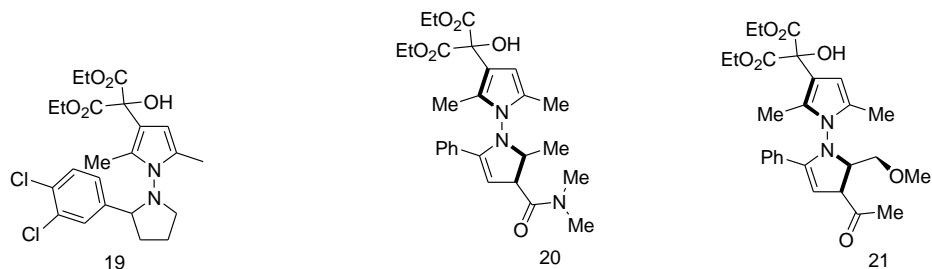


Figure 2. 6 Sample of axially chiral compounds that possess N–N axes

Hydrazides are a family of organic molecules that have a common functional group distinguished by a nitrogen-to-nitrogen covalent bond ($R-NR_1-NR_2R_3$), and non-basic due to the inductive influence of the acyl, sulfonyl, or phosphoryl substituent. They have attracted considerable attention for their properties as bioactive compounds and great efforts have been developed for the progress of new approaches in synthesis and studies of their stabilities^{31,32,33,34}

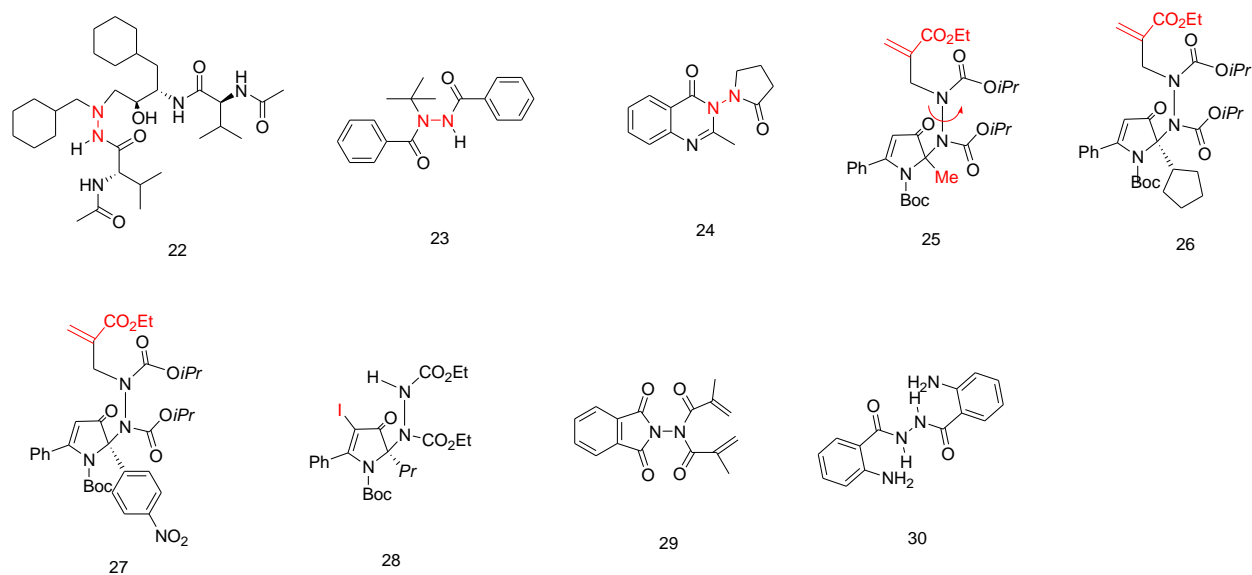


Figure 2.7 Some selected atropisomeric hydrazides

Di-, tri- and tetra-substituted hydrazine show higher barriers to rotation around the N–N bond compared to other single bonds.³⁵ This is probably because of the repulsion between the lone pairs on the nitrogen when the molecule is close to a planar conformation.^{36,37} Is may be this trend being true for hydrazides?

2.1.6 Dynamic and kinetic studies for Stereochemistry analysis

Design, synthesis, and analysis of the stereochemical stability of chiral molecules have been most fundamental works in discovery of new pharmaceutical drugs. In this part, we focus on the analysis of the stereochemical stability of chiral molecules, which are represented by axial chiral molecules. The desired enantiomer used as active pharmaceutical molecule should separate from its enantiomer which may have significant differences in the activity. Dynamic HPLC, variable temperature NMR, and kinetic analysis by off-column are the three most widely used experimental approaches to study stereochemical stabilities of an enantioenriched sample. From these approaches, we focused on the dynamic and off-column HPLC studies of chiral molecules capable of interconverting their enantiomers upon rotation of the σ bonds without bond dissociation and recombination like atropisomeric hydrazides. This approach provides us with important parameters to investigate the energy barrier to the rotation, commonly activation parameters (activation Gibbs energy, $\Delta G_{\text{rac}}^\ddagger$; activation enthalpy, $\Delta H_{\text{rac}}^\ddagger$; and activation entropy, $\Delta S_{\text{rac}}^\ddagger$) which are used to obtain Eyring plots of several kinetic constant values of racemization (k_{rac}) at different temperatures and time.

Before going to study dynamic-HPLC and kinetic analysis, it is fundamental to do screening of suitable enantioselective chromatographic conditions for samples under study. Checking the purity of the racemic compound on the achiral column is the primary work. Next, it is necessary to conduct the following activities investigate appropriate CSP for best separation of enantiomers, mobile phase composition, flow rate, wavelength (nm) of both UV and CD, and temperature of the column. This screening work helps us to group samples either as off-column or on-column studies.^{19,38,39}

2.1.6.1 Off-column HPLC approach

After optimized HPLC analytical conditions, optically pure enantiomers can be collected on the chiral column. Then, the purity of enantiomer under investigation should be controlled by

injecting on the same chiral column with the same analytical conditions. Racemization experiment can be performed by incubating the optically pure enantiomers in selected solvent at a chosen temperature and variable reaction time. Then, enantiomerization rate constants and ΔG of racemization ($\Delta G_{\text{rac}}^\ddagger$) can be obtained using unified equation. The linear correlation between the free energy of activation and the temperature of the reaction derived using Eyring equation ($1/T$ vs $\Delta G/T$).

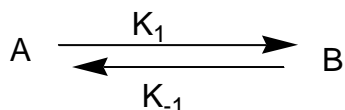


Figure 2. 8 Interconversion between atropisomers based on the rotational energy barrier

The decay of the enantiomer has been monitored over time and calculated by integration of the peaks in the elution profile. The kinetic rate constants of the racemization process can be obtained as the slope of the line resulting from the correlation between the reaction time and logarithm of the enantiomeric excess. The value extracted from $-(\Delta H^\ddagger/R)$ indicates the slope of the line while $\Delta S^\ddagger/R + \ln(kB/h)$ represents the intercept. where R, kB, and h are the gas, the Boltzmann, and the Plank constant respectively.

2.1.6.2 Dynamic-HPLC: On-column Enantiomerization

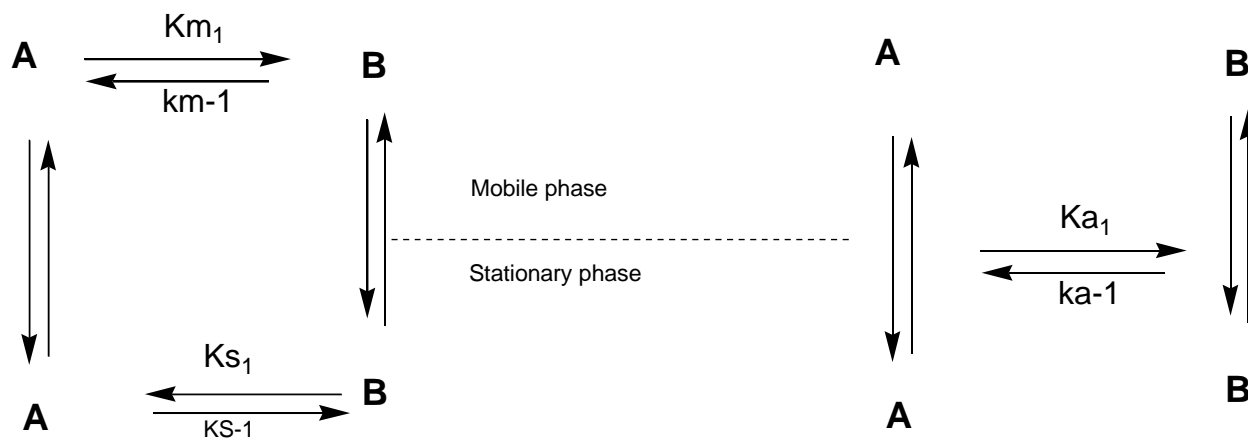
Dynamic HPLC is a well-known experimental approach for investigating enantiomerization barriers of stereolabile molecules during reversible conformational and configurational changes that operate on enantioselective stationary phases mediated by the eluent. It is one of the best available methods that provide an important role in chemistry and pharmaceutical science to understand the stereo dynamics of time and temperature-dependent enantioenriched molecules as well as help to obtain enantio-pure compounds. This experimental approach provides important parameters used to investigate the energy barrier to the rotation with the help of the simulation of a chromatogram performed in a software program that employs both stochastic and theoretical plate models. The chromatographic and kinetic parameters of the two interconverting enantiomers need to be optimized by simplex algorithm and equations. This helps to modulate peak tailing until

the simulated dynamic chromatogram is as much as possible superimposable with the experimental profile. Retention times of solutes, the theoretical plate number of each analyte, and the column hold-up time are crucial parameters to simulate peak profiles.

During stereomutation on-column approaches, the chiral stationary phase forms reversible non-covalent diastereoisomeric interactions with a chiral analyte in which the two diastereomeric complexes have different energies that translate in high selectivity. The relationship between chromatographic selectivity (α) and energy difference of the transient diastereoisomers combined in a single mathematical equation as follows

$$\Delta\Delta G^{\circ}_{2,1} = \Delta G^{\circ}_2 - \Delta G^{\circ}_1 = -RT \ln (k'_2 / k'_1) = -RT \ln \alpha \text{-----(1)}$$

$\Delta\Delta G^{\circ}_{2,1}$ is the difference between the Gibbs free energies of interaction of the two enantiomers with the selector, R is the gas constant, T is the absolute temperature and α is the ratio of the retention factors k'_2 and k'_1 of the two enantiomers.



Scheme:2.1 Enantiomers A and B equilibria happening in chromatographic column.

Where, the kinetic rate constant of the A/B interconversion in the mobile phase ($km_1 = km-1$), the kinetic rate constant of the B to A conversion in the stationary phase(ks_1), the kinetic rate constant of the A to B conversion in the stationary phase($ks-1$), apparent kinetic rate constant for B to A conversion(ka_1), apparent kinetic rate constant for B to A conversion($ka-1$). For temperature-dependent interconversion, the rapid interconversion of the enantiomers can produce a plateau

composed of racemized molecule between the two peaks, coalescence or decoalescence of peaks can be seen as the isomerization becomes faster or slower than the elution process. Apparent rate constants extracted from the simulation for the on-column interconversion and energetic barrier of isomerization (ΔG^\ddagger) from enthalpic and entropic are:

$$\ln(k/T) = -\Delta H^\ddagger/R \cdot 1/T + \ln(\kappa k_B/h) + \Delta S^\ddagger/R \quad (2)$$

$$k = (\kappa k_B T/h) e^{-\Delta G^\ddagger/RT} \quad (3)$$

where, ΔG^\ddagger = free energy activation and $\Delta G^\ddagger = \Delta H^\ddagger - T\Delta S^\ddagger$, k = Rate constants, k_B = the Boltzmann's constant (1.381×10^{-23} J/K), h = Planck's constant (6.626×10^{-34} Js).

Plotting $\ln(k/T)$ vs $1/T$, the slope of the straight line is $-\Delta H^\ddagger/R$ and hence $\Delta H^\ddagger = -(\text{slope})R$. From the same plot, the intercept is:

$$\text{intercept} = \ln(k_B/h) + \Delta S^\ddagger/R$$

$$\Delta S^\ddagger = R(\text{intercept} - \ln(k_B/h))$$

2.2 Aim of the work and research strategies

The target of this project was to study the stereochemical stability or instability of N-N atropisomeric hydrazides (DB-01 to DB-08) by chromatographic approaches and optimize resolution methods for enantiomers. Particular efforts have been made to obtain optimized conditions to separate stable atropisomeric molecules and investigate activation parameters. The HPLC-CD coupling system was employed and chiral HPLC was provided. SP achiral column was used to control the purity of each racemic molecule. The studied atropisomeric hydrazides are shown in the figure below.

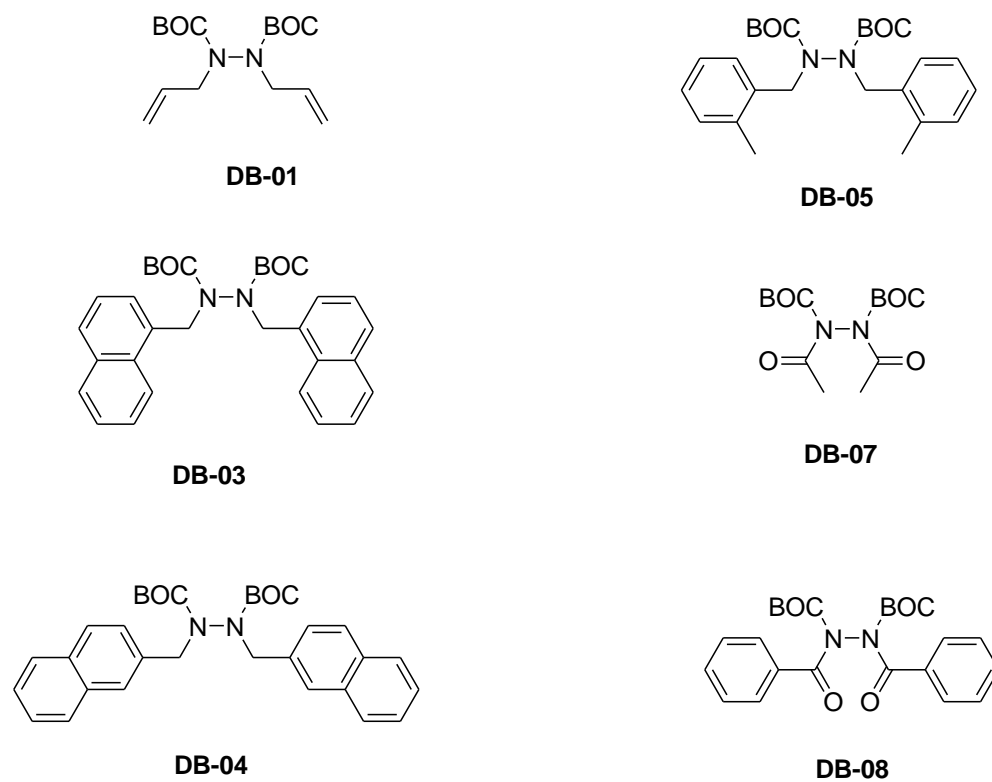
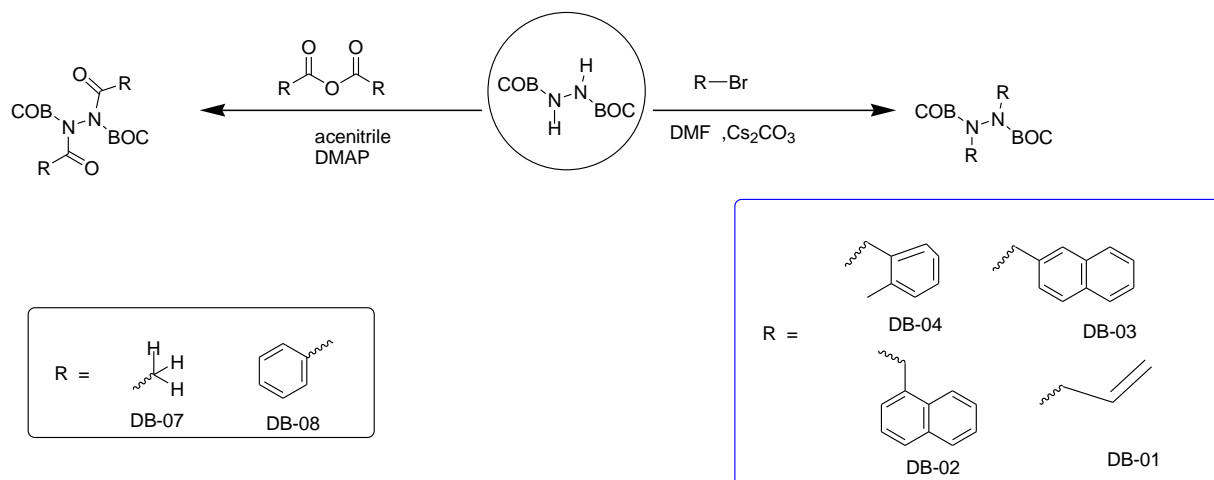


Figure 2.9. Structures of investigated hydrazides

2.3 Synthesis of the investigated hydrazides

Atropisomeric hydrazides (DB-01 to DB-08) have been synthesized as racemic with methodology indicated in reported literature.^{19,36} Di-tert-butyl hydrazine-1,2-dicarboxylate and the corresponding bromide derivatives or anhydrides were utilized to give the desired compounds.^{19,37}



Scheme.2.2 Synthetic procedures for investigated atropisomeric hydrazides.

2.4 Results and Discussion

The atropisomeric N-N interconversion of samples DB-01 to DB-08 (figure 2.9) was investigated by liquid chromatography. All the six atropisomeric are chiral and the hindered rotation around N-N single bond generates enantiomers. Two approaches were used: i) the off-column racemization process monitored by enantioselective HPLC and ii) the online enantiomerization process on chiral stationary phase at variable temperature. After initial screening aiming for the optimization of analytical conditions for each racemate, racemization and/or enantiomerization experiments were achieved. The purity of the racemic compound was checked on SP a chiral column as reported on figure 2.12. As reported in table 2.1, samples 5 and 6 were baseline separated at low temperatures (10°C and 0°C respectively) attesting to a fast-interconverting speed of each atropisomeric pair. When analyzed at room temperature, they showed a typical plateau between two peaks. Chromatographic profiles using UV and CD detectors were reported in figures 2.10 and figure 2.11 respectively. As expected, all CD traces have confirmed the enantiomeric nature of samples (opposite signals) being present only a stereogenic element. The elution conditions of each sample were listed in the experimental section.

Table 2.1. Chromatographic parameters of samples 1-6 after baseline optimized separation.

Sample	k_1	k_2	α	T °C
1	6.65	8.21	1.23	25
2	0.43	1.93	4.49	25
3	2.75	3.35	1.22	25
4	0.80	0.99	1.12	25
5	2.95	4.13	1.40	10
6	1.06	1.73	1.63	0

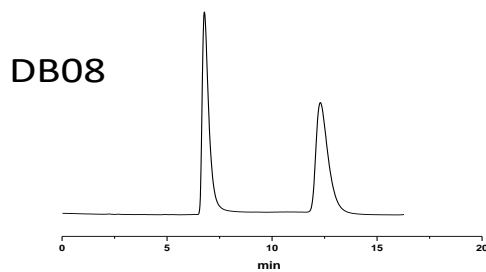
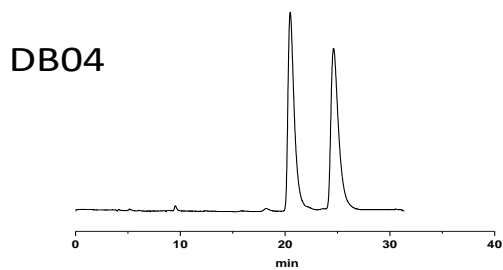
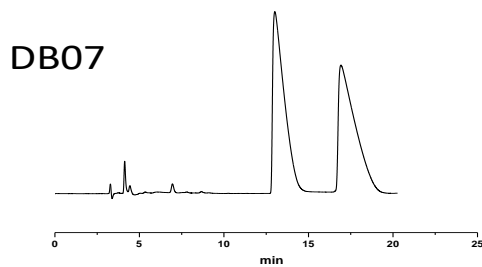
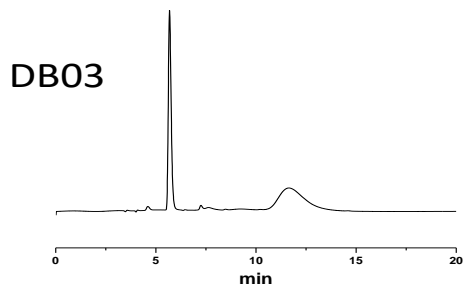
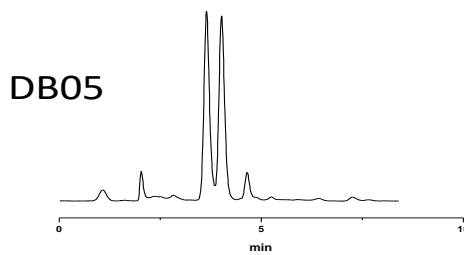
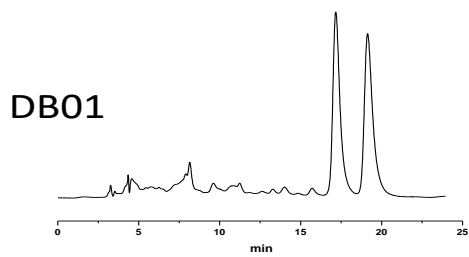


Figure 2.10. UV Chromatographic profiles of samples 1-6 (for analytical conditions see experimental section)

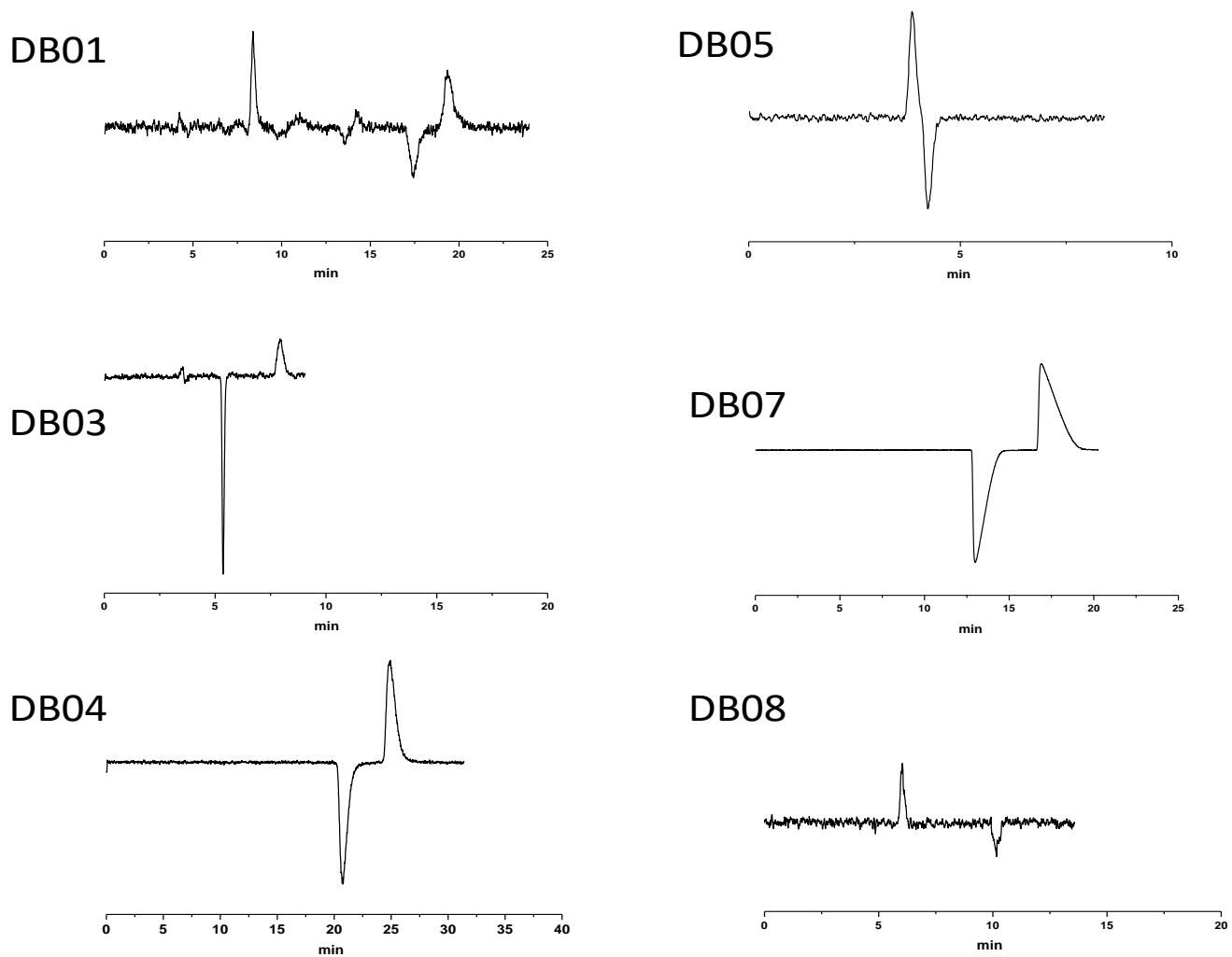


Figure 2.11. CD Chromatographic profiles of samples 1-6 (for analytical conditions see experimental section)

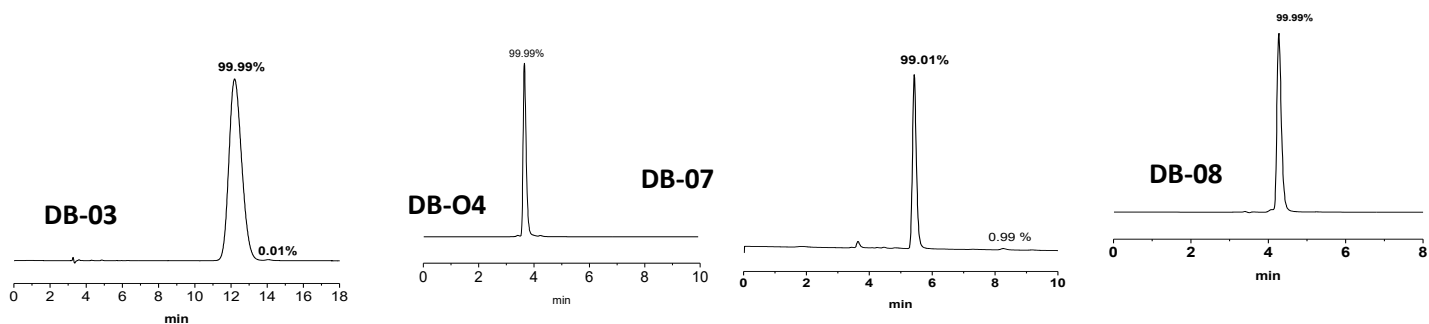


Figure 2.12 SP achiral test (for analytical conditions see experimental section)

Energy values of enantiomerization processes, temperature and speed constants were listed in table 2.2. Notably, by using the two off-column and on-column approaches, two different energy values were obtained: the ΔG of racemization from the off-column experiment and the ΔG of enantiomerization from the on-column one. The relationship between two values is: $k_{\text{racemization}} = 2k_{\text{enantiomerization}}$. To make easier the comparison of experimental data, all racemization free energies were converted into the corresponding enantiomerization values.

For samples 1-4, off-column approach was employed at 70 °C and values of free activation spanned between 24.3 Kcal/mol and 26.01 Kcal/mol. Specifically for sample 4, the value of 24.3 Kcal/mol is an estimated value due to the fast racemization (complete in less than 30 min) and to the low column performance in terms of enantioselectivity ($\alpha = 1.12$). A more flexible N-N bond is the one in sample DB-07. The plateau is visible at 40°C (see chromatogram in figure 2.13). The experimental profiles have been used to calculate the values of the energetic barriers and by Auto DHPLC y2k, simulated chromatogram furnished a $\Delta G_{\text{enant}}^{\ddagger}$ of 23.10 Kcal/mol. Unfortunately, it was not possible to acquire chromatograms at higher temperatures to preserve the integrity of polysaccharide-based stationary phase.

Table 2.2 Values of k_{rac} (min⁻¹) and k_{enantio} (min⁻¹) and the corresponding calculated $\Delta G_{\text{enantion}}^{\ddagger}$ (kcal/mol).

Sample	T (°C)	k_{rac} (min^{-1})	k_{enant} (min^{-1})	$\Delta G_{enant}^{\#}$ (Kcal/mol)	$t_{1/2}$
1	70	0.0111 ($R^2=0.9974$)	-	25.57	31 min
2	71	0.0064 ($R^2=0.9989$)	-	26.01	54 min
3	71	0.0250 ($R^2=0.9991$)	-	25.09	14 min
4	70	0.0645	-	$\approx 24.3^a$	5.4 min
5	40	-	0.0296	23.10 ^b	12 min
6	25 70	-	0.3560 ^b -	20.61 ^b 21.18 ^c	2 min

^a estimated value: the racemization is completed in 30 min. ^b averaged value between free energy of direct ($\Delta G_{1-2}^{\#}$) and reversed ($\Delta G_{2-1}^{\#}$) enantiomerization process. ^c extrapolated by Eyring equation.

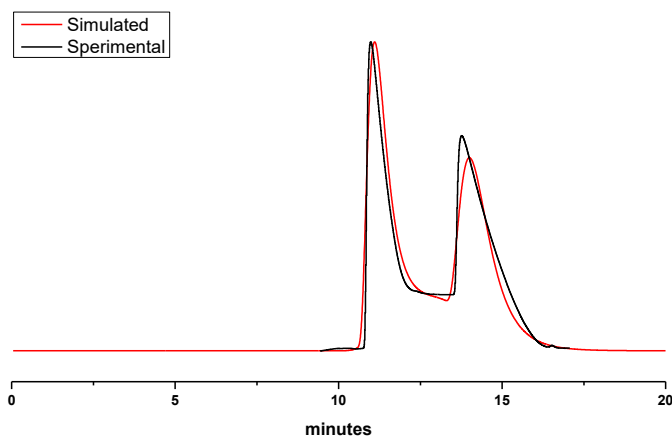


Figure 2.13. Auto DHPLC y2k simulated chromatogram based on the stochastic model: Simulated (red) and experimental (black) chromatographic profile of DB-07 at 40°C.

2.4.1 Energy barrier values at different temperatures for samples 3 and 6

Exploring the dependence of free energy versus temperature, two Eyring plots were built from sample 3 and sample 6 (Figure 2.16). Data were obtained by off-column racemization experiments for sample 3 and by on-column enantiomerization experiments for sample 6.

Table 2.3 Energy barrier values at different temperatures for samples 3 and 6

Sample	T (°C)	$\Delta G_{\text{enant}}^{\#}$ (Kcal/mol)	Chromatographic approach
3	50	24.49 ^a	Off-column
	57	24.68	
	62	24.73	
	71	25.09	
	80	25.31	
6	5	20.36 ^b	On-column
	10	20.37 ^b	
	25	20.61 ^b	

^a A value of 24.05 Kcal/mol was found when sample was dissolved in decalin. ^b Averaged value between free energy of direct ($\Delta G_{1-2}^{\#}$) and reversed ($\Delta G_{2-1}^{\#}$) enantiomerization process.

Complete separation has been achieved for sample DB-04 in presence of the (*R, R*) Whelk-01(4.6x250 mm) at room temperature (Figure 2.10 and 2.11) with complete racemization caused by interconversion started from 1st eluted enantiomer in decahydronaphthalene at 50 °C in 180min (Figure 2.14)

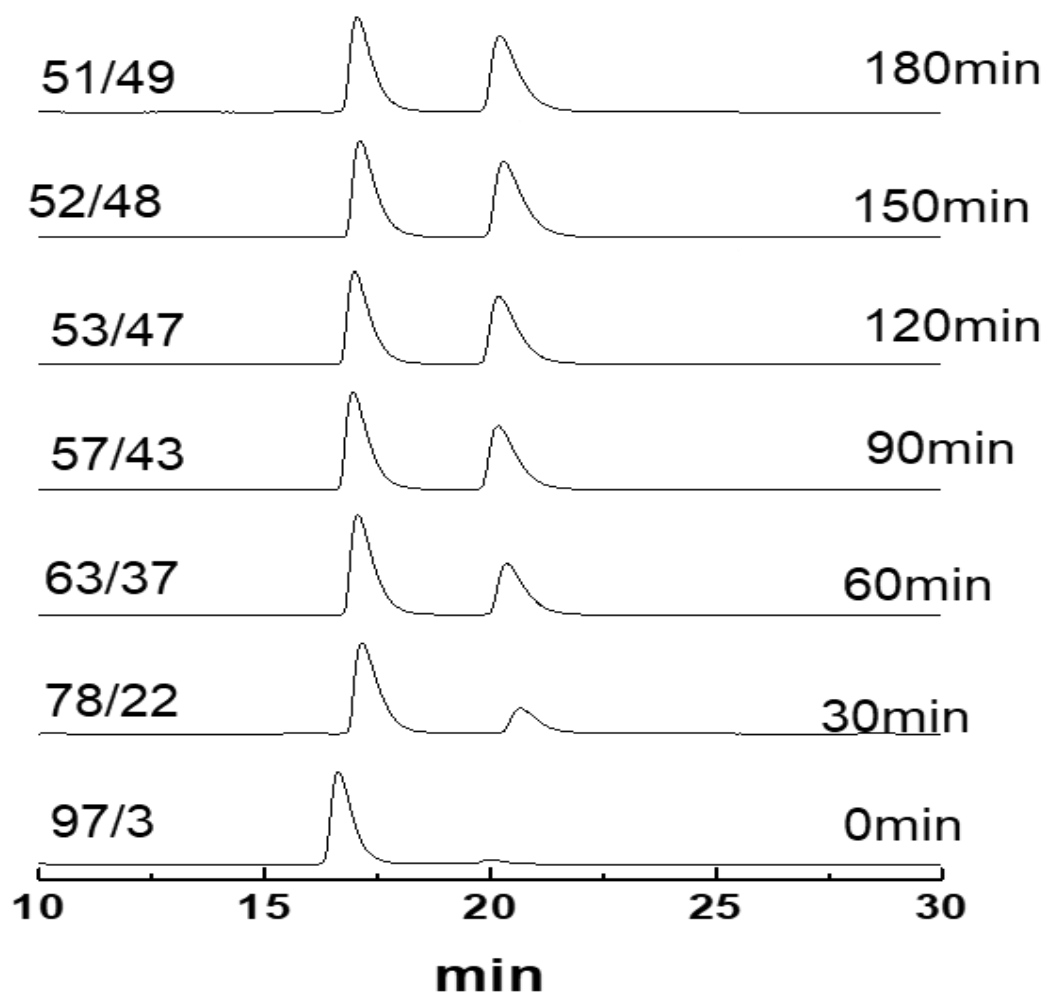


Figure 2.14 Thermal racemization of DB-04 (*R,R*) Whelk-01(4.6x250 mm), 1 mL/min, Hex/2-propanol (98/2), UV 254nm in decahydronaphthalene at 50 °C; started from 1st eluted enantiomer

The two enantiomers of DB-08 were separated on CSP IB 5 μ m (4.6x250 mm) in order of selectivity with a mobile phase composed of hexane/2-propanol (98/2) at 0 °C with the formation of plateaus caused by rapid interconversion at temperatures between 5 °C and 25 °C. The elution profiles of both UV and CD have been shown as figure 2.10 and figure 2.11 respectively. Variable temperature HPLC experiments (figure 2.15) have been performed to slow down the enantiomerization process and to reach a decoalescence of peaks at 25 °C.

The determined experimental data from the elution profiles are summarized in table 2.4. From these data, the energy barrier of benzoyl-substituted DB-08 was lower than that of the 2-methylnaphthalene substituted DB-04.

This lower energy value (ΔG_{enant}) of sample DB-08 of 20.60 Kcal/mol at 25°C has been calculated by simulation of the corresponding dynamic chromatogram (Table 2.4). The dynamic chromatographic profiles obtained at column temperatures of 0°C, 5°C, 10°C and 25°C were simulated using a stochastic model to obtain the kinetic parameters of the interconversion between 1 and 2 stereoisomers (table 2.4). A plateau between the peaks is observed starting from a temperature of the column at 10°C.

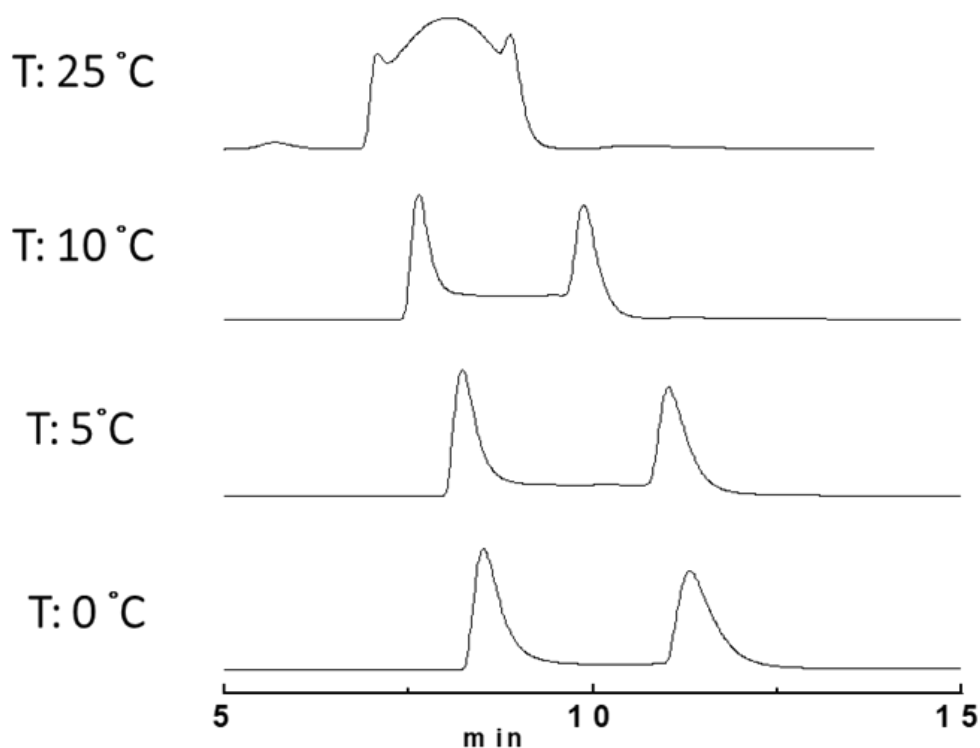


Figure 2.15. Dynamic-HPLC elution profiles(enantiomerization) of DB 08: Chiralplak IB (250 x 4.6 mm, L x ID) in hexane/2-propanol 98/2, flow rate 1.0 ml/min, UV 254. All temperatures are considered $\pm 0.1^\circ\text{C}$.

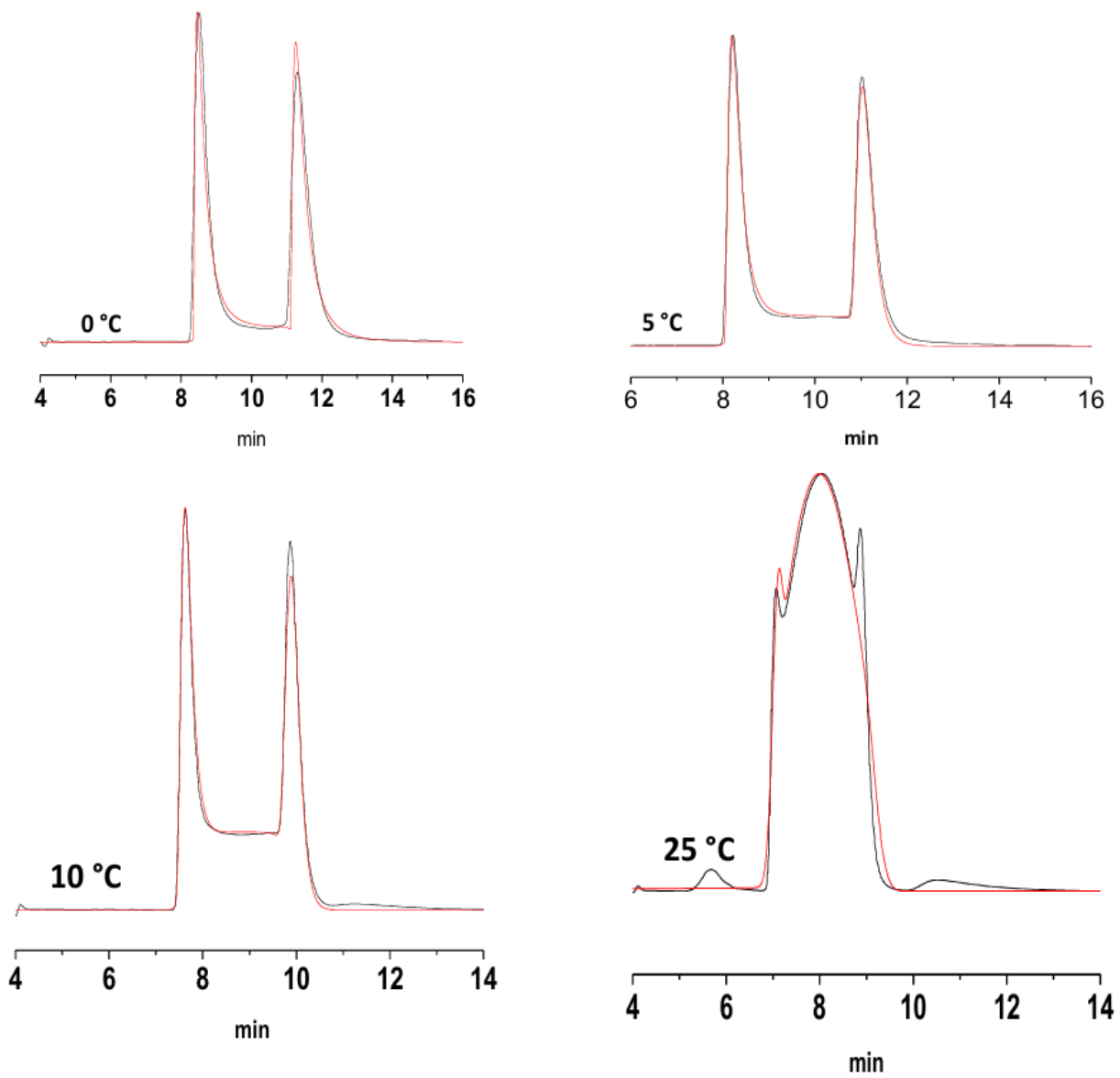


Figure 2.16 - Auto DHPLC y2k simulated chromatogram simulated (red) and experimental (black) chromatograms of DB-08.

2.4.2 Energy Barrier Values versus Temperatures: Eyring Plots

Exploring the dependence of free energy versus temperature, two Eyring plots were built from samples DB-04 and DB-08 (Table 2.4, Figure 2.17). Data were obtained by off-column racemization experiments for sample DB-04 and by on-column enantiomerization experiments for sample DB-08. In both cases, a slight increment of ΔG was recorded as temperature increased. In addition, good linearity was observed plotting $1/T$ vs $\Delta G/T$ ($R^2 = 0.994$ and $R^2 = 0.998$ for sample 3 and sample 6 respectively) and the corresponding equations have shown a not negligible entropic effect in the N-N interconversion process. The ΔH values are 15.45 Kcal/mol and 17.39 Kcal/mol while the ΔS values are -27.9 u.e. and -10.6 u.e. for sample DB-04 and sample DB-08

Table 2.4 Energetic barrier of the on-column enantiomerization of molecule DB-04. Column temperatures are intended $\pm 0,1$ °C. Errors in $\Delta G \pm 0,02$ kcal/mol.

Temperature(°C)	ΔG	1/T(k)	$\Delta G/t$
50	24,49	0,0031	0,0758
57	24,68	0,0030	0,0748
62	24,73	0,0030	0,0738
71	25,09	0,0029	0,0720
80	25,31	0,0028	0,0717

Table 2.5 Energetic barrier of the on-column enantiomerization of molecule DB-08. Column temperatures are intended $\pm 0,1$ °C. Errors in $\Delta G \pm 0,02$ kcal/mol.

Temperature(°C)	ΔG	1/T(k)	$\Delta G/t$
25	20,59	0,00335	0,06905
10	20,37	0,00353	0,07193
5	20,36	0,00360	0,07320

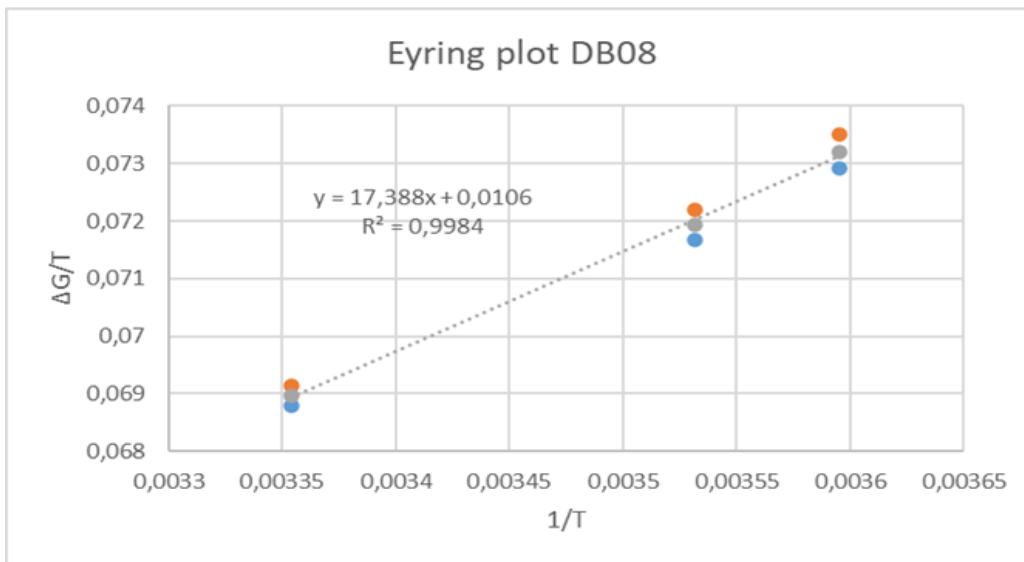
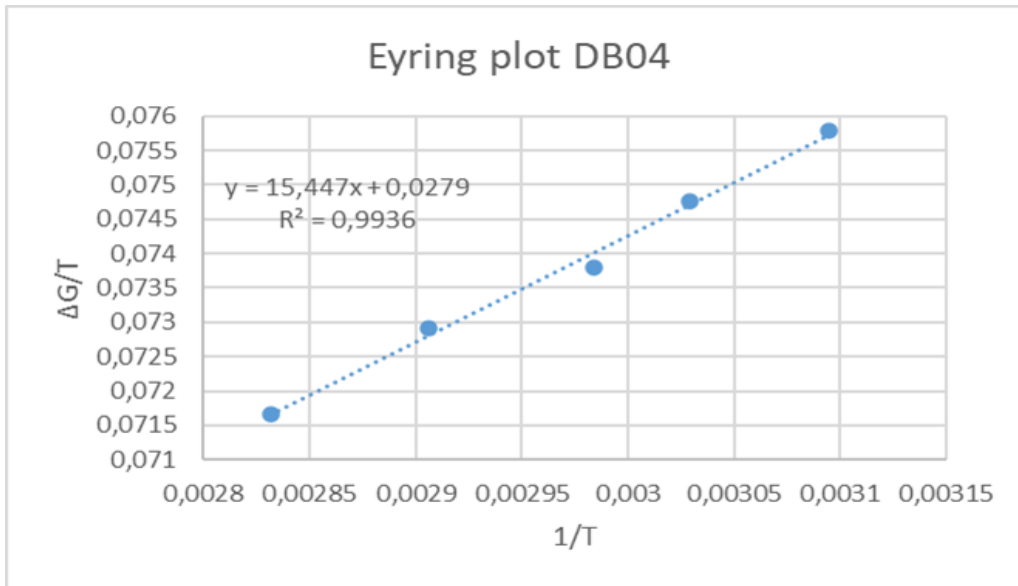


Figure 2.17. Eyring plot of atropisomeric hydrazides DB-04 and DB-08

2.4.3 Comparison: experimental and computational data

At the end, the investigated the energy barrier values by experimental have been compared with computational data (See Table 2.6, Figure 2.18). The advantage to compare these two types of data not only help to validate the obtained energy barrier but also to confirm their role in the design and development of novel atropisomeric scaffolds. The agreement of energy barrier values obtained by the on-column and off-column experimental methods with computational work, makes them a correct approach for the prediction of the rotational energy barrier of atropisomeric molecules.

The integration of these works revealed the impact of electronic and steric effects in the analyzed atropisomers hydrazides compounds (DB-01 to DB-08). The higher p-orbital character of the nitrogen atoms dominates, becoming the main reason for the barrier observed during the racemization process.

Table 2.6: Computed energy barrier values compared with the experimental ones

Samples	ΔG_{exp} [kcal/mol]	T exp [°C]	ΔG_{comp} [kcal/mol]	Deviation from experimental value [%]
DB01	25.57	70	24.81	-2.96
DB03	26.01	71	36.23	39.29
DB04	25.09	71	26.31	4.87
DB05	<24.3	70	29.23	20.29
DB07	23.10	40	28.46	23.20
DB08	20.61	25	22.57	9.52

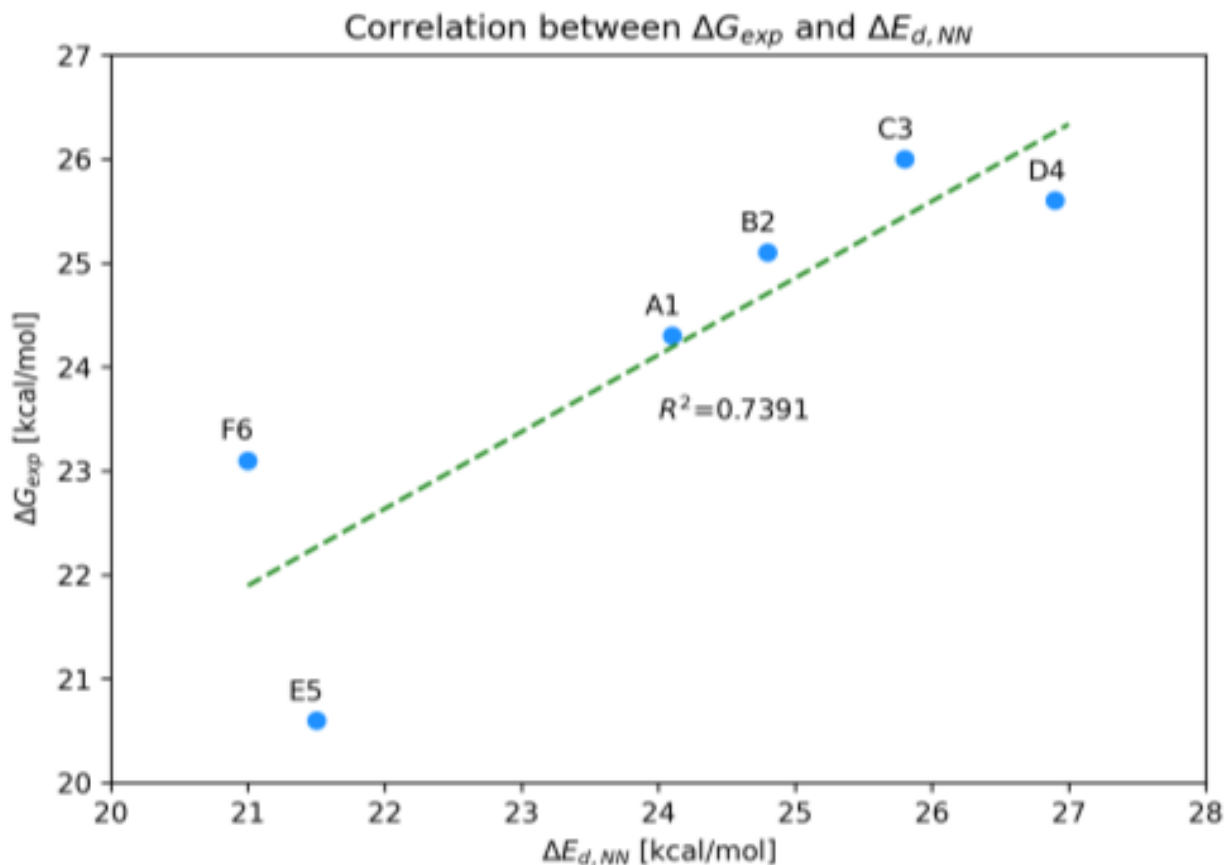


Figure 2.18 Correlation between experimental ΔG and NN distortion energy (F6 and E5 represent DB-07 and DB-08 respectively)

2.5 Conclusion

As the preliminary as well as the backbone of this work, the chiral resolution of the racemic mixtures of atropisomeric hydrazides by UV and CD on CSP HPLC has been successfully reached. Based on the stability of enantiomers, the rates of interconversion and the energetic barriers have been investigated with off-column and on-column experiments. By these two experimental approaches, the relationship between energy values of enantiomerization, temperature, and rate constants has been revealed. Generally, the combination of computational insight with thermal racemization and dynamic chromatography, the studies of the stereochemical stability of the six compounds has been achieved in a precise way.

2.6 Experimental section

Methods and Materials

Materials

All solvents were LC grade and were purchased from Sigma-Aldrich (St. Louis, MO, USA). Solutions of samples were prepared in mobile phases. Analytical HPLC columns were employed: Chiralplak IB (250*4.6 mm ID) and Chiralpak IG-3 (250*4.6 mm ID) from Daicel Corporation (Osaka, Japan), Lux-cellulose 5micron (150*4.6 mm ID) from Phenomenex (Torrance, CA, USA), (*R, R*)-Whelk-O1 (250*4.6 mm ID) and (*R, R*)-Whelk-O1 (150*4.6 mm ID) from Regis Technologies (Morton Grove, IL, USA). To control the purity of enantiomers, Luna 5u Silica (250 * 4.6mm) was used on a JASCO HPLC instrument equipped with two UV detections. The analyzed atropisomeric hydrazides samples were provided by Professor Bencivenni's research group, at Bologna University, Italy.

Instrumentation

A Jasco LC (Jasco Europe, LC, Italy) equipped with dual gradient pumps was employed and connected with UV975 and UV-CD 955 detectors and with a column module. The heating was set by using an in-house sheath with a 30°-80°C temperature range. Column temperature was maintained within ± 0.5 °C by means of an electronic controller. For lower temperatures, an ice/water-filled Dewar was employed. The uncertainty in temperature measurements can be estimated as ± 0.5 °C.

Analytical conditions

Sample 1: (*R,R*) Whelk-O1 CSP (150 x 4.6 mm, L x ID), eluent hexane/2-propanol 90/10, flow rate 1.0 ml/min, UV 254 (weak CD signal at 265 nm: 1st eluted (-), 2nd eluted (+)).

Sample 2: Chiralplak IG-3 CSP (250 x 4.6 mm, L x ID), eluent hexane/ethanol 100/5, flow rate 1.0 ml/min, UV 254 (CD signal at 265 nm: 1st eluted (-), 2nd eluted (+)).

Sample 3: (*R,R*) Whelk-O1 CSP (250 x 4.6 mm, L x ID), eluent hexane/2-propanol 98/2, flow rate 1.0 ml/min, UV 254 (CD signal at 230 nm: 1st eluted (-), 2nd eluted (+)).

Sample 4: Lux 5 μ m Cellulose-1 (150 x 4.6 mm, L x ID), eluent hexane/ethanol 100/1, flow rate 1.0 ml/min, UV 280 (CD signal at 254 nm: 1st eluted (+), 2nd eluted (-)).

Sample 5: Chiralplak IG-3 CSP (250 x 4.6 mm, L x ID), eluent hexane/2-propanol 100/1, flow rate 1.0 ml/min, UV 254 (CD signal at 265 nm: 1st eluted (-), 2nd eluted (+)).

Sample 6: Chiralplak IB (250 x 4.6 mm, L x ID), eluent hexane/2-propanol 98/2, flow rate 1.0 ml/min, UV 254 (CD signal at 254 nm: 1st eluted (+), 2nd eluted (-)).

Analytical conditions of SP achiral test

DB-03: Luna 5u Silica (250 x 4.6mm), 1 mL/min, hex/DCM (60/40) +0.05% ethanol, UV254 nm

DB-04: Luna 5u Silica (250 x 4.6mm), Eluent: hex/2-propanol (80/20), UV254 nm

DB-07: Luna 5u Silica (250 * 4.6mm), 1 mL/min, hex/IPA (98/2) ,5 °C, UV254nm

DB-08: Luna 5u Silica (250 * 4.6mm), 1 mL/min, hex/DCM (60/40) +0.05% ethanol, UV254nm

Racemization studies

The racemization experiments were made by the off-column approach. Previously HPLC separated enantiomer of each racemate was dissolved in a closed vial and it was heated at a fixed temperature. Samples were withdrawn at fixed time intervals and analyzed by enantioselective HPLC under the analytical conditions reported in the previous section. The solvent used to dissolve samples was 2-propanol in all cases. In addition, only for sample 3, some experiments were done in decalin.

Enantiomerization studies

Variable temperature chromatography was performed by placing the chiral HPLC column in the specific temperature control module and chromatograms were acquired (n.3 replicate injection for each temperature). Simulations of variable-temperature experimental chromatograms were performed by Auto DHPLC y2k ((a) J. Am. Chem. Soc. 2000, 122, 4776– 4780; (b) J. Sep. Sci. 2001, 24, 941– 952; J. of Chromatogr. A, 1647 (2021) 46214) based on the stochastic model.

Simulation of dynamic chromatograms

The simulation of variable temperature experimental chromatograms was done by employing a stochastic model in Auto-D-HPLC-Y2 K software. Chromatographic and kinetic parameters were optimized by utilizing the simplex algorithm until the agreement between experimental and simulated dynamic chromatograms. The value of error in determining the activation-free energies was estimated to be ± 0.2 kcal/mol.

Reference.

1. Ghislaine,V,;Jeanne,C.; Pasteur and chirality:A story of how serendipity favors the prepared minds.Chirality. 2021, 33,597–601
2. Joseph,G. The Discovery of Biological Enantioselectivity: Louis Pasteurand the Fermentation of Tartaric Acid, 1857—A Reviewand Analysis 150 Yr Later. Chirality,2008.20,5–19
3. Nguyen,A.; He,H.; Pham-Huy,C. Chiral Drugs: An overview. Int. J. Biomed. Sci. 2006, 2, 85–100
4. Jessica,C.; Domenico,I.;Angelica,F.; Michele,L.;Carmela.S.;Inmaculada.A.;Maria Stefania,S.;Alessia,C.A Look at the Importance of Chirality in Drug Activity: Some Significant Examples. Appl. Sci. 2022, 12, 10909.
5. Kazunobu,I.;Shusaku A.;Yuki Y.;Yuuya K.;Katsuhiko T.Analysis of Stereochemical Stability of Dynamic Chiral Molecules Using an Automated Microflow Measurement System. J. Org. Chem. 2021, 86, 9651–9657
6. Xiaoze B.;Jean R.;Damien B.EnantioselectiveSynthesis of Atropisomers with Multiple Stereogenic Axes. Angew.Chem. Int.Ed. 2020, 59, 12623–12634
7. Rosa L.;Claudio P.;Planar Chirality:AMine for Catalysis and Structure Discovery.Angew.Chem. Int.Ed. 2022, 61,e202113504
8. Michel R.;Marcel M.; Michal J.;Strain-induced helical chirality in polyaromatic systems.Chem.Soc. Rev.2016, 45, 1542-1556
9. Dawid J.;Michalina K.;Przemysław J.;A Review of Modifications of Quinoline Antimalarials: Mefloquine and (hydroxy)Chloroquine.Molecules 2022, 27, 100
10. Croft, A. A lesson learnt: the rise and fall of Lariam and Halfan. J. R. Soc. Med. 2007, 100 (4), 170–174.
11. Sean T.;Jeffrey L. Atropisomerism in medicinal chemistry: challenges and opportunities. Future Med. Chem. (2018) 10(4), 409–422.
12. Andrea Mazzanti, Maria Boffa, Emanuela Marotta,Michele Mancinelli Axial Chirality about Boron–Carbon Bond: Atropisomeric Azaborines. Org. Lett. 2016, 18, 2692–2695

13. Akila I.;Angel U.;Sivaguru.J. Understanding Conformational Preferences of Atropisomeric Hydrazides and Its Influence on Excited State Transformations in Crystalline Media. *Molecules* 2019, 24, 3001
14. Oki, M. *Topics in Stereochemistry*, 1983
15. Steven R.;Paul J.;Lee D.;Araz J.;Oliver Hucke.Revealing Atropisomer Axial Chirality in Drug Discovery. *ChemMedChem* 2011, 6, 505–513
16. Patel L.;Chandrasekhar J.;Evarts J.Discovery of orally efficacious phosphoinositide 3-kinase d inhibitors with improved metabolic stability. *J Med Chem.* 2016; 59,9228–9242
17. Peter W.Recent encounters with atropisomerism in drug discovery. *Bioorganic & Medicinal Chemistry Letters* 28 ,2018,53–60
18. Jonathan C.; Wesley J.;Paul J.;Steven R.The Challenge of Atropisomerism in Drug Discovery. *Angew. Chem. Int. Ed.* 2009, 48, 6398–6401
19. Andrea Pellegrini,Laura Marcon,Paolo Righi ,Giovanni Centonze,Chiara Portolani ,Marco Capodiferro,Shilashi Oljira ,Simone Manetto ,Alessia Ciogli ,Giorgio Bencivenni.On the Nature of the Rotational Energy Barrier of Atropisomeric Hydrazides. *Molecules* 2023, 28, 7856.
20. Clayden J.;Moran W.;Edwards P.; LaPlante S.The challenge of atropisomerism in drug discovery. *Angew.Chem.Int.Ed.Engl.*2009, 48(35), 6398–6401
21. Eveleigh P.;Hulme E.;Schudt C.;Birdsall N.The existence of stable enantiomers of telencepine and their stereoselective interaction with muscarinic receptor subtypes. *Mol. Phamacology*,1989, 35(4), 477–483
22. Bringmann G.;Mortimer A.;Keller P.; Gresser M.;Garner J.;Matthias B.Atroposelective synthesis of axially chiral biaryl compounds. *Angew.Chem.Int.Ed.*2005,44, 5384–5427
23. Bringmann G.;Gulder T.;Gulder T.;Breuning M. Atroposelective total synthesis of axially chiral biaryl natural products. *Chem. Rev.*2011,111(2), 563–639
24. Wang J.;Zeng W.;Li S.Discovery and assessment of atropisomers of (±)-lesinurad. *ACS Med. Chem. Lett.*2017, 8(3), 299–303
25. Brown D.;Bostrom J.Analysis of past and present synthetic methodologies on medicinal chemistry: where have all the new reactions gone? *J. Med. Chem.* 2016,59(10), 4443–4458
26. Roughley S.;Jordan A.The medicinal chemist’s toolbox: an analysis of reactions used in the pursuit of drug candidates. *J. Med. Chem.* 2011,54(10), 3451–3479

27. Chin C.; Roger A. Stereochemistry of, *N, N'*-dipyrryls. resolution of *N, N',2,5,2',5'*-Tetramethyl-3,3'-dicarboxydipyrryl. *J. Am. Chem. Soc.* 1931, 53, 2353–2357.
28. Rizzo, S.; Menta, S.; Faggi, C.; Pierini, M.; Cirilli, R. Influence of the nature of alkyl substituents on the high-performance liquid chromatography enantioseparation and retention of new atropisomeric 1,1-benzimidazole derivatives on amylose tris(3,5-dimethylphenylcarbamate) chiral stationary phase. *J. Chromatogr. A* 2014, 1363, 128–136.
29. Kobayashi, T.; Ishiwari, F.; Fukushima, T.; Hanaya, K.; Sugai, T.; Higashibayashi, S. Analysis of Interconversion between Atropisomers of Chiral Substituted 9,9'-Bicarbazole. *Eur. J. Org. Chem.* 2021, 2021, 449–451.
30. Jia F.; Chuan-Jun L.; Ren-Rong L. Catalytic Asymmetric Synthesis of Atropisomers Featuring an Aza Axis. *Acc. Chem. Res.* 2023, 56, 2537–2554
31. Chiara Portolani, Giovanni Centonze, Sara Luciani, Andrea Pellegrini, Paolo Righi, Andrea Mazzanti, Alessia Ciogli, Andrea Sorato, Giorgio Bencivenni. Synthesis of Atropisomeric Hydrazides by One-Pot Sequential Enantio- and Diastereoselective Catalysis. *Angew. Chem. Int. Ed.* 2022, 61, e202209895
32. Xia W.; Shao-Jie W.; Xiaolan X.; Hao A.; Zhifeng T.; Hui Y.; Ming Wah W.; Shenci L. Enantioconvergent and diastereoselective synthesis of atropisomeric hydrazides bearing a cyclic quaternary stereocenter through ternary catalysis. *Chem. Sci.*, 2024, 15, 13240–13249
33. Giovanni Centonze; Chiara Portolani; Paolo Righi; Giorgio Bencivenni. Enantioselective Strategies for The Synthesis of N-N Atropisomers. *Angew. Chem. Int. Ed.* 2023, 62, e202303966
34. Akila I.; Angel U.; Sivaguru. J. Understanding Conformational Preferences of Atropisomeric Hydrazides and Its Influence on Excited State Transformations in Crystalline Media. *Molecules* 2019, 24, 3001
35. Fabrizio P. Atropisomeric bis-heterocycles as chiral pools for asymmetric transformations. Cardiff University, 2018/ DOI: <http://dx.medra.org/10.17374/targets.2018.21.348>
36. Wang, X.; Zhang, P.; Xu, Q.; Guo, C.; Zhang, D.; Lu, C.; Liu, R. Enantioselective Synthesis of Nitrogen–Nitrogen Biaryl Atropisomers via Copper-Catalyzed Friedel–Crafts Alkylation Reaction. *J. Am. Chem. Soc.* 2021, 143, 15005–15010

37. Rasmussen, L. Facile Synthesis of Mono-, Di-, and Trisubstituted Alpha-Unbranched Hydrazines. *J. Org. Chem.* 2006, 71, 3627–3629.
38. Ciogli, A.; Vivek Kumar, S.; Mancinelli, M.; Mazzanti, A.; Perumal, A.; Severic, C.; Villania, C. Atropisomerism in 3-arylthiazolidine-2-thiones. A combined dynamic NMR and dynamic HPLC study. *Org. Biomol. Chem.*, 2016, 14, 11137–11147
39. Ciogli, A.; Wolfgang, B., Wolfgang, L. determination of enantiomerization barriers of hypericin and pseudohypericin by dynamic high-performance liquid chromatography on immobilized polysaccharide-type chiral stationary phases and Off-Column racemization experiments. *CHIRALITY*, 2010, 22:463–471.

Part-C

Symmetric Amido-thiourea Organocatalysts for the Synthesis of α -Aminonitriles

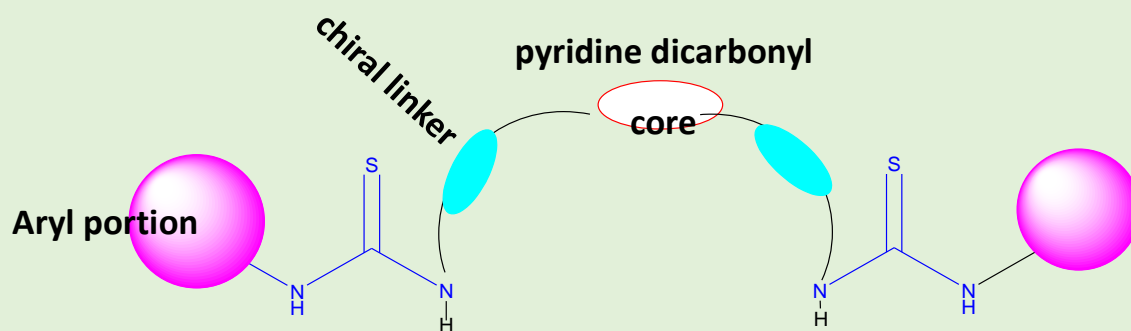
Research period abroad

This research work was carried out at the Institute of Organic Chemistry, University of Munster (Germany) in the research group of Prof. Olga Garcia Mancheño for 6 months (27/11/2023-31/05/2024). During my stay, I have been involved in the ‘Synthesis of Symmetric amido-thiourea Organocatalysts for the Synthesis of α -aminonitriles

3.1 Aim of the Research Work

Since, *N, N*-dimethylformamide (**12**), novel chiral amide-organocatalyst **16**, and symmetric chiral amide **19** proved to be effective catalysts for the Strecker reaction, we become more interested in the rational design and synthesis of new symmetric chiral amido-thiourea aiming at developing a more powerful and effective three-component Strecker reaction. Different thiourea-organocatalysts displayed hydrogen bonding catalysis for the synthesis of α -aminonitriles. However, symmetric thiourea-organocatalysts containing pyridines as spacer have never been investigated for the three-component Strecker reaction of an aldehyde, amine, and cyanide source. With this research strategy, we aimed to develop new catalysts that may avail an additional activation approach with H-bonding catalysis. To develop novel thiourea-catalytic based pyridine spacer that may act as hydrogen-bonding catalysis and Lewis-base has become the focus of attention. It was postulated that the presence of lone pair of electrons in the spacer would allow for greater reactivity and selectivity. We have considered that the presence of this lone pair on the pyridine molecule may avail new influence of catalysis that allow the activation of both nucleophilic and electrophilic reactants and lead to chemical transformation towards to excellent catalytic activity and stereochemical control.

Generally, our target is to develop symmetric thiourea-organocatalysts using spacer containing pyridine structure where hydrogen-bonding catalysis, anion-binding and Lewis-base has become the focus of attention.



3.2 Introduction

3.2.1 H-bond donor catalysis: Focus of thiourea organocatalysts

Covalent and non-covalent catalysis are the two common approaches to activate substrates and reactants through organocatalysis.^{1,2} In the first approach, the catalyst covalently binds the substrate, whereas in the latter case, activation of the substrate towards the asymmetric transformation is accomplished through non-covalent contacts with the substrates such as hydrogen bonds, van der Waals or ionic interactions, etc.^{3,4} Organocatalysts exhibit insensitivity to air and moisture, as well as display a lower environmental problem than metal-containing materials. From this point of view, the catalysis involving hydrogen bonding interactions between a catalyst and substrates has gotten great attention for more than one decade.^{5,6,7}

Thiourea-organocatalysis is a powerful tool in the synthesis of optically active molecules used in different medicinal and industrial fields. Thioureas have a crucial role in asymmetric catalysis as they can form strong hydrogen bonds that activate the substrates.^{8,9,10} This class of organocatalysts can act as Brønsted bases (through the S-atom)¹¹ and Brønsted acids^{12,13} by hydrogen bonding (through the NH-groups). Thiourea-organocatalysis became an acceptable protocol in different chemical reactions due to the excellent catalytic activity and stereochemically control.

To boost dissymmetric reactions and enhance the rates with the addition of a variety of structural motifs, the structure of thiourea catalysts can easily be modified. The introduction of electron-withdrawing groups at the nitrogen, which pulls electron density away from the nitrogen atoms, is widely used in thiourea organocatalysts, since it makes them stronger hydrogen donors and allows them to donate in multiple hydrogen bonding interactions.^{14,15} In this regard, the 3,5-bis(trifluoromethyl)phenyl group was introduced as a key structural motif in thiourea catalysts in 2003 (Figure 3.1)¹⁹, and used to increase catalyst polarity, polarizability, acidity, and π - π interactions through the highly polarized aryl groups.^{16,17,18}

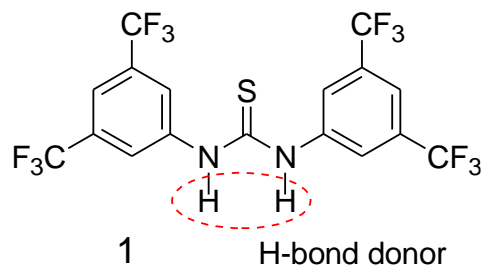


Figure 3.1. Symmetrical H-bond donor Schreiner's thiourea ¹⁹

As mentioned above, organic molecules capable of activating substrates via noncovalent hydrogen-bond interactions have turned up as an important approach in organocatalysis. It is a type of catalysis that activates substrates through inter- or intramolecular H-bond formation or attractive interaction between a hydrogen atom of the compound or a fragment X–H, where X is more electronegative than H.²¹ The Jacobsen's and Schreiner's thioureas shown in Figure 3.2 are exemplary for this class of organocatalysts.^{22,23}

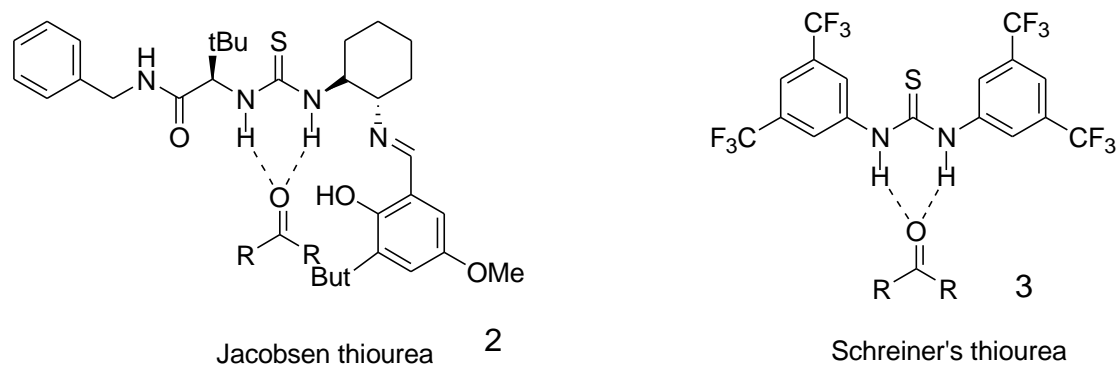


Figure 3.2. H-bonding organocatalysts activating a carbonyl

The development of bifunctional H-bond donor organocatalysts had a remarkable influence on the advance of noncovalent catalysis since they allow the simultaneous activation and coordination of both nucleophilic and electrophilic reactants.^{24,25,26} For instance, an H-bond donor bifunctional organocatalyst derived from a chiral 1,2-diamine scaffold such as quinuclidine or cyclohexane-1,2-diamine, that contains a tertiary amine functionality and a hydrogen bonding donor moiety in the form of thiourea or (thio)squaramide has been often applied ²⁷ (Figure 3.3).

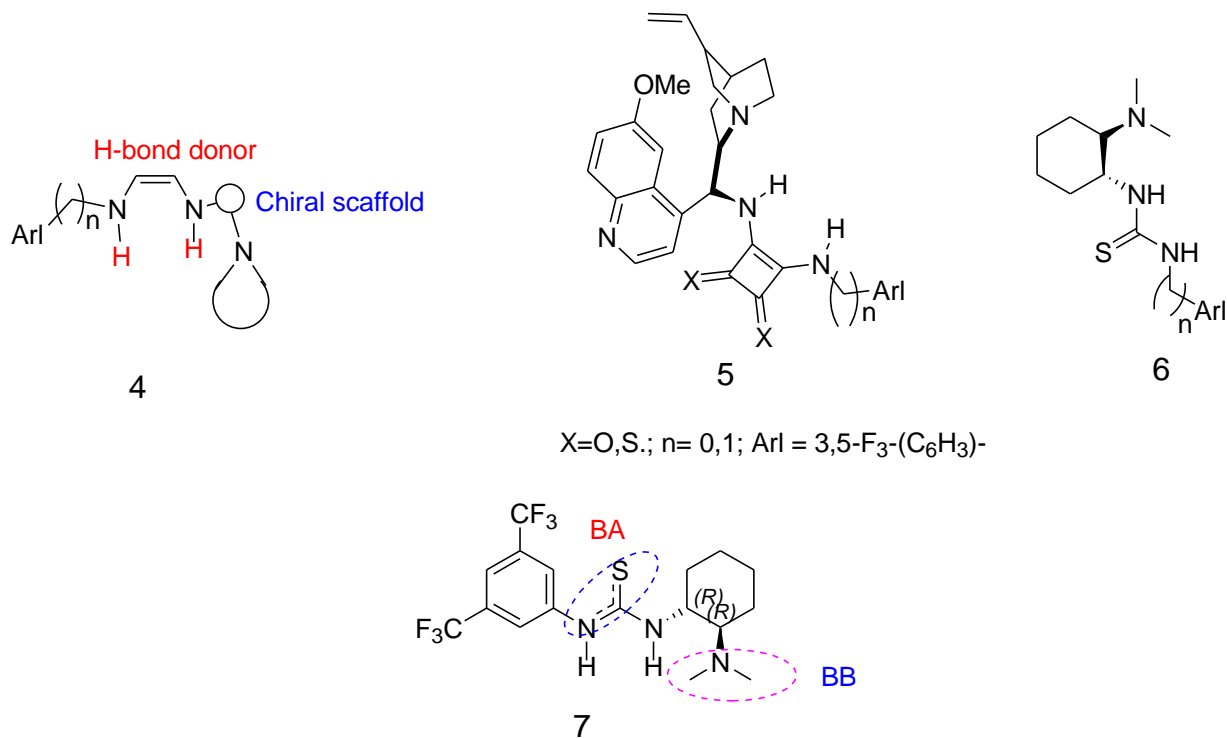
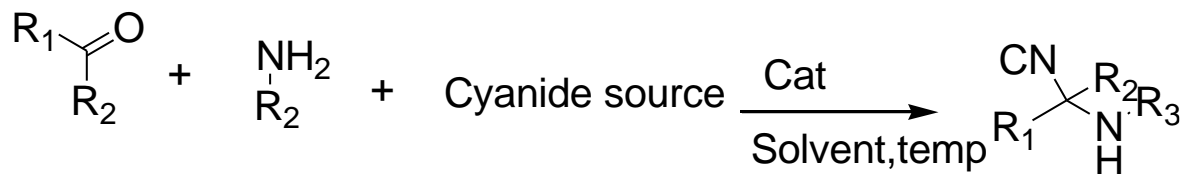


Figure 3.3 H-bond donor and Brønsted acid/bases bifunctional thiourea ²⁰

3.2.3 Hydrogen bond catalyzed synthesis of α -aminonitriles

The asymmetric Strecker reaction represents one of the well-known reactions via hydrocyanation of imines to afford α -amino nitriles, which can be synthesized from the three components of an aldehyde or ketone, amine, and a cyanide source ^{28,29} (Scheme 3.1).

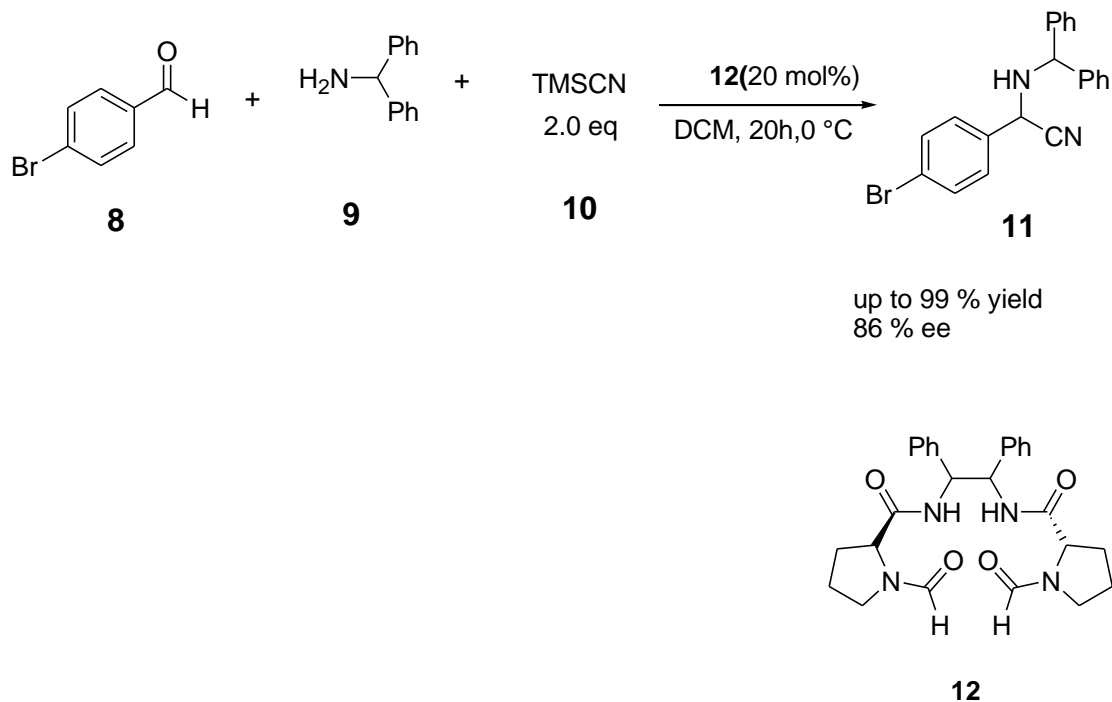


R₂ =H or other group

Scheme 3.1. General reaction scheme in synthesis of three-component Strecker reaction

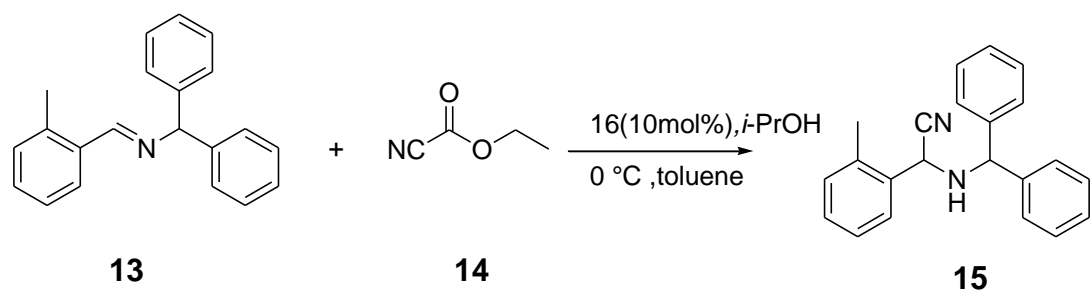
Different metal-free catalysts have been developed by employing chiral guanidines, ureas and thioureas, bis(N-oxides), Brønsted acids, and ammonium salts. In 2007, Xiaoming Feng and

coworkers developed C_2 -symmetric chiral bisformamides that have shown excellent performance in asymmetric one-pot, three-component Strecker reaction, which produced the *R*-amino nitriles in excellent yields (up to 99%) with good enantioselectivities (up to 86% ee)²⁹ (Scheme 3.2).

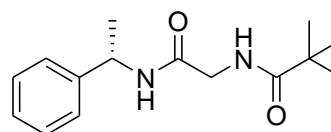


Scheme 3.2. Performance of C_2 -symmetric chiral bis-formamides in asymmetric Strecker reaction

In 2013, a novel chiral amide-based organocatalyst **16** was developed for the asymmetric Strecker reaction, where excellent enantioselectivities and good yields were achieved³⁰ (Scheme 3).



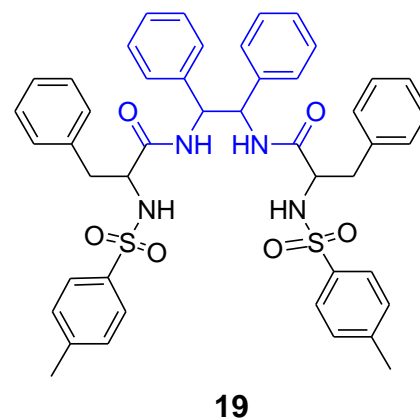
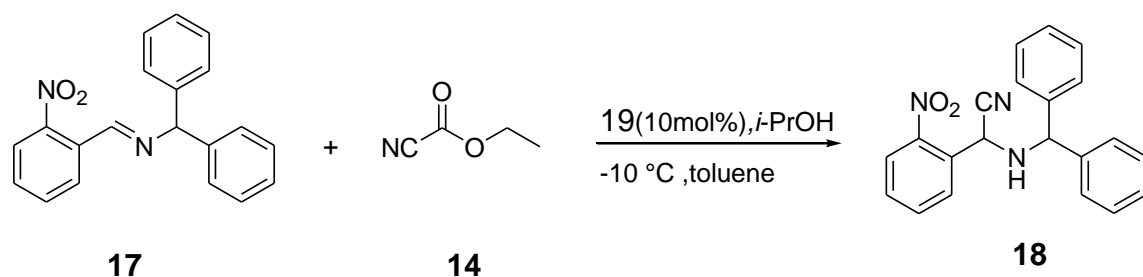
up to 99 % yield
88 % ee



16

Scheme 3.3. Evaluation of novel chiral amide-based organocatalyst 16 asymmetric Strecker reaction

Furthermore, in 2012, C₂-symmetric chiral amide-based organocatalyst **19** was developed for the enantioselective Strecker reaction (Scheme 3.4). It displayed remarkable substrate scope in the reaction of various aromatic and aliphatic *N*-benzhydryl imines with ethyl cyanofornate as cyanide source at $-10\text{ }^\circ\text{C}$, providing the α -aminonitriles in high yield (95%) and with excellent chiral induction (up to 99% ee)³¹.

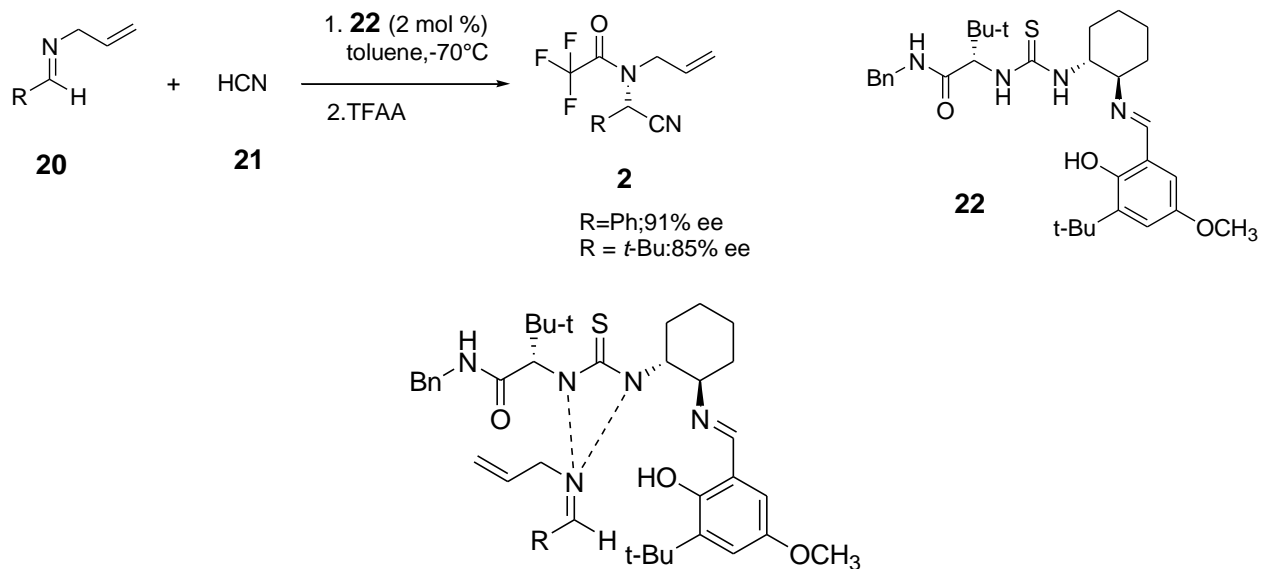


Scheme 3.4. The efficiency of C₂-symmetric recyclable organocatalyst **19** in asymmetric Strecker reaction

As most organocatalysts, thioureas can be synthesized simply from primary amine, and easy to handle since no inert gas atmosphere is required. These catalysts have been shown effective catalysis in several organic reactions and provide high atom economy, and a high chance to insert additional functional groups through the choice of the corresponding precursors.

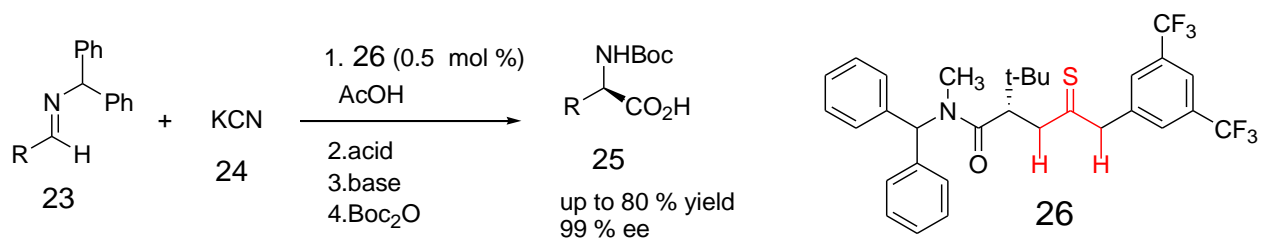
α -Aminonitriles are important and widely used molecules because they are used as starting materials for the synthesis of different products like α -amino acids, amides, α -amino alcohols, α -amino carbonyls, thiadiazoles, or imidazoles.^{32,33} Different cyanide sources are thus employed in the enantioselective α -aminonitrile synthesis through nucleophilic addition to imines. The availability of -CN and -NH₂ functional groups makes α -aminonitriles a crucial, versatile building block in agrochemicals, pharmaceuticals, and heterocyclic chemistry.^{34,35} Various synthetic methods have been developed for the synthesis of this building block over a century.³⁷ Despite the rapid advances in using thiourea-containing molecules as privileged catalysts for organocatalysis, the synthesis of chiral α -aminonitriles by symmetric thiourea-organocatalysis is still limited. Sigman and Jacobsen described that urea and thiourea derivatives **22** catalyze enantioselective

hydrocyanation reactions of imines derived from both aromatic and aliphatic aldehydes (Scheme 5)³⁸. NMR based mechanistic analysis, structure-activity, kinetic and theoretical studies disclosed that the thiourea functionality was responsible for the catalytic activity and that the imine substrate interacts with the catalyst via a dual H-bond interaction to the urea protons.³⁹



Scheme 3.5. First-generation catalyst for the thiourea-catalyzed Strecker reaction

The second generation of catalysts uses simple hydrogen bonding thiourea **26** to catalyze the Strecker reaction, where solid KCN was used as a cyanide source, in a biphasic toluene/water solution (Scheme 3.6). This reaction could be run on the multi-gram scale. While the ee's range from 73-98%, the products can be recrystallized up to 99% ee for a broad range of aliphatic and aryl imine substrates.⁴⁰



Scheme 3.6. Second-generation catalyst for the thiourea-catalyzed Strecker reaction

Through a flow-based methodology, Margherita Brindisi and coworkers designed cinchona-based thiourea as chiral catalysts **27** (Figure 3.4) for enantioselective Strecker by employing ethyl cyanoformate as a relatively safe cyanide source and methanol as additive. The corresponding α -amino nitriles were then obtained in good yields (up to 96%) and enantioselectivities (up to 90% ee).⁴¹

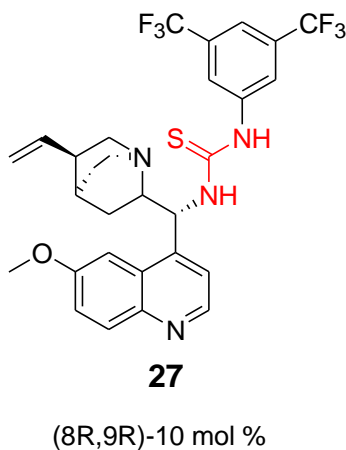


Figure 3.4. Cinchona-based thiourea catalyst as chiral catalysts for enantioselective Strecker

3.3 Results and Discussion

3.3.1 Synthesis of symmetric amido-thiourea (Cat-1 to Cat-5)

The symmetric chiral amido thiourea catalysts **Cat-1** to **Cat-5** (Figure 3.5) were prepared in quantitative yield by reaction of a commercially available chiral diamine **28**, **35**, or **40** with the corresponding spacers **31** and **36**.

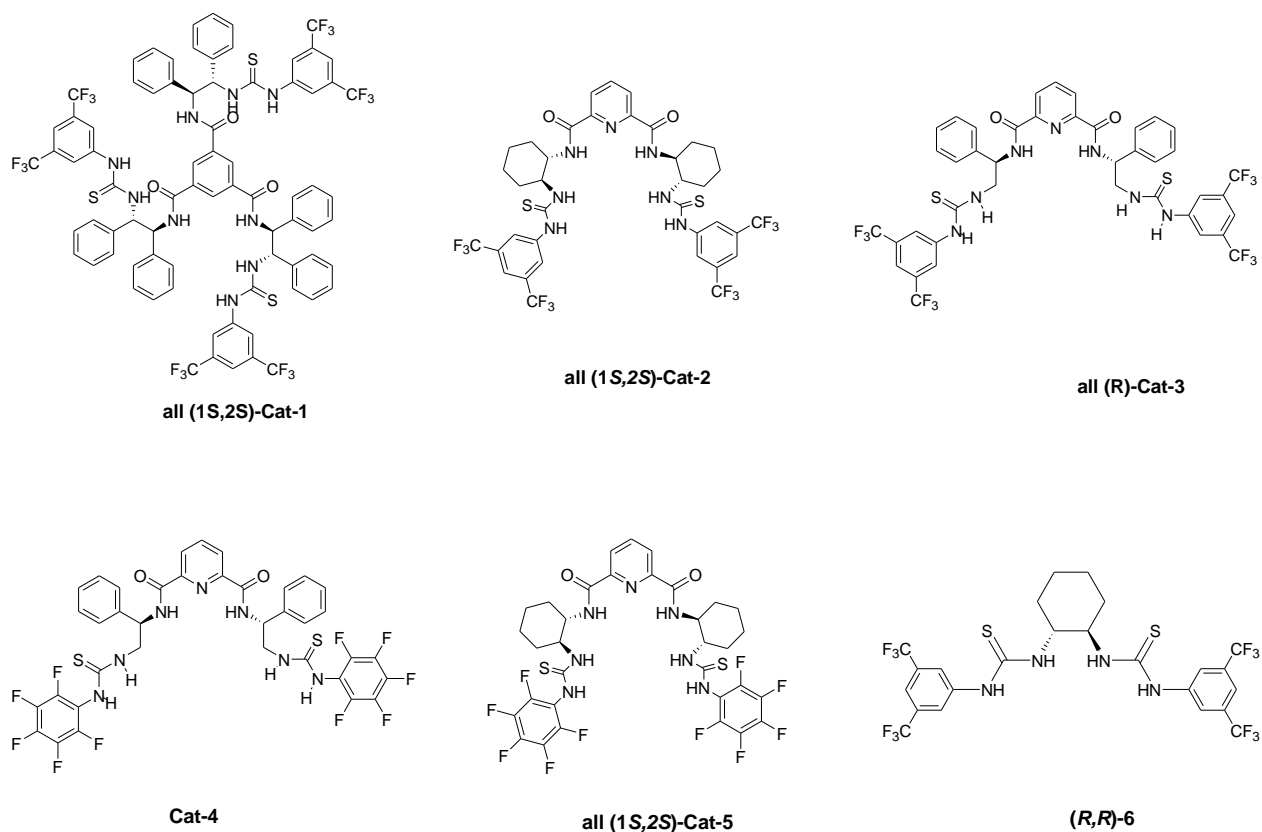
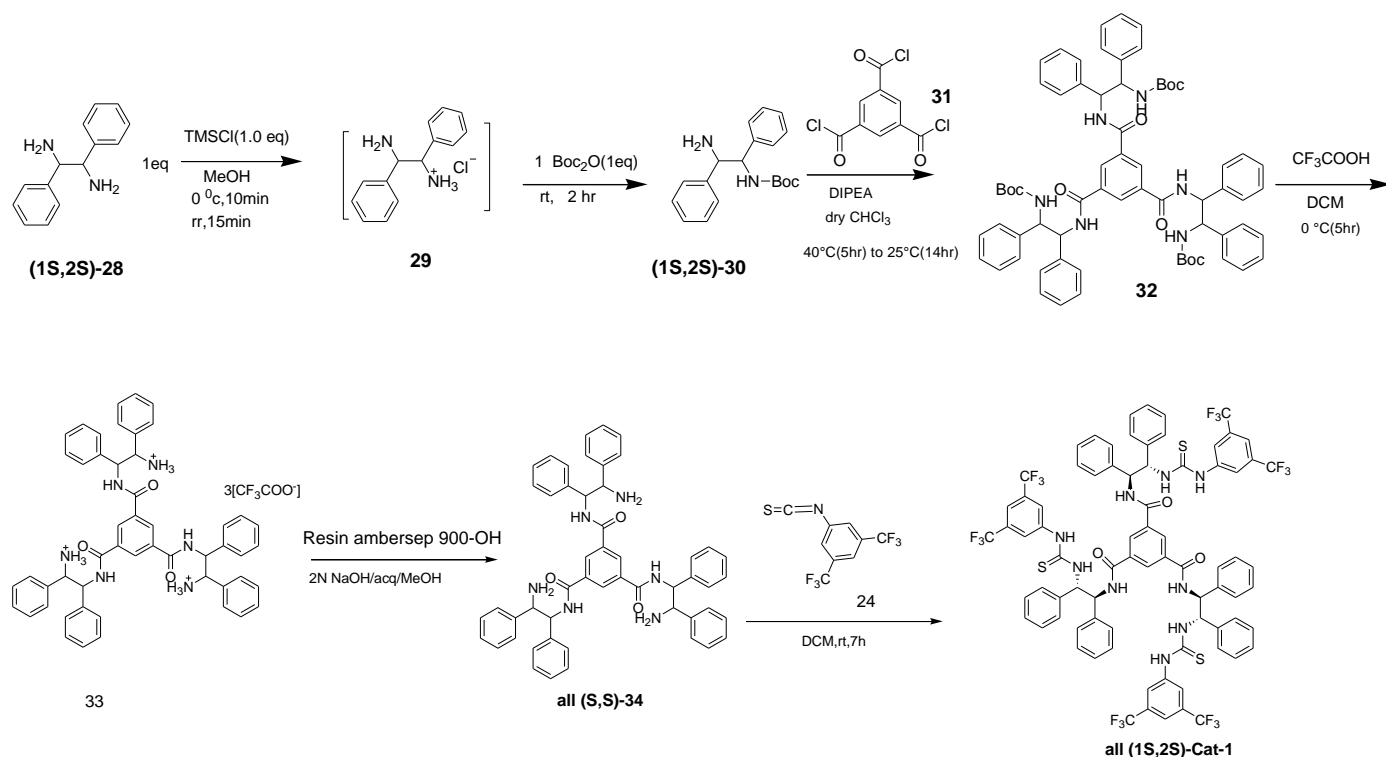


Figure 3.5. Symmetric amido-thiourea organocatalysts

C3-Symmetric amido thiourea (**Cat-1**) was smoothly synthesized in good yield via six steps starting from the diamine (**31**) using equimolar amounts of di-*tert*-butyl dicarbonate to protect one N-group in the presence of trimethylsilyl chloride (Scheme 3.7).

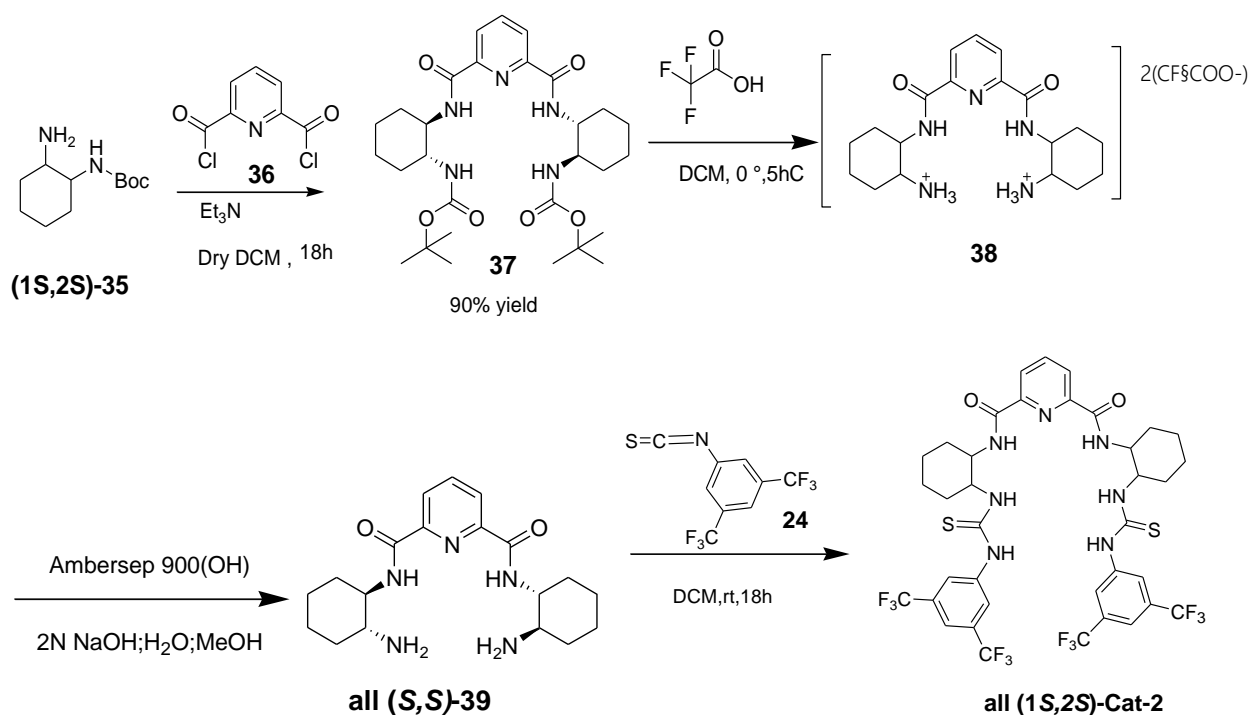


Scheme 3.7. Synthesis of (1S,2S)-DPEDA based C3-amido-thiourea (Cat-1)

Next, we shifted our attention to the design and synthesis of C_2 -symmetric chiral amido thiourea catalysts based on the pyridine spacer to increase the Lewis's basicity and ion-binding properties of our catalysts in addition to their hydrogen bonding catalysis.

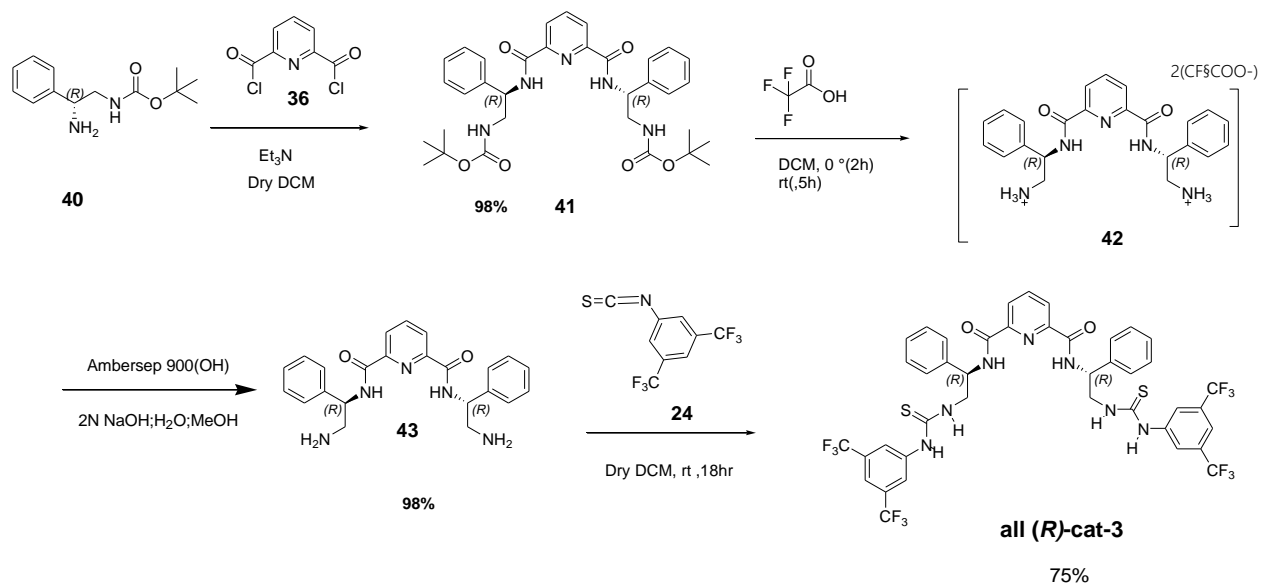
The synthesis of C_2 -symmetric chiral amido thiourea catalysts: **Cat-2**, **Cat-3**, **Cat-4**, and **Cat-5** was accomplished with spacer **36** and in dry DCM. In a dried flask equipped with a stir bar, compound (1S,2S)-*N*-Boc-1,2-cyclohexanediamine (**35**) was stirred with one equivalent of spacer pyridine-2,6-dicarbonyl dichloride (**36**) in presence of triethyl amine in dry DCM, providing the product **37** in 90% yield. The deprotection was carried out with TFA in DCM, affording the diamine **39** in 99% yield. The preparation of catalysts **Cat-2** was carried out by passing a solution of **39** in methanol through ambersep 900-OH. The resin was activated with 2N NaOH and the solution of compound **39** was loaded. The collected solution was evaporated on a vacuum and dried on high vacuum to provide the bisamine intermediate in 99% yield. Finally, **Cat-2** was

synthesized in 85% yield by reacting **39** with bis(trifluoromethyl)phenyl isothiocyanate (**24**) in DCM at 0 °C (Scheme 8).

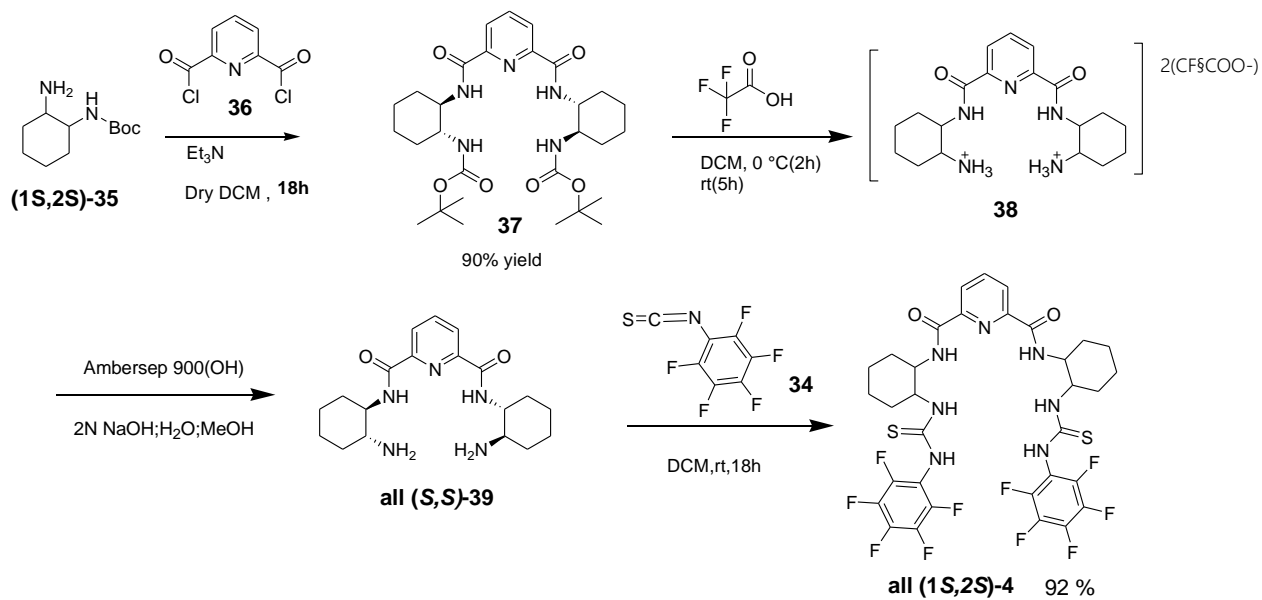


Scheme 3.8. Synthesis of (1S,2S)-diaminocyclohexane derived C2-amido-thiourea (Cat-2)

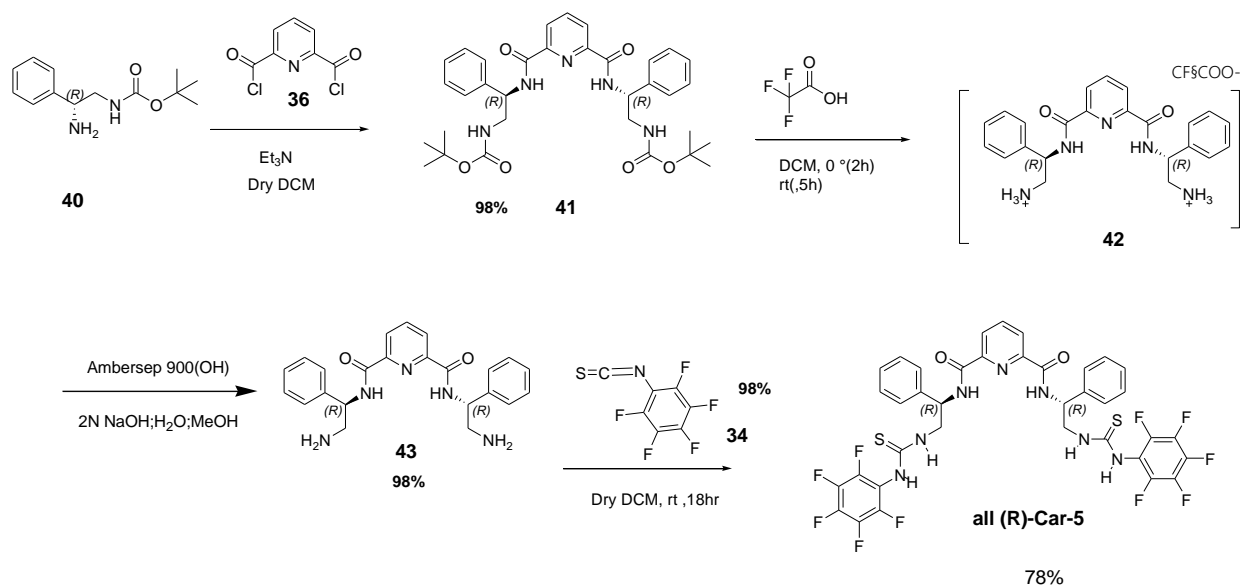
Following the same procedure of catalyst **Cat-2**, chiral amido thiourea catalysts **Cat-3** was prepared using a different chiral amine in 98% yield. At the end, **Cat-4** and **Cat-5** have been synthesized successfully with 1,2,3,4,5-pentafluoro-6-isothiocyanato-benzene **34** in 92% and 78% yield, respectively.



Scheme 3.9. Synthesis of *(R)*-(2-amino-2-phenyl-ethyl)-carbamic acid *tert*-butyl ester based C2-amido-thiourea (Cat-3)



Scheme 3.10. Synthesis of *(1S,2S)*-diaminocyclohexane derived C2-amido-thiourea (Cat-4)



Scheme 3.11. Synthesis of (*R*)-(2-amino-2-phenyl-ethyl)-carbamic acid *tert*-butyl ester based C2-amido-thiourea (Cat-5)

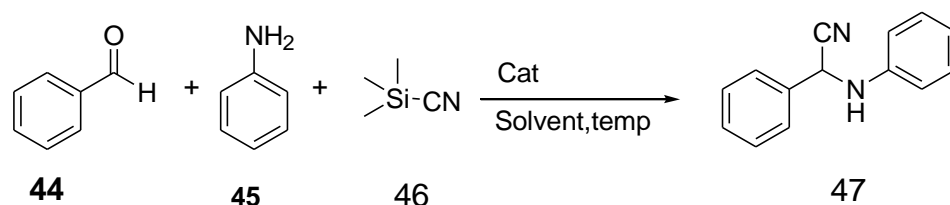
3.3.2 Enantioselective Strecker reaction

After the successful preparation of catalysts **Cat-1** to **Cat-5**, their activity, and stereoselection in the enantioselective Strecker reaction was investigated (Table 3.1). Initially, the C_3 -symmetric chiral amido thiourea catalysts **Cat-1** was applied in the three components Strecker reaction of an aldehyde, amine, and TMS-CN as cyanide source (Table 3.1, entries 2-4). Surprisingly, 97% yield of α -amino nitrile **47** was obtained employing 2 mol% of this catalyst (**Cat-1**) in dry DCM at -20°C , however, it provided almost a racemic product (57:43 e.r.) (Table 3.1, entry 4).

Next, we have continued to examine the efficiency of catalysts **Cat-1** to **Cat-5** for the Strecker reaction (Table 3.1, entries 5-10). To study the effectivity of each catalyst, the aldehyde, and the amine were combined in a dried Schlenk flask containing dry solvent and activated molecular sieve 5\AA (150 mg), and the mixture was stirred at room temperature for 2h under an argon atmosphere. After a while, the catalyst was added to the mixture and stirred for 10 min. The TMS-CN was finally added and the mixture was stirred overnight. Catalyst (1*S*,2*S*)-**Cat-2** showed superior performance over the other tested catalysts in terms of both yield (up to 99%) and enantioselectivity, achieving a moderate 65:35 e.r. in DCM at -40°C (Table 1, entry 7). Finally,

we have used the available symmetric chiral amido bis-thiourea catalyst **Cat-6** (Table 3.1, entry 11). However, the result obtained with this catalyst is the same line with the newly synthesized catalysts (95% yield and low 58:42 e.r).

Table 1. Catalyst, solvent and temperature screening in the three-component Strecker reaction using TMSCN as cyanide source



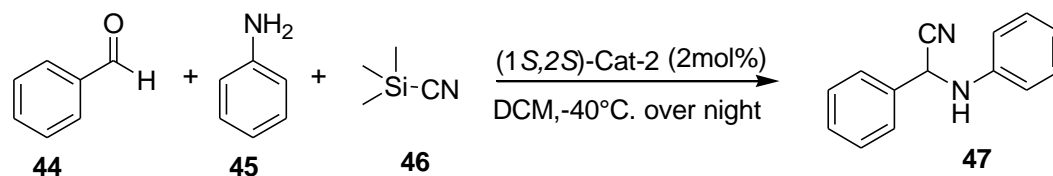
Entry	Cat.	Mol%	Solvent (dry)	Temp. (°C)	Time (h)	Yield (%)	e.r
1	-	-	DCM	-40	18	48	50:50
2	Cat-1	2	Toluene	rt	24	97	55:45
3	Cat-1	2	Toluene	-20	24	90	55:45
4	Cat-1	2	DCM	-20	24	98	57:43
5	Cat-2	2	DCM	rt	18	99	62:38
6	Cat-3	2	DCM	rt	18	97	39:61
7	Cat-2	2	DCM	-40	18	83	65:35
8	Cat-3	2	DCM	-40	18	77	41:59
9	Cat-4	2	DCM	-40	18	99	58:42
10	Cat-5	2	DCM	-40	18	98	57:43
11	Cat-6	2	DCM	-40	18	95	58:42

Further optimization work with this catalyst was carried out by increasing the loading from 2 mol % to 5 mol %, as well as the use of additives (Table 3.2). However, the increased catalyst loading didn't make change in enantioselectivity (table 3.2). This may be rise from due to a solubility problem of the catalyst within the same volume of solvent. According to our research strategy and

plan, we aimed to enhance the yield and enantioselectivity of the α -amino nitrile product with the developed symmetric chiral amido thiourea catalysts **Cat-1** to **Cat-5**. This protocol didn't display a broad substrate scope for reactants in enantioselectivity. In this case, we have achieved highest yield, but, the performance of catalyst in enantioselectivity remained moderate.

Table 3.1 Screening of catalysts

Table 3.2 The additives, solvent and catalyst loading effect in the reaction catalyzed by **Cat-2**

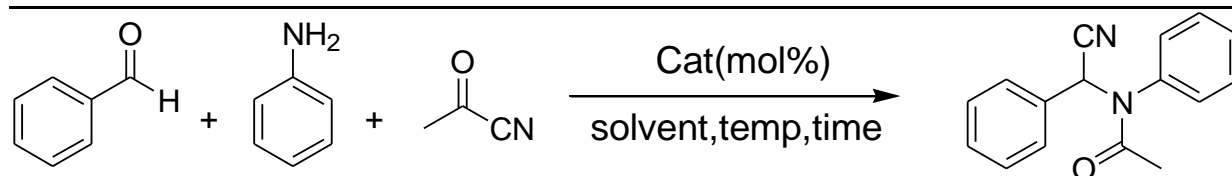


Entry	Mol%	Additive	Solvent	Temp.	Time (h)	Yield (%)	e.r
1	2	-	Toluene	-40 °C	18	88	51/49
2	2	-	Et ₂ O	-40 °C	18	72	56/44
3	2	-	CH ₃ CN	-40 °C	18	62	57/43
4	5	-	DCM	-40 °C	18	99	59/41
5	2	-	DCM	40 °C	18	100	57/48
6	2	-	DCM	-70 °C	18	62	63/37
7	1	-	DCM	-40 °C	18	72	50/50
8	5	-	DCM	-40 °C	18	99	58/42
9	2	H ₂ O	DCM	-40 °C	18	63	55/45
10	2	IPA	DCM	-40 °C	18	99	55/45
11	2	IPA	Toluene	-40 °C	18	89	55/45

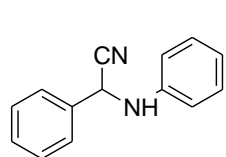
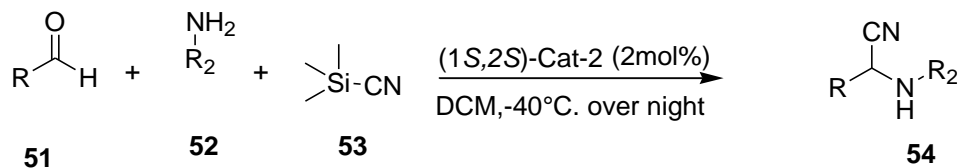
To improve the enantioselectivity, the reaction using pyruvitrile as a cyanide source was explored under the same best reaction conditions obtained with **Cat-2** and TMSCN. With these optimal conditions (Table 3.1, entry 7), the effect of the catalyst loading and temperature was investigated and the results are summarized in Table 3.3. Higher yields were generally obtained (up to 99%), however, dismissed enantioselectivities were observed and the products were almost racemic (up to 56:44) (Table 3.3, entry 6).

Table 3.3. Optimization for Solvent, catalysts loading and temperature Effect

Entry	Cat.	Mol%	Solvent	Temp.	time	Yield (%)	e.r
1	Rac-4	5	DCM	rt	18	85	49:51
2	(<i>S,S</i>)-1	2	DCM	-40 °C	18	95	55:45
3	(<i>S,S</i>)-1	2	DCM	rt	18	98	54:46
4	(<i>R,R</i>)-1	2	DCM	rt	18	93	49:50
5	(<i>S,S</i>)-1	2	Toluene	-40 °C	18	80	53:47
6	(<i>S,S</i>)-1	2	Et₂O	-40 °C	18	59	56:44
7	(<i>S,S</i>)-1	2	CH ₃ CN	-40 °C	18	68	52:48
8	(<i>S,S</i>)-1	5	DCM	-40 °C	18	99	52:48
9	(<i>S,S</i>)-1	2	DCM	40	18	100	49:51
10	(<i>S,S</i>)-1	2	DCM	-70	18	57	49:51

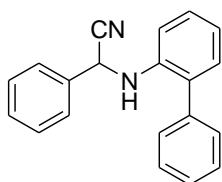


Survey of scope of reactions with Cat-2 for the three-component Strecker reaction



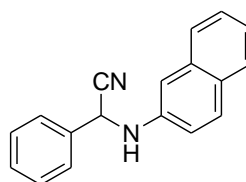
54a

yield 83%, 65/35 e,r



54b

yield 89%



54c

yield 92%

3.3 Anion-binding studies of the catalyst Cat-2

Determining binding constants is the most intuitive method for the evaluation of the binding force of anions. ^1H NMR titration is one of the most used and effective method for determining the binding constant.

The anion binding ability of dual hydrogen bond donor symmetric amido-thiourea (**Cat-2**) has been investigated by the addition of four anions as the tetrabutylammonium (TBA^+) salts to solutions of the catalysts in THF- d_8 (Table 3.4). This helps us to identify the performance of **Cat-2** in enantioselective Strecker reaction from the correlations between catalyst and anion.

The analysis of anion binding abilities of the **Cat-2** was performed by the addition of (0–10 equiv) of a range of monovalent anions (Cl^- , CN^-), bidentate benzoate and tridentate OTf^- as the tetrabutylammonium (TBA^+) salts to solutions in THF- d_8

Based on the obtained results, weak binding to bidentate benzoate and tridentate OTf^- anions, but not observable binding to monodentate Cl^- or CN^- anions in THF- d_8 could be determined. Maybe this explain why low enantioselectivities in the Strecker reaction were observed, since the binding

to the CN-anion or carbonyl substrate might also be weak and may lead to a low control of enantioselectivity.

As we can see from table 3.4 and 3.5, a 1:2 host-guest complex could be identified for the multidentate anions. Thus, the benzoate binding affinity for the 1:1 complex is $k_{1:1}$: $4.74 \times 10^{13} \text{ M}^{-1}$ and $k_{1:2}$: 0.24 M^{-1} for the 1:2 complex; while the tridentate OTf anion binding constants were determined to be $k_{1:1}$: -0.009 M^{-1} and $k_{1:2}$: -0.97 M^{-1}). By comparing to the two binding constant, the binding affinity to the benzoate anion is significant stronger than to the OtF anion

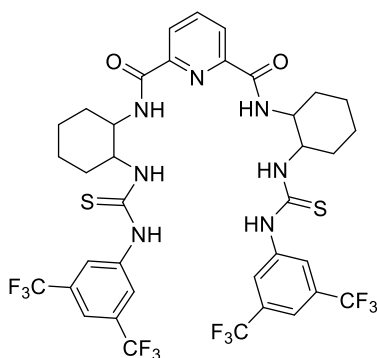
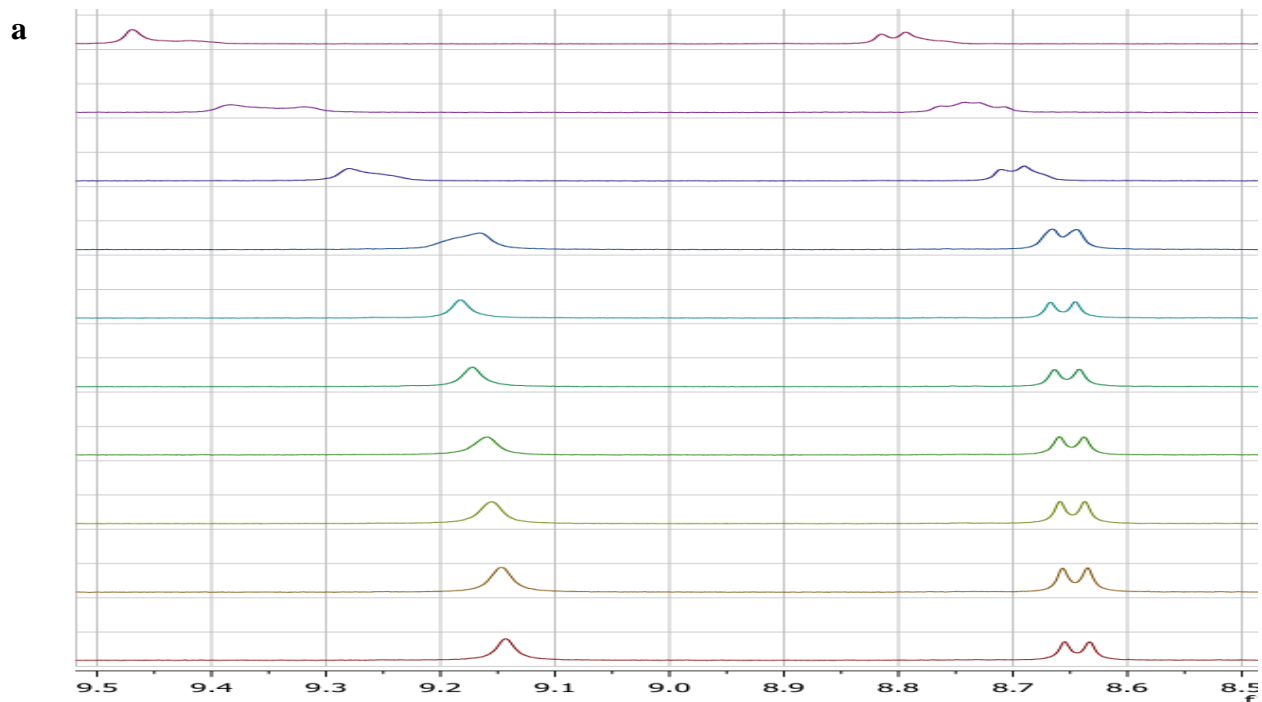


Figure 3.6. Participating protons of Cat-2 to the binding to different anions

Binding to benzoate anion:



b

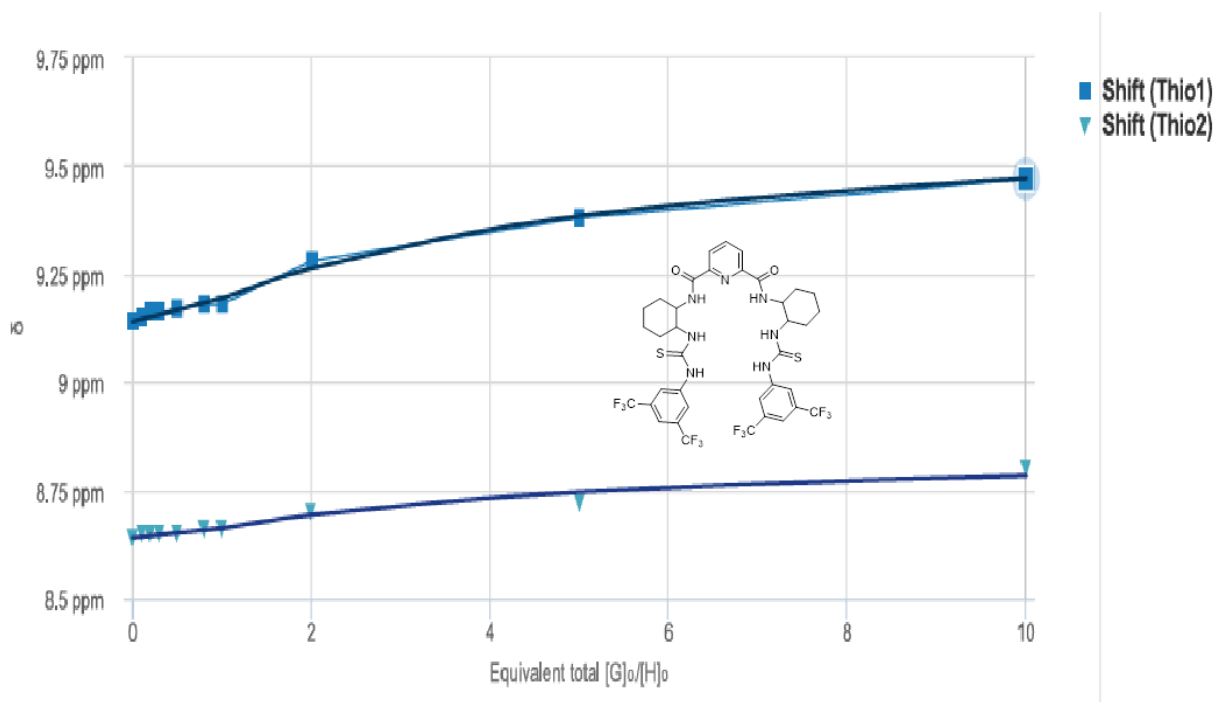


Figure:3.7. a) Stack plots of ¹H NMR spectra of addition of TBA-Benzoate (0–10 equiv) in THF-d₈ at rt. b) Corresponding chemical shift changes of thio-1 and thio-2 during titration.

Table 3.4 Anion-binding constant (M⁻¹) of Cat-2 to bidentate benzoate anion

Parameter (bounds)	Optimised	Error(M ⁻¹)
k_{1:1}	4.74x10 ¹³ M ⁻¹	± 1.39x10 ⁹
k_{1:2}	0.24 M ⁻¹	± 0.16

Figure: 3.8 a) Stack plots of ^1H NMR spectra of addition of TBA-OTf (0–10 equiv) in THF-d8 at rt b) Corresponding chemical shift changes of thio-1 and thio-2 during titration

Table 3.5 Anion-binding constant (M^{-1}) of Cat-2 to tridentate OTf anion

Parameter (bounds)	Optimised	Error(M^{-1})
$k_{1:1}$	-0.093 M^{-1}	± -0.21
$k_{1:2}$	-0.97 M^{-1}	± -0.09

3.4 Conclusion

Surprisingly, symmetric amido-thiourea (Cat-1-Cat-5), which contains pyridine as a core has been developed in good to excellent yield. To investigate the performance of each catalyst, we have applied them for three components of Strecker reactions in the presence of different cyanide sources, solvents, and additives. From good to excellent yield of α -aminonitriles obtained illustrated how the effectiveness of symmetric amido-thiourea (Cat-1-Cat-5) for three components of Strecker reactions. However, these catalysts provide low enantioselective of α -aminonitriles

Furthermore, we have tried to investigate the reason for the low performance of enantioselectivity of α -aminonitriles in the presence of symmetric chiral amido thiourea catalysts. We have investigated the anion binding ability of dual hydrogen bond donor (Cat-2) in the presence of four anions as the tetrabutylammonium (TBA⁺) salts to solutions of the catalysts in THF-d8 (Table 3.4). From the results of NMR titrations of cat-2 by cyanide, the shift of proton of -N-H happened which may become a reason for the low enantioselectivities in the Strecker since the binding to

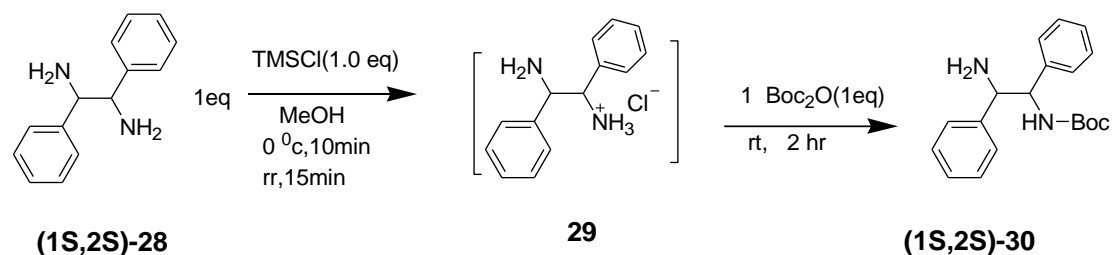
the CN-anion or carbonyl substrate might also be weak and may lead to a low control of enantioselectivity.

3.5 Experimental Section

Synthesis of Symmetric amido-thiourea (Cat-1 to Cat-5)

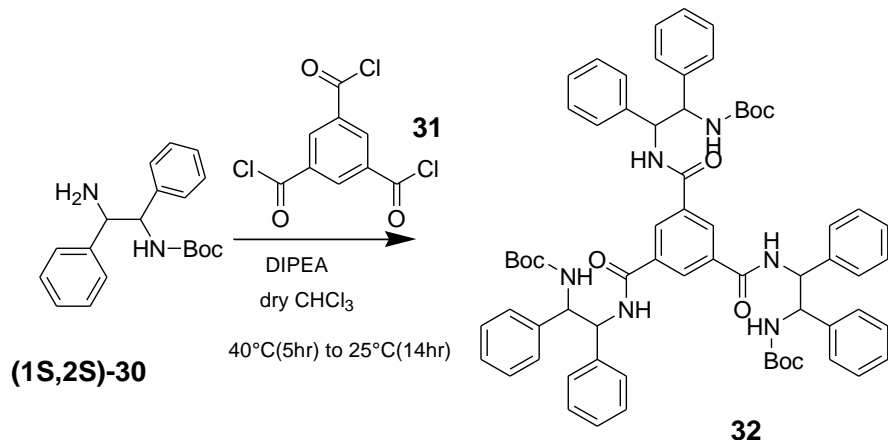
Synthesis of Cat-1

Synthesis of (2-amino-1,2-diphenyl-ethyl)-carbamic acid *tert*-butyl ester (1*S*,2*S*)-**30**



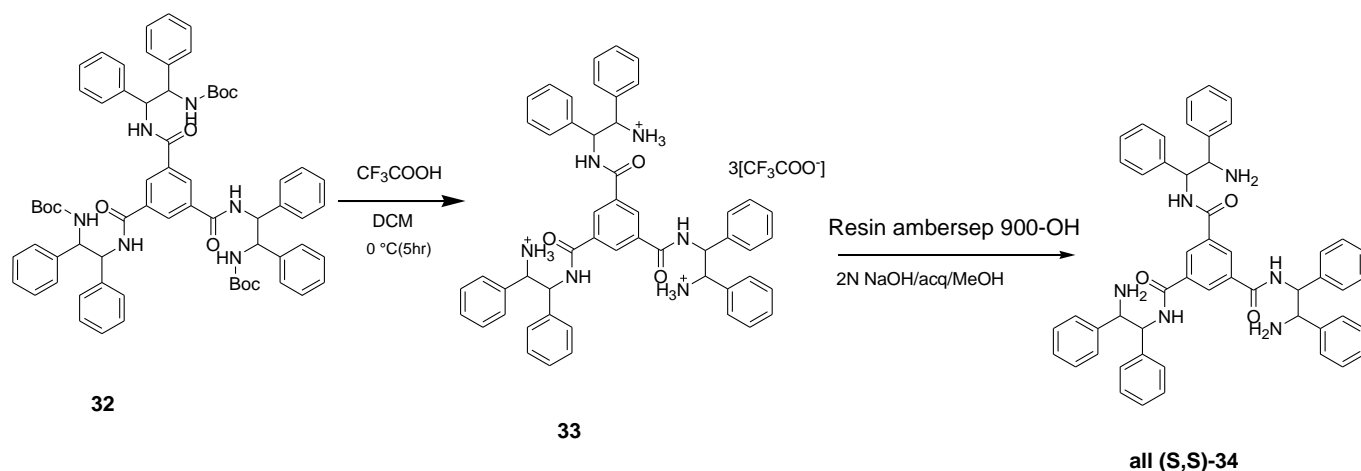
A round bottom flask contain methanol (3 ml) was charged with TMSCl (1.415 mmol, 178.5 μ L) at 0 °C. After 10 min stirring, 1,2-diphenylethylenediamine (**28**) (1.415 mmol, 300.0 mg) was added. The solution was continued to stirred at room temperature for 15 min. The solution of di-*tert*-butyl dicarbonate (Boc)₂O (1.4151 mol, 308.5 mg) in MeOH (2 mL) was added dropwise for 30 min. The resulting solution was stirred for 2h at room temperature. The mixture was concentrated in vacuo. The residue was washed with diethyl ether (3 \times 4 mL) and pale-yellow solid was treated with the 3N NaOH solution (1.2 mL) and water (3 \times 1.5mL). The product was dried in vacuo at low pressure. The product **3** was isolated by column chromatography (Hex/EA 50/50 +1% TEA) as a white solid (87%). H NMR (400 MHz, CDCl₃) δ 7.47 – 7.24 (m, 10H), 5.88 (1, J = 8.1 Hz, 1H), 4.89 (s, 1H), 4.37 (s, 1H), 1.44 (s, J = 27.6 Hz, 2H), 1.36 (s, 9H). MS (ESI) m/z for C₁₉H₂₄N₂O₂ [M +H]⁺: 313.17 and [M +Na]⁺: 335.17. The analytic data is in concordance with the one previously reported in the literature ⁴².

Synthesis of {2-[3,5-bis-(2-tert-butoxycarbonylamino-1,2-diphenyl-ethylcarbamoyl)-benzoylamino]-1,2-diphenyl-ethyl}-carbamic acid tert-butyl ester (Molecule-32)



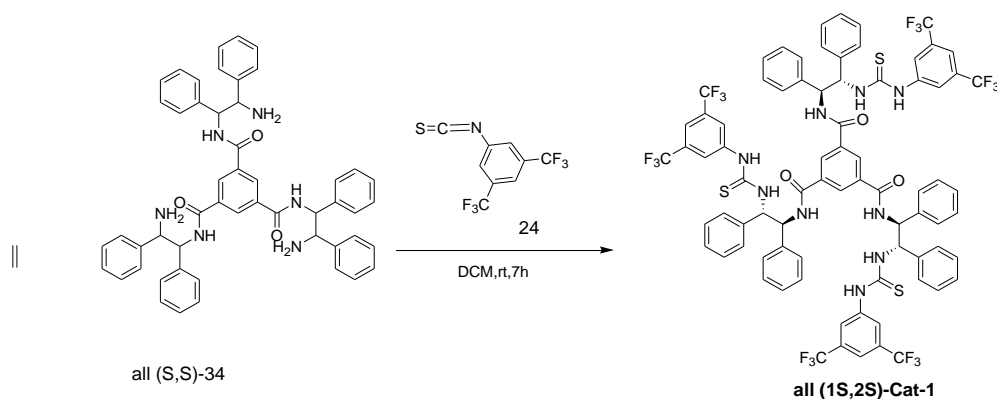
Compound-30 (380 mg, 1.22 mmol) was dissolved in 8 ml of dry CHCl₃. Next, DIPEA (167.7 μl) was added to the reaction mixture. Then, the solution of 1,3,5-Benzenetricarbonyl trichloride 31 (107.8 mg, 0.41 mmol) in 4 ml of dry CHCl₃ was added to the reaction mixture dropwise. The solution was stirred under nitrogen atmosphere at 40 °C. After 5h stirring, the temperature of the reaction was decreased to 25 °C for 14h. The reaction progress was controlled with TLC (Hex/EA 50/50 +1% MeOH, R_fspot1 =0.037, R_fspot2 =0.278, R_fspot3 =0.667). Then, 2 ml of MeOH was added slowly. The crude of reaction was concentrated in vacuo. The residue was purified by column chromatography on silica gel, obtaining the product in 85% yield. The structure was confirmed by both NMR and mass spectroscopy. ¹H NMR (400 MHz, DMSO) δ 9.02 (d, *J* = 9.1 Hz, 3H), 8.23 (s, 3H), 7.69 (d, *J* = 9.7 Hz, 3H), 7.35 (m, *J* = 13.2, 7.5 Hz, 11H), 7.28 – 7.11 (m, 10H), 5.52 (dd, *J* = 8.9, 6.4 Hz, 3H), 5.13 (dd, *J* = 9.4, 6.3 Hz, 3H), 1.23 (d, *J* = 9.9 Hz, 27H). MS (ESI) *m/z* for C₆₆H₇₂N₆O₉ [M +H]²⁺: 569.33 and [M +Na]⁺: 1115.58.

Synthesis of benzene-1,3,5-tricarboxylic acid tris-[(2-amino-1,2-diphenyl-ethyl)-amide] (1S,2S)-34



TFA (165 μl) was added to a solution of compound-**32** (1 g, 1.00 mmol) in DCM (7 ml) at 0 $^\circ\text{C}$. The reaction was stirred at room temperature for 6h. The progress of deprotection was controlled by TLC (Hex/EA 50/50 +1% methanol), then after completion, the crude of reaction was concentrated in vacuo. After activation of resin(ambersep-900-OH) with 2N NaOH, water and methanol, the solution of product **33** ($\text{C}_{51}\text{H}_{51}\text{N}_6\text{O}_3$)⁺³ in methanol was loaded and collected. The solvent was evaporated in vacuo and 98% of product was obtained. Finally, the product was characterized by ¹H NMR and mass spectroscopy. ¹H NMR (400 MHz, MeOD) δ 8.40 (s, 3H), 7.28 – 7.07 (m, 33H), 5.28 (d, J = 8.6 Hz, 3H), 4.32 (d, J = 13.3, 8.6 Hz, 3H). MS (ESI) m/z $\text{C}_{51}\text{H}_{48}\text{N}_6\text{O}_3$ $[\text{M} + \text{H}]^{2+}$: 397.13, $[\text{M} + \text{H}]^+$: 793 and $[\text{M} + \text{Na}]^+$: 815.41.

Synthesis of (1S,2S)-Cat-1

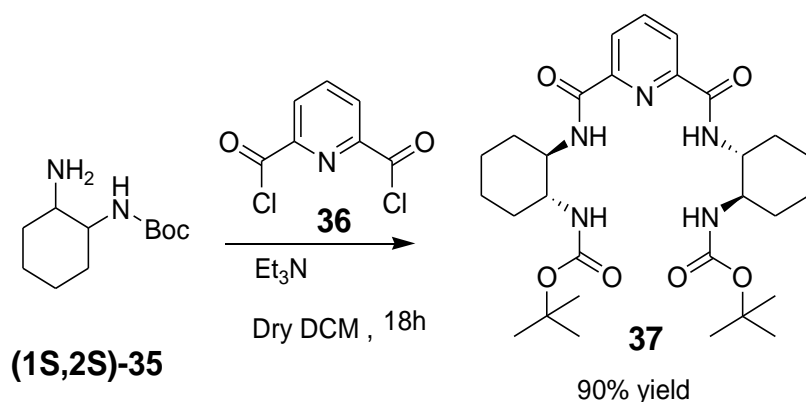


The first catalyst (**Cat-1**) was synthesized by addition of 1-isothiocyanato-3,5-bis-trifluoromethylbenzene (0.265 mmol, 50.0 μL) to a solution of compound-**34** (0.075 mmol, 120.0 mg) in 3 ml of

dry DCM at 0 °C under N₂ gas. The reaction was performed for 7 h at room temperature. The crude of reaction was extracted with DCM/NaCl solution(brine) three times. The collected organic phase was filtered two times to minimize the amount of water. The solution was dried over Na₂SO₄ and the purified by column chromatography, providing the product as a white solid in 96% yield. ¹H NMR (400 MHz, CDCl₃) δ 10.63 (d, *J* = 4.8 Hz, 3H), 9.58 (d, *J* = 7.1 Hz, 3H), 9.42 (s, 3H), 7.57 – 6.84 (m, 42H), 5.77 – 5.65 (m, 3H), 5.59 (dd, *J* = 10.9, 5.2 Hz, 3H). HRMS (ESI): *m/z* for C₇₈H₅₇F₁₈N₉O₃ [M +Na]²⁺: 815, found: [M +Na]⁺: 1629.

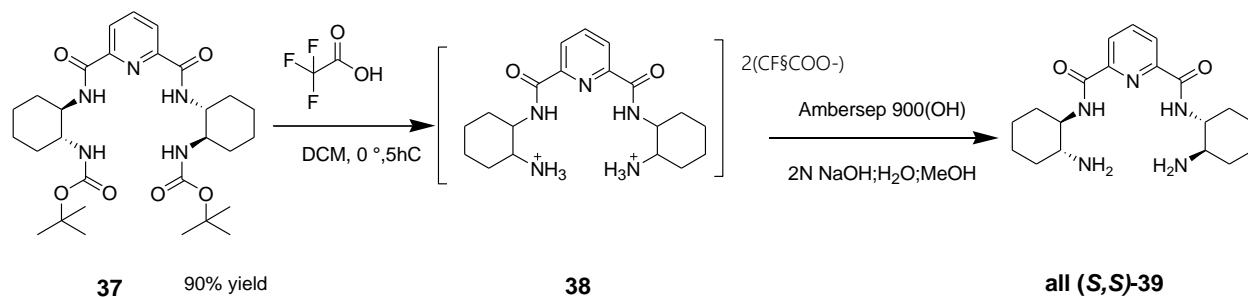
Synthesis of Cat-2

Synthesis of compound-37



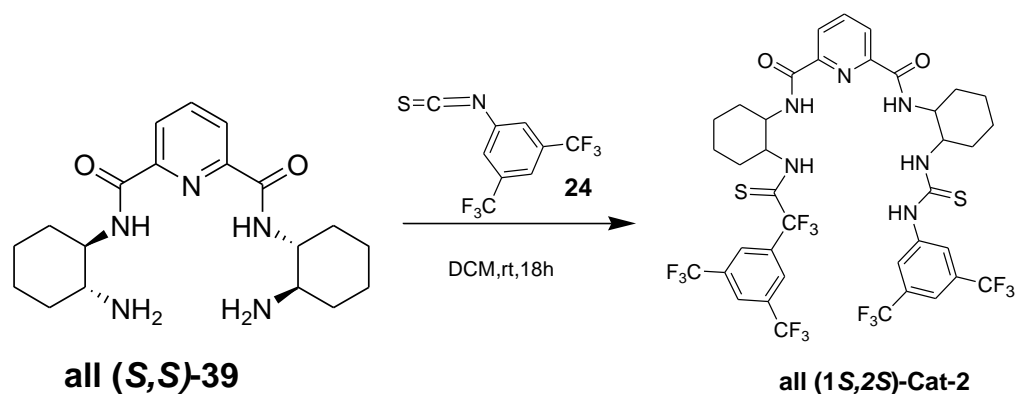
In a dried Schlenk flask containing dry DCM (6 mL), commercially available chiral amine-**35** (500.0 mg, 2.334 mmol) was added under argon gas. Et₃N (325.3 μL, 0.9333 mmol) was added to the solution at 0 °C. Then, the solution of 2,6-pyridinedicarbonyl dichloride **36** (238.1 g, 1.167 mmol) in dry CH₂Cl₂ (4 mL) was added dropwise. The mixture was stirred overnight at room temperature. The progress of the reaction was monitored via TLC. After completion, the crude product was concentrated and purified by column chromatography on silica gel (Hex/EA 50/50) leading to product **37** in 90% yield. ¹H NMR (400 MHz, CDCl₃) δ 8.01 (d, *J* = 8.5 Hz, 2H), 7.54 (d, *J* = 7.7 Hz, 2H), 7.26 (t, *J* = 7.7 Hz, 1H), 3.90 (d, *J* = 9.0 Hz, 2H), 3.19 – 2.91 (m, 4H), 1.39 (dd, *J* = 28.4, 12.6 Hz, 4H), 1.09 (s, 4H), 0.99 – 0.85 (m, 2H), 0.79 – 0.54 (m, 7H), 0.45 (s, 18H). HRMS (ESI): *m/z* for C₂₉H₄₉N₅O₄ [M +H]⁺ 560.3446, found [M +Na]⁺ 582.3262, [2M +Na]⁺ 1141.6646.

Synthesis of Pyridine-2,6-dicarboxylic acid bis-[(2-amino-cyclohexyl)-amide]-39



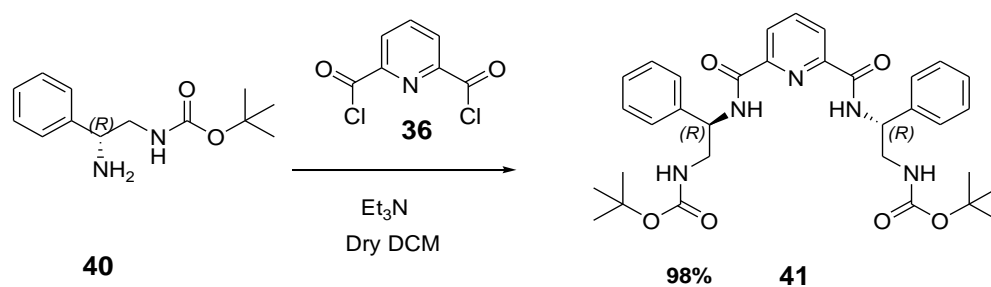
To the solution of **37** (19mg 0.3680 mmol) in DCM (10 ml), TFA (170.1 μ L, 2.21 mmol) was added at 0 °C. Then, the reaction was stirred at 0 °C for 2h and the temperature of the reaction was increased to room temperature for another 5h. The progress of the reaction was controlled by TLC (Pentane/EOAc 50/50). After completion of the reaction, the solvent was removed in a rotavapor. Then, product **39** was obtained after passing through Ambersep 900-OH. Half of the column was filled with resin and activated with 2N NaOH. Then, water and MeOH were passed consecutively. At the end, the solution of compound **38** in methanol was loaded to column. The solution was collected and evaporated, providing the desired product **39** in 99% yield. ^1H NMR (400 MHz, CDCl_3) δ 7.92 (d, $J = 7.8$ Hz, 2H), 7.58 (dd, $J = 18.1, 10.2$ Hz, 1H), 7.49 (d, $J = 8.3$ Hz, 2H), 3.26 (qd, $J = 11.1, 3.7$ Hz, 2H), 2.19 (td, $J = 10.3, 3.8$ Hz, 2H), 1.74 (dd, $J = 7.2, 4.2$ Hz, 2H), 1.66 – 1.54 (m, 2H), 1.37 (dd, $J = 23.0, 20.2$ Hz, 4H), 0.92 (tt, $J = 22.0, 11.2$ Hz, 10H). HRMS (ESI): m/z calculated for $\text{C}_{19}\text{H}_{29}\text{N}_5\text{O}_2$ found: $[\text{M} + \text{H}]^+$ 360.2393, $[\text{M} + \text{Na}]^+$ 382.2212, $[2\text{M} + \text{H}]^+$ 719.4719.

Synthesis of (1S,2S)-Cat-2



3,5-Bis(trifluoromethyl)phenyl isothiocyanate **24** (904.2 μ L) was added to a solution of chiral amine **39** (387.0 mg, 1.10 mmol) in dry CH_2Cl_2 (30 mL) at 0 $^\circ\text{C}$ and stirred at overnight at rt. The reaction was monitored by TLC (Pentane/EA 50/50). After completion, the crude was extracted with brine, dried over Na_2SO_4 , and the solvent was removed under reduced pressure. Then, the purification was carried out on column chromatography, leading to the desired (1*S*,2*S*)-**Cat-2** in 96% yield. $^1\text{H NMR}$ (400 MHz, DMSO) δ 9.91 (s, 2H), 8.77 (s, 2H), 8.28 (d, $J = 8.7$ Hz, 2H), 8.19 – 8.10 (m, 3H), 7.95 (s, 4H), 7.62 (s, 2H), 4.68 (s, 2H), 3.93 (d, $J = 11.7$ Hz, 2H), 1.91 – 1.22 (m, 16H). HRMS (ESI): m/z calculated for $\text{C}_{37}\text{H}_{35}\text{F}_{12}\text{N}_7\text{O}_2\text{S}_2$, found: $[\text{M} + \text{Na}]^+$ 924.1995.

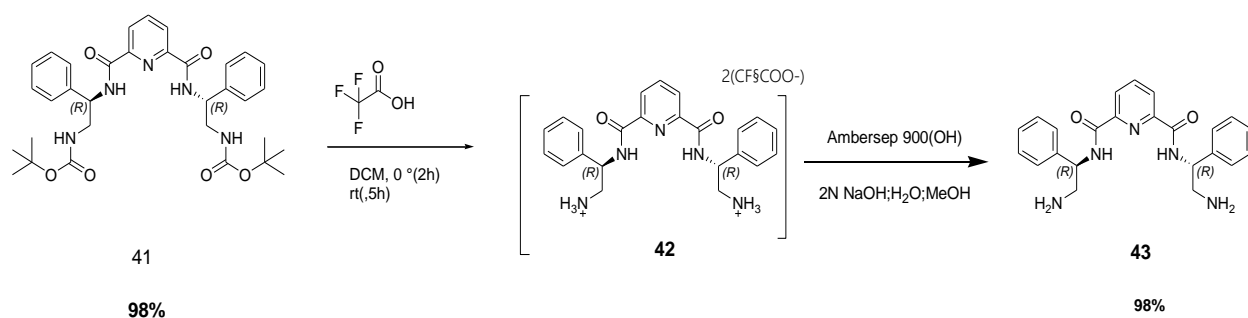
Synthesis of (2-[[6-(2-*tert*-Butoxycarbonylamino-1-phenylethylcarbamoyl)-pyridine-2-carbonyl]-amino]-2-phenylethyl)-carbamic acid *tert*-butyl ester (compound-41)



To the solution of chiral amine **40** (400.0 mg, 1.70 mmol) in dry CH_2Cl_2 (7 mL), Et_3N (237 μ L, 1.70 mmol) was added. The solution of 2,6-pyridinedicarbonyl dichloride (173.4 mg, 1.70 mmol)

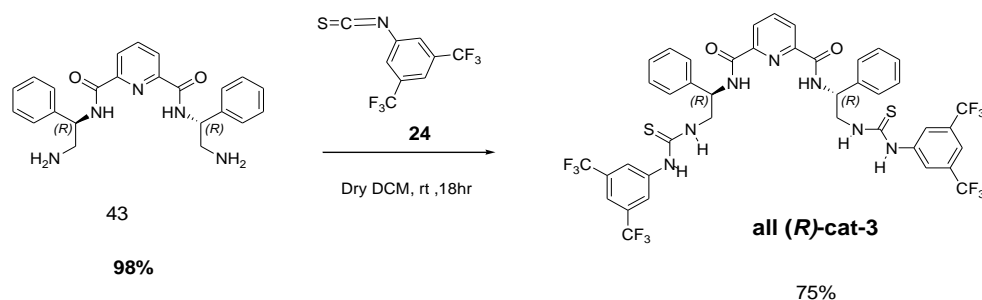
in CH₂Cl₂ (4 mL) was added dropwise. The mixture was stirred at room temperature overnight. The crude was concentrated and purified by column chromatography on silica gel (Hex/EA 50/50), providing a 98% yield. ¹H NMR (400 MHz, CDCl₃) δ 9.00 (d, *J* = 4.5 Hz, 2H), 8.20 (d, *J* = 7.7 Hz, 2H), 7.91 (t, *J* = 7.8 Hz, 1H), 7.27 (ddd, *J* = 29.9, 24.4, 7.0 Hz, 10H), 5.27 (d, *J* = 91.5 Hz, 4H), 3.84 – 3.32 (m, 4H), 2.04 (d, *J* = 49.6 Hz, 2H), 1.21 (s, *J* = 21.2, 13.9 Hz, 18H). HRMS (ESI): *m/z* calculated for C₃₃H₄₁N₅O₆, found: [M+Na]⁺ 626.2949, [2M +Na]⁺ 1229.6012.

Synthesis of Cpd-43



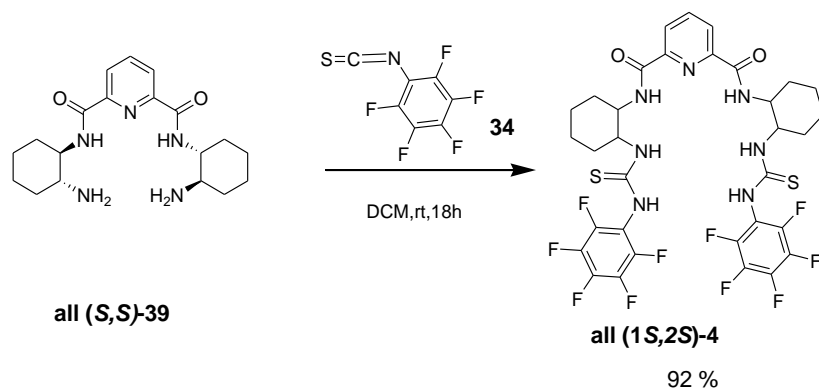
To the solution of product, **41** (306.0 mg, 0.51 mmol) in DCM (14 ml) was added TFA (391 μL, 5.10 mmol) at 0 °C and stirred at rt for 5h. After removing the solvent under reduced pressure, the resin was activated by 2N NaOH. Product **42** in methanol was loaded into the column, the solution was collected, concentrated, and dried, providing the product with a 98% yield. ¹H NMR (400 MHz, MeOD) δ 8.21 – 8.13 (m, 2H), 8.08 – 7.97 (m, 1H), 7.39 – 7.16 (m, 12H), 5.13 (dd, *J* = 7.9, 5.7 Hz, 2H), 3.15 – 2.98 (m, 4H), 1.80 (s, 4H). HRMS (ESI): *m/z* calculated for C₂₃H₂₅N₅O₂, found, [M+Na]⁺ 426.1901, [2M +Na]⁺ 829.3909.

Synthesis of all (*R*)-cat-3



To a solution of chiral amide, **43** (393.8 mg, 0.98 mmol) in CH₂Cl₂ (25 mL) was added 3,5-bis(trifluoromethyl)phenyl isothiocyanate (766 μL) at 0 °C. Then, the reaction was stirred at rt for 18h. After being monitored by TLC, the crude reaction was extracted with DCM/NaCl solution(brine) three times. The collected organic phase was filtered two times to minimize the amount of water. The solution was dried over Na₂SO₄ and purified by column chromatography, providing the product as a white solid with a 75% yield. ¹H NMR (400 MHz, DMSO) δ 9.47 (d, *J* = 8.5 Hz, 2H), 8.42 (d, *J* = 5.4 Hz, 2H), 8.30 – 8.10 (m, 8H), 7.70 (s, 2H), 7.52 (d, *J* = 7.2 Hz, 4H), 7.33 (dd, *J* = 8.3, 6.9 Hz, 3H), 7.27 – 7.12 (m, 2H), 5.48 (dd, *J* = 9.0, 5.2 Hz, 2H), 4.15 (dt, *J* = 15.7, 4.9 Hz, 4H), 3.47 (s, 2H). HRMS (ESI): *m/z* calculated for C₄₁H₃₁F₁₂N₇O₂S₂, found, [M+Na]⁺ 968.1688, [M+Na]²⁺ 492.5704.

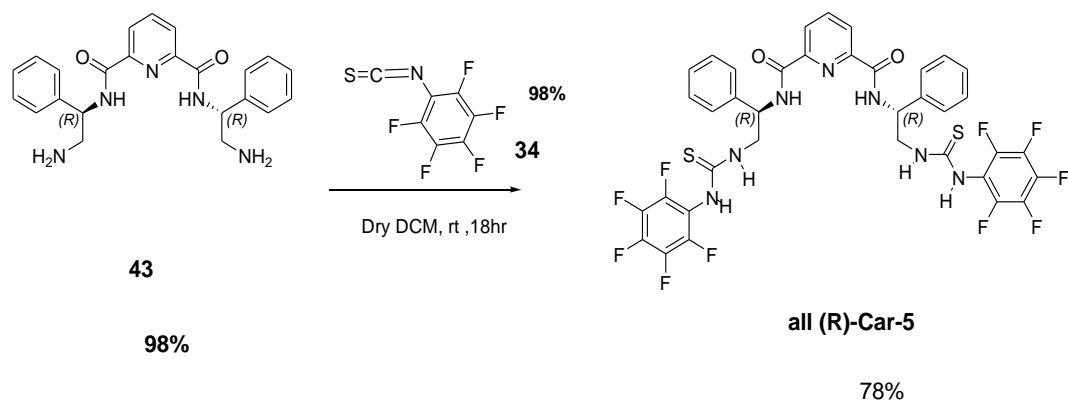
Synthesis of Cat-4



To a solution of chiral amide, **13** (0.42mmol,150mg) in CH₂Cl₂ (6mL) was added pentafluorophenyl-Isothiocyanat (0.88 mmol, 270.5 μL) at 0 °C. Then the reaction was stirred overnight at rt. The progress of the reaction was monitored by TLC (pentane/EA 50/50), After 18h, the crude of the reaction was concentrated and extracted with DCM/NaCl solution(brine) three times. The organic phase was filtered two times to minimize the amount of water and the

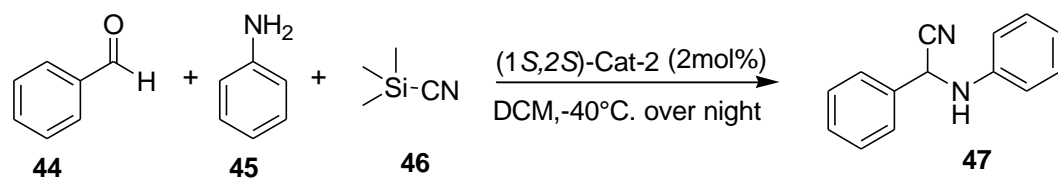
solution was filtered again. The solution was dried over Na₂SO₄ and the solvent evaporated under reduced pressure, providing the product with a 92% yield. ¹H NMR (400 MHz, CDCl₃) δ 7.99 – 7.76 (m, 2H), 7.74 – 7.52 (m, 2H), 7.26 (s, 6H), 4.32 – 3.90 (m, 2H), 3.43 – 3.21 (m, 2H), 1.34 – 0.66 (m, 16H). HRMS (ESI): m/z calculated for C₃₃H₂₉F₁₀N₇O₂S₂, found [M + H]⁺ 808.1560, [2M + H]⁺ 1617.3229.4

Synthesis of Cat-5

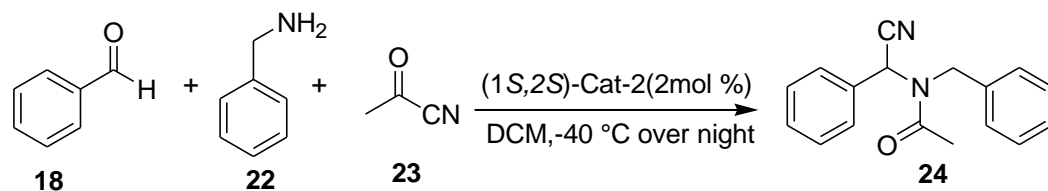


To a solution of chiral amide, **43** (100.0 mg, 0.248 mmol) in CH₂Cl₂ (7 mL) was added 1,2,3,4,5-pentafluoro-6-isothiocyanatobenzene (162 μL, 0.52mmol) at 0 °C and the reaction was stirred overnight at rt. After completion of the reaction (monitored by TLC: pentane/EAOc 50/50), then the crude solution was washed with a brine solution (three times). After dried, directed to column (pentane/ 78%: ¹H NMR (400 MHz, MeOD) δ 8.35 – 8.26 (m, 1H), 7.57 – 7.47 (m, 7H), 7.36 – 7.24 (m, 11H), 5.48 (dt, *J* = 12.7, 5.1 Hz, 2H), 3.95 – 3.80 (m, 4H). HRMS (ESI): m/z calculated for C₃₇H₂₅F₁₀N₇O₂S₂ found, [M + Na]⁺ 876.1243· [2M + Na]⁺ 1729.2597.

Procedure for the synthesis of Strecker Reactions



In a dried Schlenk flask containing dry CH_2Cl_2 (1.5 ml) and activated molecular sieve 5\AA (150 mg), aldehyde **44** (0.3 mmol) and aniline **45** (0.3 mmol) were added, and the mixture was stirred for 2 h at rt. Then, **Cat-2** (3.1 mg, 2 mol%) was added to the mixture and stirred for 10 min. **TMSCN 53** (0.75 mmol, 2 equiv.) was added and the mixture was stirred overnight. The crude of reaction was concentrated and subjected to silica gel column chromatography to give pure product. $^1\text{H NMR}$ (400 MHz, CDCl_3) δ 8.13 – 7.98 (m, 1H), 7.98 – 7.85 (m, 1H), 7.79 – 7.66 (m, 1H), 7.38 (tt, $J = 7.4, 1.0$ Hz, 1H), 7.29 – 7.19 (m, 1H), 5.89 (s, 0H), 4.56 – 4.46 (m, 0H).



In a dried Schlenk flask containing dry CH_2Cl_2 (1.5 ml) and activated molecular sieve 5\AA (150 mg), aldehyde **18** (0.5 mmol) and amine **22** (0.5 mmol) were added. After 2 h stirring at rt, catalyst **Cat-2** (2 mol%) was added, and the mixture will be stirred for 10 min. Acylcyanide (0.75 mmol, 1.5 equiv.) was added and the mixture was stirred -40°C . The concentrated crude was subjected to silica gel column chromatography to give pure product. $^1\text{H NMR}$ (400 MHz, CDCl_3) δ 7.34 (t, $J = 6.6$ Hz, 1H), 7.28 (dd, $J = 6.6, 3.6$ Hz, 2H), 7.23 – 7.14 (m, 2H), 7.05 – 6.94 (m, 1H), 4.52 – 4.31 (m, 1H), 2.14 – 1.93 (m, 2H).

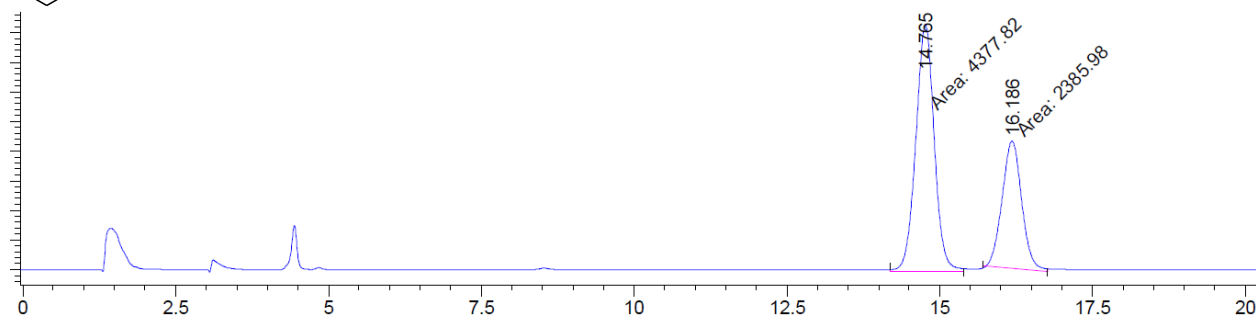
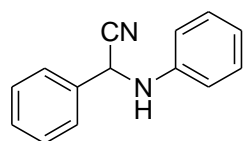
Biphenyl-2-ylamino)-phenyl-acetonitrile (**26b**)

^1H NMR (400 MHz, CDCl_3) δ 7.85 (dd, $J = 7.1, 1.8$ Hz, 2H), 7.78 – 7.68 (m, 4H), 7.52 (s, 1H), 7.46 (dd, $J = 10.2, 5.9$ Hz, 1H), 7.33 (dd, $J = 17.7, 9.7$ Hz, 4H), 7.13 (dt, $J = 13.1, 6.6$ Hz, 1H), 7.03 (dd, $J = 7.0, 5.1$ Hz, 1H), 5.67 (d, $J = 8.0$ Hz, 1H), 4.38 (d, $J = 7.7$ Hz, 1H).

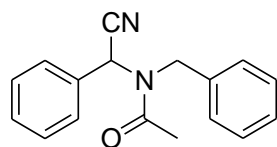
(Naphthalen-2-ylamino)-phenyl-acetonitrile(26c)

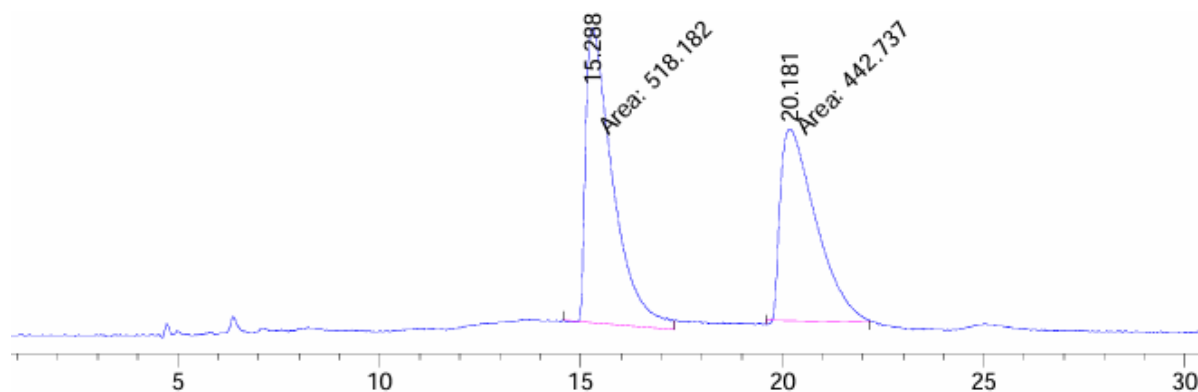
^1H NMR (400 MHz, CDCl_3) δ 7.85 – 7.66 (m, 7H), 7.61 – 7.48 (m, 2H), 7.44 – 7.34 (m, 2H), 7.16 (d, $J = 1.9$ Hz, 2H), 5.37 (s, 1H), 4.30 (s, $J = 6.9$ Hz, 1H).

HPLC chromatogram of enantioenriched /Strecker products



Peak	Time(Min)	Area(%)
1	14.765	65
2	16.186	35





Peak	Time(Min)	Area(%)
1	15.29	56
2	20.18	44

References

1. MacMillan, D. The advent and development of organocatalysis. *Nature* **2008**, *455*, 304–308.
2. Palumbo, C.; Guidotti, M. Organocatalysts for enantioselective synthesis of fine chemicals: definitions, trends and developments. *Sci. Open Res.* **2014**, *0*, 1–14.

3. Perera,D.; Aakery,B Organocatalysis by a multidentate halogen-bond donor: an alternative to hydrogen-bond based catalysis. *New J. Chem.* **2019**, *43*, 8311–8314.
4. Zhu,Y.; Hu,Y.; Li,Z.; Li,Y.; Gao,L.; Guo,K A genuine H-bond donor and Lewis base amine cocatalyst in ring-opening polymerizations. *Eur. Polym. J.* **2021**, *143*, 110184.
5. Novikov,A.; Bolotin,D.Halonium, chalconium, and pnictonium salts as noncovalent organocatalysts: a computational study on relative catalytic activity. *Org. Biomol. Chem.* **2022**, *20*, 7632–7639.
6. Oliveira,V.; Cardoso,M.; Forezi,L.Organocatalysis: A Brief Overview on Its Evolution and Applications. *Catalysts*, **2018**, *8*, 605.
7. Qin.Y.; Zhu,L.;Luo,S. Organocatalysis in Inert C–H Bond Functionalization. *Chem. Rev.* **2017**, *117*, 9433 9520.
8. Čmelová, P.; Šramel, P.; Zahradníková, B.; Modrocká, V.; Szabados, H.; Mečiarová, M.;Sebesta.M.Pro-Pro Dipeptide-Thiourea Organocatalyst in the Mannich Reaction between α -Imino Esters and Pyruvates. *Eur. J. Org. Chem.* **2022**, e202200106.
9. Zhang,Z.; Schreiner.P.(Thio)Urea Organocatalysis - What Can Be Learnt from Anion Recognition? *Chem. Soc. Rev.* **2009**, *38*, 1187–1198.
10. Fang,X.;Wang,C.Recent Advances in Asymmetric Organocatalysis Mediated by Bifunctional Amine-Thioureas Bearing Multiple Hydrogen-Bonding Donors. *Chem. Commun.* **2015**, *51*,1185–1197.
11. Vera, S.; García-Urricelqui, A.; Mielgo, A.;Oiarbide.M.Progress in (Thio)urea- and Squaramide-Based Brønsted Base Catalysts with Multiple H-Bond Donors. *Eur. J. Org Chem.* **2023**, *26*, e202201254.
12. Madarász, A.; Dósa, Z.; Varga, S.; Soós, T.; Csámpai, A.; Pápai,I.Thiourea Derivatives as Brønsted Acid Organocatalysts. *ACS Catal.* **2016**, *6*, 4379–4387.
13. Bradshaw,G.;Colgan,AQ.;Allen,N.;Pongener,L.;Boland,M.;Ortin,Y.;McGarrigle.E. Stereoselective organocatalyzed glycosylations-thiouracil, thioureas and mono thiophthalimide act as Brønsted acid catalysts at low loadings. *Chem. Sci.* **2019**, *10*, 508–514.
14. Madarász,A.; Z.Dósa,Z.;Varga,S.;Soós,T.;Csámpai,A.;Pápai.I.Thiourea Derivatives as Brønsted Acid Organocatalysts. *ACS Catal.* **2016**, *6*, 4379-4387.
15. Otevrel,J.;Bobal.P.Diamine-Tethered Bis(thiourea) Organocatalyst for Asymmetric Henry Reaction. *J. Org. Chem.* **2017**, *82*, 8342-8358.

16. Wittkopp, A.; Schreiner, P. Metal-Free, Noncovalent Catalysis of Diels ± Alder Reactions by Neutral Hydrogen Bond Donors in Organic Solvents and in Water. *Chem. Eur. J.* **2003**, *9*, 407–414.
17. Okino, T.; Hoashi, Y.; Takemoto, Y. Enantioselective Michael Reaction of Malonates to Nitroolefins Catalyzed by Bifunctional Organocatalysts. *J. Am. Chem. Soc.* **2003**, *125*, 12672–12673.
18. Schreiner, P.; Wittkopp, A.; H-Bonding Additives Act Like Lewis Acid Catalysts. *Org. Lett.* **2002**, *4*, 217–220.
19. Kotke, M.; Schreiner, P. Acid-Free, Organocatalytic Acetalization. *Tetrahedron* **2006**, *62*, 434–439.
20. Yamaoka, Y.; Miyabe, H.; Takemoto, Y. Catalytic Enantioselective Pétasis-Type Reaction of Quinolines Catalyzed by a Newly Designed Thiourea Catalyst. *J. Am. Chem. Soc.* **2007**, *129*, 6686–6687.
21. Matienko, L.; Mil, E.; Albantova, A.; Goloshchapov, A. The Role of H-Bonding and Supramolecular Structures in Homogeneous and Enzymatic Catalysis. *Int. J. Mol. Sci.* **2023**, *24*, 16874.
22. Wittkopp, A.; Schreiner, P. Metal-free, noncovalent catalysis of diels–alder reactions by neutral hydrogen bond donors in organic solvents and in water. *Chem Eur J.* **2003**, *9*, 407–414.
23. Sigman, M.; Vachal, P.; Jacobsen, E. A general catalyst for the asymmetric Strecker reaction. *Angew. Chem. Int. Ed.* **2000**, *39*, 1279–81.
24. Torres, R. (Ed.). *Stereoselective Organocatalysis: Bond Formation Methodologies and Activation Modes*, 1st ed.; John Wiley & Sons: Hoboken, NJ, USA, 2013.
25. Okino, T.; Hoashi, Y.; Takemoto, Y. Enantioselective Michael Reaction of Malonates to Nitroolefins Catalyzed by Bifunctional Organocatalysts. *J. Am. Chem. Soc.* **2003**, *125*, 12672–12673.
26. Alemán, J.; Parra, A.; Jiang, H.; Jørgensen, K. Squaramides: Bridging from Molecular Recognition to Bifunctional Organocatalysis. *Chem. Eur. J.* **2011**, *17*, 6890–689.
27. Ciber, L.; Požgan, F.; Brodnik, H.; Štefane, B.; Svete, J.; Grošelj, U. Synthesis and Catalytic Activity of Organocatalysts Based on Enaminone and Benzenediamine Hydrogen Bond Donors. *Catalysts* **2022**, *12*, 1132.

28. Kouznetsov, V.; Galvis, C. Strecker reaction and α -amino nitriles: Recent advances in their chemistry, synthesis, and biological properties. *Tetrahedron*, **2018**, *74*, 773–810.
29. Wang, J.; Liu, X.; Feng, X. Asymmetric Strecker Reactions. *Chem. Rev.* **2011**, *111*, 6947–6983.
30. Saravanan, S.; Khan, N.; Kureshy, R.; Abdi, S.; Bajaj, H. Small Molecule as a Chiral Organocatalyst for Asymmetric Strecker Reaction. *ACS Catal.* **2013**, *3*, 2873–2880.
31. Saravanan, S.; Sadhukhan, A.; Khan, N.; Kureshy, R.; Abdi, S.; Bajaj, H. C₂-Symmetric Recyclable Organocatalyst for Enantioselective Strecker Reaction for the Synthesis of α -Amino Acid and Chiral Diamine- an Intermediate for APN Inhibitor. *J. Org. Chem.* **2012**, *77*, 4375–4384.
32. Wen, Y.; Xiong, Y.; Chang, L.; Huang, J.; Liu, X.; Feng, X. Chiral Bisformamides as Effective Organocatalysts for the Asymmetric One-Pot, Three-Component Strecker Reaction. *J. Org. Chem.* **2007**, *72*, 7715–7719.
33. Kouznetsov, V.; Galvis, C. Strecker Reaction and α -Amino Nitriles: Recent Advances in Their Chemistry, Synthesis, and Biological Properties. *Tetrahedron* **2018**, *74*, 773–810.
34. Grundke, C.; Vierengel, N.; Opatz, T. Aminonitriles: From Sustainable Preparation to Applications in Natural Product Synthesis. *Chem. Rec.* **2020**, *20*, 989–1016.
35. Eppinger, E.; Gröning, J.; Stolz, A. Chemoenzymatic Enantioselective Synthesis of Phenylglycine and Phenylglycine Amide by Direct Coupling of the Strecker Synthesis with a Nitrilase Reaction. *Front. Catal.* **2022**, *2*, 952944.
36. Masamba, W. Petasis vs. Strecker Amino Acid Synthesis: Convergence, Divergence and Opportunities in Organic Synthesis. *Molecules* **2021**, *26*, 1707.
37. Cai, X.; Xie, B. Recent Advances on Asymmetric Strecker Reactions. *Arkivoc* **2014**, *2014*, 205–248.
38. Sigman, M.; Jacobsen, E. Schiff Base Catalysts for the Asymmetric Strecker Reaction Identified and Optimized from Parallel Synthetic Libraries. *J. Am. Chem. Soc.* **1998**, *120*, 4901.
39. Vachal, P.; Jacobsen, E. Asymmetric Cooperative Catalysis of Strong Brønsted Acid-Promoted Reactions Using Chiral Ureas. *J. Am. Chem. Soc.* **2002**, *124*, 10012.
40. Zuend, S.; Coughlin, M.; Lalonde, M.; Jacobsen, E. Scaleable Catalytic Asymmetric Strecker Syntheses of Unnatural α -Amino Acids. *Nature* **2009**, *461*, 968–970.

41. Alfano, A.; Sorato, A.; Ciogli, A.; Lange, H.; Brindis, M. Enantioselective catalytic Strecker reaction on cyclic (Z)-aldimines in flow: reaction optimization and sustainability aspects. *J. Flow Chem.* **2024**, *14*, 197–210.
42. Kochetkov, V.; Kucherenko, S.; Sergei, Z. Asymmetric synthesis of warfarin and its analogs catalyzed by C₂ symmetric squaramidebased primary diamines. *Org. Biomol. Chem.*, 2018

List of Publications

1. Andrea Pellegrini, Laura Marcon, Paolo Righi, Giovanni Centonze, Chiara Portolani, Marco Capodiferro, Shilashi Oljira, Simone Manetto, Alessia Ciogli, Giorgio Bencivenni. On the Nature of the Rotational Energy Barrier of Atropisomeric Hydrazides. *Molecules* 2023, *28*, 7856.
2. Andrea Sorato; Martina DeAngelis; Shilashi Badasa Oljira; Marco Pierini; Giulia Mazzocanti; Maria Pia Donzello; Alessia Ciogli. A C₃-Symmetric Amino Organocatalyst for Asymmetric Synthesis of Warfarin and Analogues: Mechanistic Insight From ESI-MS Spectrometry and Computational Calculations. *ChemCatChem*, 2024, e202400031